The human SCCRO gene family: characterization of its molecular function and role in carcinogenesis

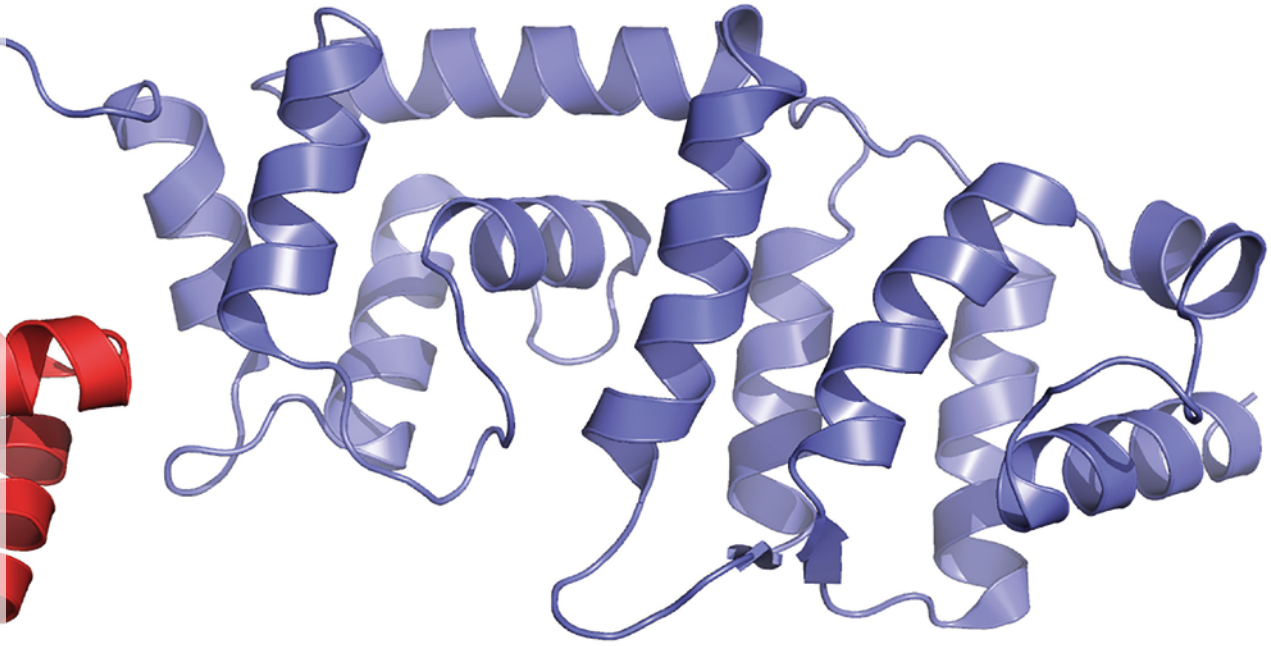

Claire C. Bommeljé

The Human SCCRO Gene Family: Characterization of its molecular function and role in carcinogenesis

Claire Cornelia Bommeljé

The Human SCCRO Gene Family: Characterization of its molecular function and role in carcinogenesis.

The research in this thesis was financially supported by Bekker La Bastide Fonds, Stichting Fundatie van de Vrijvrouwe van Renswoude, Dr. Catherine van Tussenbroek Fonds and Trustfonds Rotterdam.

Publication of this thesis was financially supported by:
ABN AMRO Bank N.V., ALK-Abello B.V., Atos Medical B.V., ChipSoft B.V., Daleco Pharma B.V., de Nederlandse Vereniging voor KNO-heelkunde en Heelkunde van het Hoofd-Halsgebied, Dos Medical B.V./kno-winkel.nl, Entercare, Erasmus Universiteit Rotterdam, Meda Pharma B.V., Olympus Nederland B.V., Phonak en Specsavers.

ISBN: 978-94-6299-109-5

Printed by: Ridderprint BV – www.ridderprint.nl
Layout: Ridderprint BV – www.ridderprint.nl

The Human SCCRO Gene Family: Characterization of its molecular function and role in carcinogenesis

De menselijke SCCRO gen familie: karakterisering van hun moleculaire functie en rol in het ontstaan van kanker

Proefschrift

ter verkrijging van de graad van doctor aan de
Erasmus Universiteit Rotterdam
op gezag van de rector magnificus

prof.dr. H.A.P. Pols

en volgens besluit van het College voor Promoties.
De openbare verdediging zal plaatsvinden op
woensdag 8 juli 2015 om 09.30 uur

door
Claire Cornelia Bommeljé
geboren te Breda

Erasmus University Rotterdam

Promotiecommissie

Promotoren:	Prof.dr. R.J. Baatenburg de Jong
	Prof.dr. B. Singh
Overige leden:	Prof.dr. F.J. van Kemenade
	Prof.dr. L.H.J. Looijenga
	Prof.dr. E-J.M. Speel

Index

Chapter 1	General introduction	7
Chapter 2	SCCRO (DCUN1D1) is an essential component of the E3 complex for neddylation	19
Chapter 3	The ubiquitin associated domain of SCCRO (DCUN1D1) serves as a feedback regulator of biochemical and oncogenic activity	43
Chapter 4	SCCRO3 (DCUN1D3) antagonizes the neddylation and oncogenic activity of SCCRO (DCUN1D1)	69
Chapter 5	Oncogenic function of SCCRO5 (DCUN1D5) requires its neddylation E3 activity and nuclear localization	97
Chapter 6	SCCRO and its paralogs are frequently dysregulated in human cancers and are associated with an aggressive clinical course and activation of neddylation	129
Chapter 7	General discussion	151
Chapter 8	Summary / Samenvatting	163
List of abbrevations		171
PhD portfolio		173
Acknowledgments		174
About the author		176
List of publications		177

Chapter 1

General introduction

Cancer

Cancer is an international public health problem. A total of 1,665,540 new cancer cases and 585,720 cancer deaths are projected to occur in the United States in 2015. Although the combined cancer death rate (deaths per 100,000 population per year) has been continuously declining for two decades, from a peak of 215 in 1991 to 172 in 2010, cancer is still a big health problem (1).

Head and neck squamous cell carcinoma

Head and neck cancer represents the sixth most common malignancy worldwide. The vast majority of these patients are diagnosed with head and neck squamous cell carcinoma (HNSCC) (Figure 1). HNSCC and its treatment can result in cosmetic deformity and functional impairment of vital functions, including breathing, swallowing, speech, phonation, taste, hearing, and smell. The estimated yearly incidence worldwide is half a million people. Nearly 50% of patients die due to tumor-related complications (2,3). The disease ranks age dependently among the leading types of solid cancer and is responsible for more than 65,000 deaths annually in Europe (4,5). More than 50% of patients suffering from HNSCC sustain local relapses after primary treatment while up to 25% develop distant metastases (6). Despite significant improvements in treatment options of these cancers, with combinations of radiotherapy (RT), surgery and systemic therapy, the five-year disease-free survival of those patients remains unacceptably poor (7).

Figure 1. Squamous cell carcinoma on the left side of the tongue.

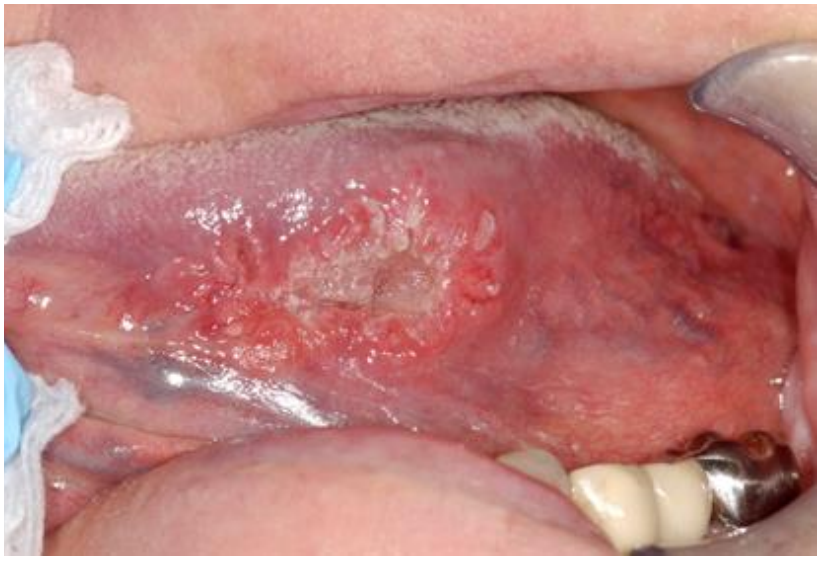

For many years, the main prognostic factors of HNSCC have been the conventional grading, staging, and site of the tumor (8,9). Since the human genome project has been finished and a better understanding of the molecular basis of cancer has resulted, an enormous scientific field has arisen. Nowadays, an important goal of basic science research is to define the tumor "biological fingerprint" and to find key molecular components that are involved in carcinogenesis. An example is the epidermal growth factor receptor (EGFR). EGFR is a transmembrane tyrosine kinase receptor belonging to the HER/erbB family, it is overexpressed in up to 90% of HNSCC patients (10). High EGFR gene copy number has been reported in 10% - 58% of HNSCC. In HNSCC, in contrast to other cancers such as lung cancer, activating EGFR mutations are rare. Overexpression of EGFR and high EGFR gene copy number are associated with poor prognosis and radioresistance (11-16). EGFR is a relevant target in HNSCC since cetuximab, an immunoglobulin G1 (IgG1) monoclonal antibody targeting EGFR, improves overall survival (OS) when combined with RT or chemotherapy. However, only a minority of patients will benefit from anti-EGFR monoclonal antibodies, and the objective response rate in monotherapy is between 6% and 13% (17,18). The goal of research nowadays is to be able to treat the majority of patients with individualized cancer therapy by elucidating the major genetic and epigenetic changes per tumor. Thus, further research is necessary for this still deadly disease to expand the array of targeted therapies. An in-depth understanding of head and neck tumorigenesis and new developments in molecular biology may lead to personalized cancer treatment with improved overall outcomes.

Squamous cell carcinoma related oncogene (SCCRO a.k.a. DCUN1D1)

In an attempt to elucidate the biological background of HNSCC, low-resolution mapping studies utilizing comparative genomic hybridization (CGH) and spectral karyotyping (SKY) were performed and refined a region of frequent amplification to 3q25-27 (19-21). Several tumor types originating from mucosal squamous cell epithelium demonstrated a similar recurrent gain of the long arm of chromosome 3, including squamous-type non-small-cell lung cancer (NSCLC), and cancer of the uterine cervix (19). FISH-based fine-resolution mapping of a region of maximal amplification at 3q26.3 in head and neck cancer cell lines identified squamous cell carcinoma related oncogene (SCCRO a.k.a. DCUN1D1) as a candidate oncogene within this region of frequent amplification. *SCCRO* gene amplification correlated significantly with mRNA and SCCRO protein overexpression in tissue and cell lines derived from head and neck and lung cancers. In primary human tumors, highly significant overexpression of *SCCRO* mRNA relative to normal tissue controls was detected in 36% of HNSCC, 44% of cervical carcinoma, and 48% of NSCLC tested. *SCCRO* overexpression is shown to correlate negatively with cause-free survival in non-small cell lung cancer (22). Functional evidence of *SCCRO's* oncogenic activity came from experiments in which *SCCRO* was transgenically overexpressed in mouse fibroblasts and human immortalized keratinocytes. *SCCRO*-transfected keratinocytes gained anchorage-independent growth, while stably *SCCRO* overexpressing fibroblasts showed dedifferentiated morphology, increased proliferation, serum-independent

growth, enhanced invasiveness and tumorgenicity in nude mice (22). Altogether, these data established SCCRO as a potential novel oncogene. The next step was to characterize the molecular function of SCCRO. At that time, completion of the human genome sequencing project revealed that SCCRO was known as Defective in Cullin Neddylation 1 (DCUN1D1) in the gene database. During that same period, Kurz and colleagues showed that in the nematode Caenorhabditis elegans Defective in Cullin Neddylation (DCN-1) and in the yeast Saccharomyces Cerevisiae Dcn1p, both homologs of the human SCCRO/DCUN1D1, were required for the covalent modification of cullin proteins by the ubiquitin-like protein Nedd8 (23). This led the focus of our research, described in this thesis, to SCCRO's involvement in the neddylation pathway, a pathway known to regulate protein ubiquitination.

Ubiquitination

The ubiquitination of proteins involves the hierarchical action of three ubiquitin enzymes (Figure 2). An E1 enzyme must first activate ubiquitin (Ub), a highly conserved 76 amino acid polypeptide. The thioesterified ubiquitin passes from the E1 active site to the next member of the cascade, the E2 or ubiquitin-conjugating enzyme. Finally, the E3 ubiquitin ligase binds to both the E2-bound ubiquitin and the protein substrate, promoting the transfer of ubiquitin onto the substrate. There are several hundred different ubiquitin pathway E3 ligases (24). Cullin-Ring ubiquitin ligases (CRL's) comprise the largest known category of ubiquitin ligases. Eukaryotic species contain multiple cullins. Each cullin forms a distinct class of CRL complex with distinct adaptors and/or substrate-recognition subunits. Despite this diversity, each of the classes of CRL complexes is subject to similar regulatory mechanisms (25).

Figure 2 shows the neddylation and ubiquitin pathway.

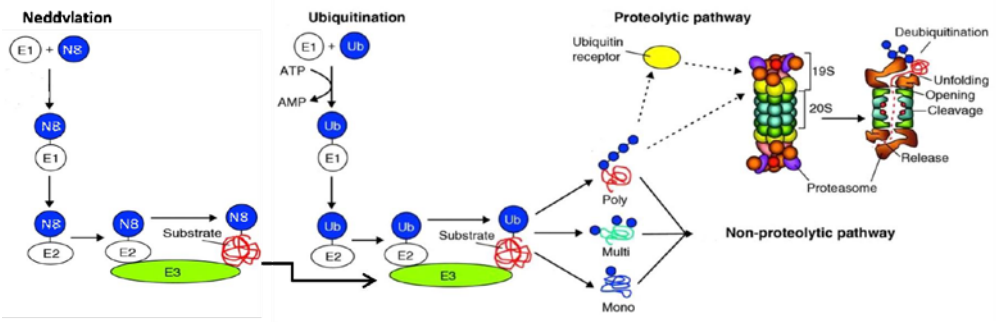

In the ubiquitin pathway proteins can either be conjugated to one ubiquitin monomer, referred to as mono-ubiquitination, or to several ubiquitins to form a poly-ubiquitin chain. Mono-ubiquitination modifies proteins, changes their activity and in that way mediates downstream effects. Proteins conjugated to chains of ubiquitin may be directed to the 26S proteasome where they then become degraded or undergo alteration of their activity. Degradation occurs through the ubiquitin-proteasome system (UPS), a highly complex process (26). The ubiquitin system plays important roles in a variety of basic cellular processes. Among these are regulation of cell cycle and division, apoptosis, transcription, modulation of the immune and inflammatory responses and development and differentiation (27). The association between ubiquitination and cancer is evident from the multiple tumor suppressor genes and oncogenes that are regulated in this manner (27).

Neddylation

Like ubiquitination, neddylation results from an enzymatic cascade involving the sequential activity of a dedicated E1 (APPBP1/Uba3), E2 (Ubc12), and E3 enzyme (Figure 2) (27,28). Covalent modification of cullins by the ubiquitin like protein (UBL) Nedd8 regulates protein ubiquitination by promoting the assembly of CRL E3 complexes, thus activating protein ubiquitination. Nedd8 modification of cullins is crucial for CRL dependent ubiquitination (30,31). Most UBL's don't target their substrates for degradation, but rather change their activity by, for example, providing a (new) binding surface for interaction partners (26,32).

SCCRO family

Completion of the human genome sequencing project revealed that SCCRO is a member of a protein family that contains four other highly conserved paralogs in higher organisms, all of which contain a conserved C-terminal potentiating of neddylation (PONY) domain with a variable N-terminal region. SCCRO paralogs are subdivided into three subfamilies on the basis of the N-terminal sequence: SCCRO and SCCRO2 (a.k.a. DCUN1D2) contain a ubiquitin associated (UBA) domain, SCCRO3 (a.k.a. DCUN1D3) contains a myristoylation sequence and SCCRO4 (a.k.a. DCUN1D4) and SCCRO5 (a.k.a. DCUN1D5) contain a nuclear localization sequence (NLS) (Figure 3). Like *SCCRO* (at 3q26), its paralogs are located in chromosomal loci that are recurrently amplified in human cancers (*SCCRO2* at 13q34, *SCCRO4* at 4q12, and *SCCRO5* at 11q22) (33-40). Therefore, we sought to unravel their molecular function and their clinical relevance and to evaluate their potential roles in carcinogenesis.

Figure 3. Phylogenetic analyses of the SCCRO gene family.

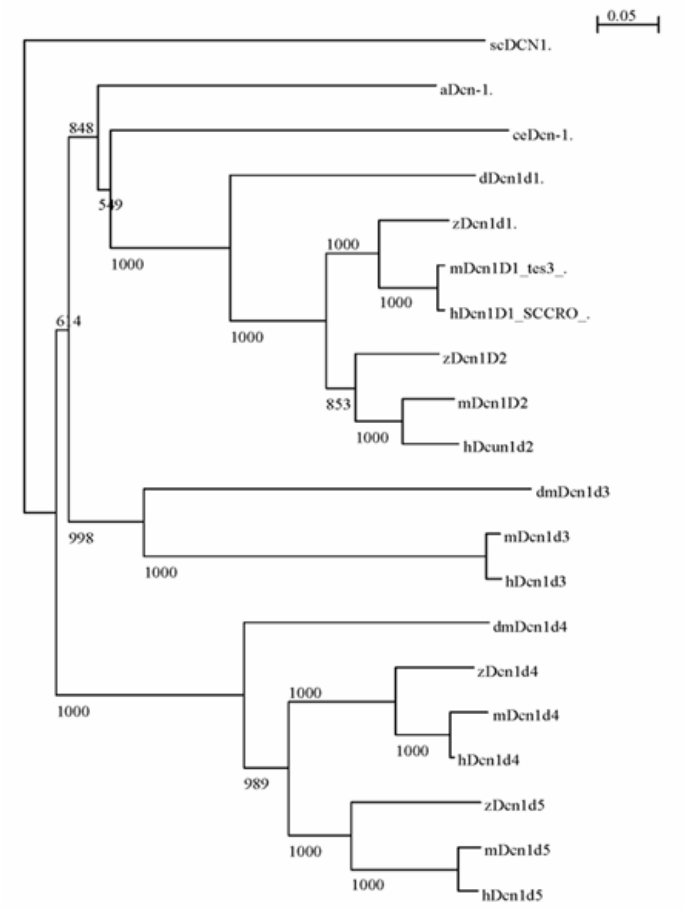

Evolutionary tree showing the inferred evolutionary relationships among various biological species – their phylogeny based upon similarities and differences in their physical or genetic characteristics. Here shown the phylogenetic or evolutionary tree of the SCCRO/DCUN1D genes. Numbers: boot strap comparison.
a, Anopheles gambiae ; ce, C.elegans; dm, Drosophila melanogaster; h, Homo sapiens; m, Mus musculus; Sc, S. cerevisiae.

Translational relevance

Targeted therapy based on common molecular aberrations consitutes the future of cancer therapy. In this regard, the characterization of SCCRO in the neddylation pathway is not only important in the understanding of basic cellular biology, but also for oncogenesis. The observation that changes in protein homeostatis drive human cancer pathogenesis has led to the discovery of several important anticancer therapies. In this regard, the ubiquitin proteasome system is of significance, as

there is a high prevalence of aberrations among the components of this pathway. The link between abnormal CRL activity and dysregulation of proteins involved in neddylation in human cancers has only recently been appreciated (41). These observations have led to the development of a small molecule inhibitor of neddylation E1, MLN4924. Inhibition of neddylation by the Nedd8 activating enzyme (NAE) inhibitor MLN4924 has shown statistically significantly suppressed proliferation, survival, migration and motility of lung cancer cells *in vitro* and tumor formation and metastasis *in vivo* and has shown promise in preclinical and early human trials (42). Also, the therapeutic potential of inhibition of the ubiquitin proteosome system (UPS) has been validated with the first-in-class proteasome inhibitor, Bortezomib, which is approved for the treatment of multiple myeloma and the treatment of relapsed mantle cell lymphoma (43,44).

Altogether, this underscores the importance of elucidating the function of the ubiquitin and neddylation pathways. In this thesis we solve a piece of this puzzle by characterizing the role of the human SCCRO gene family in the neddylation pathway and in carcinogenesis.

Outline of the thesis

In this thesis we have set the first steps in understanding the molecular function of the human SCCRO gene family in neddylation and in carcinogenesis.

Chapter 2 describes the molecular function of SCCRO in the neddylation pathway. We show that SCCRO binds to the components of the neddylation pathway (Cullin-ROC1, Ubc12, and CAND1) and augments, but is not required for cullin neddylation in reactions using purified recombinant proteins. We show that SCCRO enhances recruitment of Ubc12~Nedd8 to the CRL complex and is necessary to dissociate CAND1.

In **chapter 3** we define the contribution of the N-terminal UBA domain to SCCRO's function. We show that binding of polyubiquitin chains to the UBA domain inhibits SCCRO's neddylation activity by inhibiting SCCRO-promoted nuclear translocation of neddylation components. We suggest that the UBA domain of SCCRO functions as a negative regulator of SCCRO's function.

Chapter 4 describes the function of SCCRO3. We find that SCCRO3 is often underexpressed in various human cancers and we attempt to define the cause of decreased expression of SCCRO3. We show by structure-function and cell based assays that SCCRO3 may function as a tumor suppressor. Our findings suggest that SCCRO3 antagonizes SCCRO mediated neddylation and oncogenic activity by blocking nuclear localization of cullins and hence cullin neddylation.

In **chapter 5** we elucidate the role of SCCRO5 as a target that drives selection for 11q22 amplification in human cancers. Gene expression levels and protein levels are assessed and clinical correlations are described. The molecular mechanism is unraveled by showing its function in the neddylation pathway and further explored by cell based assays.

Finally, **chapter 6** further illustrates the translational importance of this basic science research as we examine the role of the SCCRO family of genes in various human cancers and describe a novel biochemical assay to look for ubiquitination activities in human tissue and use this in a subset of thyroid cancer.

In **chapter 7** we recapitulate the role of the human SCCRO gene family, the importance of neddylation and ubiquitination in cell function and in carcinogenesis. Finally, topics for further investigation are discussed in this chapter.

References

1. Siegel R, Ma J, Zou Z, Jemal A. Cancer statistics, 2014.CA Cancer J Clin 2014; Jan-Feb;64(1):9-29.
2. Parkin DM, Bray F, Ferlay J, Pisani P. Estimating the world cancer burden: Globocan 2000. Int J Cancer. 2001;94:153-156.
3. Haddad RI, Shin DM. Recent advances in head and neck cancer. N Engl J Med. 2008;359:1143-1154.
4. Barnes L. World health organisation classification of tumours, pathology and genetics, head and neck tumours. Lyon: IARC Press; 2005.
5. Kademani D, Bell RB, Bagheri S, Holmgren E, Dierks E, Potter B, Homer L. Prognostic factors in intraoral squamous cell carcinoma: the influence of histologic grade. J Oral Maxillofac Surg. 2005;63:1599-1605.
6. Zbären P, Lehmann W. Frequency and sites of distant metastases in head and neck squamous cell carcinoma. An analysis of 101 cases at autopsy. Arch Otolaryngol Head Neck Surg. 1987;113:762-764.
7. Machiels JP, Lambrecht M, Hanin FX, Duprez T, Gregoire V, Schmitz S, Hamoir M. Advances in the management of squamous cell carcinoma of the head and neck. F1000Prime Rep. 2014. Jun2;6:44.
8. Wennerberg J. Predicting response to therapy of squamous cell carcinoma of the head and neck (review). Anticancer Research. 1996; 16:4: 2389–2396.
9. Woolgar JA. Histopathological prognosticators in oral and oropharyngeal squamous cell carcinoma. Oral Oncology. 2006; 42:3: 229–239.
10. Kalyankrishna S, Grandis JR: Epidermal growth factor biology in head and neck cancer. J Clin Oncol 2006, 24:2666-72.
11. Temam S, Kawaguchi H, El-Naggar AK, Jelinek J, Tang H, Liu DD, Lang W, Issa JP, Lee JJ, Mao L. Epidermal growth factor receptor copy number alterations correlate with poor clinical outcome in patients with head and neck squamous cancer. J Clin Oncol 2007, 25:2164-70.
12. Mrhalova M, Plzak J, Betka J, Kodet R: Epidermal growth factor receptor-its expression and copy numbers of EGFR gene in patients with head and neck squamous cell carcinoma. Neoplasm. 2005. 52:338-43.
13. Chung CH, Ely K, McGavran L, Varella-Garcia M, Parker J, Parker N, Jarrett C, Carter J, Murphy BA, Netterville J, Burkey BB, Sinard R, Cmelak A, Levy S, Yarbrough WG, Slebos RJ, Hirsch FR. Increased epidermal growth factor receptor gene copy number is associated with poor progonis in head and neck squamous cell carcinomas. J Clin Oncol. 2006, 24:4170-76.
14. Chiang WF, Liu SY, Yen CY, Lin CN, Chen YC, Lin SC, Chang KW. Association of epidermal growth factor receptor (EGFR) gene copy number amplification with neck lymph node metastasis in areca-associated oral carcinoma.Oral Oncol. 2008. 44:270-6.
15. Ang KK, Berkey BA, Tu X, Zhang HZ, Katz R, Hammond EH, Fu KK, Milas L. Impact of epidermal growth factor receptor expression on survival and pattern of relapse in patients with advanced head and neck carcinoma. Cancer Res. 2002. 62:7350-56.
16. Wheeler S, Siwak DR, Chai R, LaValle C, Seethala RR, Wang L, Cieply K, Sherer C, Joy C, Mills GB, Argiris A, Siegfried JM, Grandis JR, Egloff AM: Tumor epidermal growth factor receptor and EGFR PY1068 are independent prognostic indicators for head and neck squamous cell carcinoma. Clin Cancer Research. 2012. 18:2278-89.
17. Vermorken J, Mesia R, Rivera F, Remenar E, Kawecki A, et al. Hitt R: Platinum-based chemotherapy plus cetuximab in head and neck cancer. N Eng J Med 2008, 11:1116-27.
18. Bonner JA, Harari PM, Giralt J, Cohen RB, Jones CU, Sur RK, Raben D, Baselga J, Spencer SA, Zhu J, Youssoufian H, Rowinsky EK, Ang KK: Radiotherapy plus cetuximab for locoregionally advanced head and neck cancer: 5-year survival data from a phase 3 randomised trial, and relation between cetuximab-induced rash and survival. Lancet Oncol 2010, 11:21-8.
19. Singh B, Gogineni S, Goberdhan A, Sacks P, Shaha A, Shah J, et al. Spectral karyotyping analysis of head and neck squamous cell carcinoma. Laryngoscope. 2001;111:1545–50.
20. Singh B, Stoffel A, Gogineni S. Amplification of the 3q26.3 locus is associated with progression to invasive cancer and is a negative prognostic factor in head and neck squamous cell carcinomas. Am J Pathol. 2002;161:365–71.
21. Singh B, Gogineni SK, Sacks PG, Shaha AR, Shah JP, Stoffel A, Rao PH. Molecular cytogenetic characterization of head and neck squamous cell carcinoma and refinement of 3q amplification. Cancer Res. 2001. 61:4506-13.

22. Sarkaria I, O-charoenrat P, Talbot SG, Reddy PG, Ngai I, Maghami E, et al. Squamous cell carcinoma related oncogene/DCUN1D1 is highly conserved and activated by amplification in squamous cell carcinomas. Cancer Res. 2006;66:9437–44.
23. Kurz T, Ozlu N, Rudolf F, O'Rourke SM, Luke B, Hofmann K, Hyman AA, Bowerman B, Peter M. The conserved protein DCN-1/Dcn1p is required for cullin neddylation in C.elegans and S.cerevisiae. Nature. 2005;Jun;435(7046):1257-61.
24. Dye BT, Schulman BA. Structural mechanisms underlying posttranslation modification by ubiquitin-like proteins. Annu Rev Biophys Biomol Struct. 2007;36:131-50.
25. Sarikas A, Hartmann T, Pan ZQ. The cullin protein family. Genome Biol. 2011; 12(4):220.
26. Chiechanover A, Orian A, Schwartz AL. The ubiquitin-mediated proteolytic pathway: mode of action and clinical implications. J Cell Biochem Suppl. 2000;34:40-51
27. Ang XL, Wade Harper J. SCF-mediated protein degradation and cell cycle control. Oncogene. 2005;24(17):2860-70.
28. Wu K, Chen A, Pan ZQ. Conjugation of Nedd8 to Cul1 enhances the ability of the ROC1-CUL1 complex to promote ubiquitin polymerization. J Biol Chem. 2000. 13;275(41):32317-24.
29. Gong L, Yeh ET. Identification of the activating and conjugating enzymes of the Nedd8 conjugation pathway. J Biol Chem 1999; 274:12036–42.
30. Kawakami T, Chiba T, Suzuki T, Iwai K, Yamanaka K, Minato N, et al. Nedd8 recruits E2-ubiquitin to SCF E3 ligase. EMBO J 2001;20:4003–12.
31. Sakata E, Yamaguchi Y, Miyauchi Y, Iwai K, Chiba T, Saeki Y, et al. Direct interactions between Nedd8 and ubiquitin E2 conjugating enzymes upregulate cullin-based E3 ligase activity. Nat Struct Mol Biol 2007;14:167–8.
32. Bosu DR, Kipreos ET. Cullin-RING ubiquitin ligases: global regulation and activation cycles. Cell Div. 2008. Feb 18;3-7.
33. Abba MC, Fabris VT, Hu Y, Kittrell FS, Cai WW, Donehower LA, et al. Identification of novel amplification gene targets in mouse and human breast cancer at a syntenic cluster mapping to mouse ch8A1 and human ch13q34. Cancer Res 2007;67:4104–12.
34. Salgado R, Toll A, Alameda F, Baro T, Martin-Ezquerra G, Sanmartin O, et al. CKS1B amplification is a frequent event in cutaneous squamous cell carcinoma with aggressive clinical behaviour. Genes Chromosomes Cancer 2010;49:1054–61.
35. Barrow J, Adamowicz-Brice M, Cartmill M, MacArthur D, Lowe J, Robson K, et al. Homozygous loss of ADAM3A revealed by genome-wide analysis of pediatric high-grade glioma and diffuse intrinsic pontine gliomas. Neuro Oncol 2011;13:212–22.
36. Lockwood WW, Chari R, Chi B, Lam WL. Recent advances in array comparative genomic hybridization technologies and their applications in human genetics. Eur J Hum Genet 2006;14:139–48.
37. Brown J, Bothma H, Veale R, Willem P. Genomic imbalances in esophageal carcinoma cell lines involve Wnt pathway genes. World J Gastroenterol 2011;17:2909–23.
38. Ambatipudi S, Gerstung M, Gowda R, Pai P, Borges AM, Schaffer AA, et al. Genomic profiling of advanced-stage oral cancers reveals chromosome 11q alterations as markers of poor clinical outcome. PLoS ONE 2011;6:e17250.
39. Dai Z, Zhu WG, Morrison CD, Brena RM, Smiraglia DJ, Raval A, et al. A comprehensive search for DNA amplification in lung cancer identifies inhibitors of apoptosis cIAP1 and cIAP2 as candidate oncogenes. Hum Mol Genet 2003;12:791–801.
40. Swords RT, Kelly KR, Smith PG, Garnsey JJ, Mahalingam D, Medina E, et al. Inhibition of Nedd8-activating enzyme: a novel approach for the treatment of acute myeloid leukemia. Blood. 2010. 115:3796-800.
41. Chairatvit K, Ngamkitidechakul C. Control of cell proliferation via elevated Nedd8 conjugation in oral squamous cell carcinoma. Mol Cell Biochem. 2007. 306(1-2):163-9.
42. Milhollen MA, Traore T, Adams-Duffy J, Thomas MP, Berger AJ, Dang L, et al. MLN4924, a Nedd8-activating enzyme inhibitor, is active in diffuse large B-cell lymphoma models: rationale for treatment of NF-B-dependent lymphoma. Blood. 2010. 116:1515-23.
43. Li L, et al. Overactivated neddylation pathway as a therapeutic target in lung cancer. J Natl Cancer Inst. 2014. May 22;106(6):dju083.
44. Boeckx C, Baay M, Wouters A, Specenier P, Vermorken JB, Peeters M, Lardon F. Anti-epidermal growth factor therapy in head and neck squamous cell carcinoma: focus on potential molecular mechanisms of drug resistance. Oncologist. 2013. 18(7): 850-64.

Chapter 2

SCCRO (DCUN1D1) is an essential component of the E3 complex for neddylation

C.C. Bommeljé*, A.Y. Kim*, B.E. Lee, Y. Yonekawa, L. Choi, L.G. Morris, R. Ryan, A. Kaufman, B.Hao, Y. Ramanathan, B. Singh

*These authors contributed equally to this work

J. Biol. Chem, 2008 Nov 28; 283(48):33211-20

Abstract

Covalent modification of cullins by the ubiquitin-like protein Nedd8 (neddylation) promotes protein ubiquitination by fostering the assembly of cullin-RING ligase (CRL) E3 complexes. Like ubiquitination, neddylation results from an enzymatic cascade involving the sequential activity of a dedicated E1 (APPBP1/Uba3), E2 (Ubc12) and an ill-defined E3. We show that SCCRO (a.k.a. DCUN1D1) binds to the components of neddylation pathway (Cullin-ROC1, Ubc12, and CAND1) and augments but is not required for cullin neddylation in reactions using purified recombinant proteins. We also show that SCCRO recruits Ubc12~Nedd8 to the CAND1-Cul1-ROC1 complex, but that this is not sufficient to dissociate CAND1 or overcome its inhibitory effects on cullin neddylation in purified protein assays. In contrast to findings in cellular systems, we show that SCCRO and CAND1 can bind to the neddylated Cul1-ROC1 complex in assays using purified recombinant proteins. Although neddylated (not unneddylated) Cul1-ROC1 is released from CAND1 upon incubation with testis lysate from SCCRO$^{+/+}$ mice, the addition of recombinant SCCRO is required to achieve the same results in lysate from SCCRO$^{-/-}$ mice. Combined, these results suggest that SCCRO is an important component of the neddylation E3 complex that functions to recruit charged E2 and is involved in the release of the inhibitory effects of CAND1 on CRL E3 complex assembly and activity.

Introduction

Post-translational modification of proteins by ubiquitin (Ub) regulates diverse cellular functions including protein turnover, differentiation, apoptosis, cell cycle and transcription (1-5). Given its essential role, ubiquitination is a highly regulated process that involves the sequential action of three enzymes termed as E1, E2 and E3. In this enzymatic cascade, E1 initiates the process by forming a high energy thioester bond with Ub in an ATP coupled reaction. The Ub is then transferred to E2 as a thioester intermediate. Finally, E3s serve as the targeting arm in the ubiquitination process mediating the transfer of Ub from E2 to the target protein to create an isopeptide bond between the c-terminal glycine in Ub and a lysine residue on the substrate protein. Once attached, the Ub itself can be modified to generate poly-ubiquitin chains on the target protein (6). The signal initiated by ubiquitination is influenced by the chain length and the residue on the Ub to which the chain is attached. Poly-ubiquitination promotes the translocation to the 26S proteosome for degradation. Other functional effects of mono- and poly-ubiquitination include protein translocation, interaction and activation.

Although there is only one known E1 (except in plants) and relatively few E2s, E3s exist in multiple forms to allow for specific protein targeting (6). In general, E3s are modular multiprotein complexes that can be divided into two broad categories based on the presence of either a HECT (homologous to E6-AP carboxy terminus) or RING (Really Interesting New Gene) finger domain containing protein at their core. While HECT E3s form a thioester intermediate with the Ub before its transfer, RING containing complexes serve as scaffolds to facilitate the direct transfer of Ub from E2 to the target protein.

Cullin RING ligases (CRLs) constitute the largest class of E3s in mammals (7,8). All CRLs are anchored by cullins, a highly conserved protein family with 7 known isoforms in humans (Cul1, Cul2, Cul3, Cul4a, Cul4b, Cul5, and Cul7). A small RING protein (ROC1) and a variable substrate recognition subunit bind to the cullin core to form the CRL complex. The SCF (SKP1 cullin1 F-box) complex is the prototypic CRL E3 complex and is made up of ROC1 bound to the C-terminus and SKP1 adaptor protein bound to the N-terminus of Cul1. SKP1 in turn binds to a host of different F-box containing proteins to confer target specificity and ROC1 binds to E2 to form the catalytic core of the SCF complex.

Assembly of CRL complexes serves as a key regulatory step for ubiquitination. Cullins normally exist as part of two mutually exclusive complexes in cells. The majority of cullins are in complex with CAND1 (Cullin Associated Nedd8 Dissociated-1) which sterically inhibits assembly of CRL complexes. The covalent modification of cullins with the ubiquitin like protein (Ublp) Nedd8, in a process termed neddylation, dissociates CAND1 and promotes assembly of CRL complexes (9-12). In addition, cullin neddylation also enhances CRL activity through the recruitment of ubiquitin E2s to the complex and possible facilitation of cullin heterodimer formation (13-15). Conversely, deneddylation of cullins, principally by the COP9 signalosome, promotes dissociation

of CRL complexes and binding to CAND1. Several studies suggest that cycling of neddylation and deneddylation is required for normal CRL function. (8,16,17). Neddylation occurs by mechanisms analogous to Ub or Ublp conjugation, involving the sequential activity of a dedicated E1, E2 and E3. While APPBP1/Uba3 functions as the E1 and Ubc12 as the E2, the precise components of the neddylation E3 remain to be established. Using a positional cloning strategy, we identified *SCCRO* (Squamous Cell Carcinoma Related Oncogene) within a recurrent amplification peak at 3q26.3 in squamous cell carcinomas (18). Here we show that SCCRO interacts with known cullin isoforms as well as ROC1, Ubc12 and CAND1. SCCRO preferentially binds to Ubc12~Nedd8 thioester and augments cullin neddylation in both lysate and purified systems. Although SCCRO is not essential in a purified system, lack of neddylation in extracts made from *SCCRO*$^{-/-}$ mice suggest that it plays an important role *in vivo*. Details of the *SCCRO* knock-out mouse construction and characterization will be published elsewhere (Kaufman et. al., manuscript in preparation). Although purified recombinant SCCRO on its own does not overcome CAND1 inhibition of cullin neddylation, lysate from *SCCRO*$^{+/+}$ mice and not *SCCRO*$^{-/-}$ mice could dissociate CAND1. These findings suggest that SCCRO plays an essential role in neddylation and supports its inclusion as a component of the E3 complex for neddylation.

Experimental procedures

Alignment and sequence analyses

Database and Blast searches were carried out at NCBI (http://www.ncbi.nlm.nih.gov). Multiple sequence alignments were performed using the ClustalW program.

Reagents

All constructs were generated by standard PCR-ligation based methods and verified by automated sequencing. Proteins were expressed as GST fusions in *E. coli* and induced overnight at 18°C with the addition of 1 mM IPTG, purified by passing through Glutathione Sepharose 4B beads (GE Healthcare, WI) followed by thrombin cleavage where required. Cul1-ROC1 was expressed and purified from *E. coli* essentially as described (19). APPBP1/Uba3, Ubc12 and Nedd8 were obtained from a commercial source (Boston Biochem, MA).

cDNAs for mammalian transfection were cloned into pUSEamp or pCMV-HA vector (Clontech, DE). Anti-SCCRO RNAi, and scrambled RNAi were generated, validated and used as previously described (18). Transfection was carried out with Lipofectamine 2000 (Invitrogen, CA) or FuGene (Roche, NJ) using manufacturer's specifications.

All cell lines used in this study were obtained from ATCC (American Type Culture Collection, Rockville, MD) and grown at 37°C in 5% CO_2. HeLa cells were maintained in minimal essential media (MEM) supplemented with 10% fetal calf serum (FCS) containing antibiotics.

The following antibodies were used in this study: anti-Cul1 (Zymed, CA), anti-Cul2 (Abcam, MA), anti-Cul3 (BD Biosciences, CA), anti-Cul4, anti-Cul5 (Santa Cruz, CA), anti-ROC1 (Abcam, MA), anti-SKP1 (Abnova, Taiwan), anti-Ubc12 (Rockland, MA), anti-Nedd8 (Invitrogen, CA), anti-CAND1 (BD Biosciences, CA), anti-α-tubulin (CalBiochem, WI), anti-HA (Abcam, MA), and Anti-Flag (Sigma, MO). Anti-SCCRO (rabbit polyclonal) antibody was produced and utilized as described previously (Sarkaria et al., 2006). Secondary antibodies conjugated to horseradish peroxidase (Santa Cruz, CA) were used according to the manufacturers' specifications.

GST pull down assay

GST tagged proteins were bound to Glutathione Sepharose beads by gentle rocking at 4°C for 30 minutes. The beads were washed three times with EBC buffer (50 mM Tris-HCl pH (7.5), 2.5 mM $MgCl_2$, 150 mM NaCl, and 0.5% NP40) at 20x bead volume. The beads were incubated with 500 µg of HeLa cell lysate or purified proteins as indicated at 4°C for 1 hour followed by three washes with EBC buffer at 20x bead volume. Bound proteins were eluted by the addition of 6x Lamelli buffer, resolved on SDS-PAGE and analyzed by western blot. For mass spectrometric analysis, the resolved proteins were stained with Coomassie R250. Bands were excised and subjected to matrix-assisted laser-desorption/ ionization reflectron time-of-flight (MALDI-reTOF) mass spectrometric analysis.

Immunoprecipitations

Immunoprecipitations were performed essentially as described earlier (18). In brief, all cells were lysed using mammalian cell lysis buffer (20 mM Tris-HCl (pH 7.5), 150 mM NaCl, 1 mM EDTA, 1 mM EGTA, 1% Triton X-100, 2.5 mM sodium pyrophosphate, 1 mM β-glycerophosphate, 1 mM Na_3VO_4, 1 µg/ml leupeptin (Cell Signaling, MA). One mg of cell lysate was incubated with HA antibody bound to agarose beads by gentle rocking at 4°C for 2 hours. The same wash and detection sequence was used as for the GST pull down assay.

Thioester reactions

Reactions were performed at room temperature in a buffer (50 mM Tris-HCl (pH 7.6), 50 mM NaCl, 10 mM $MgCl_2$, 0.5 mM DTT) with 4 mM ATP, 80 nM APPBP1/Uba3, 800 nM Ubc12 and 9 µM Nedd8. Reactions were quenched with 3x non-reducing Lamelli buffer (without DTT) and the presence of Ubc12~Nedd8 thioester complexes were verified by western blot for Ubc12 and/or Nedd8 in the presence and absence of 50 mM DTT. Time course experiments showed that incubation times greater than 10 minutes resulted in the formation of a small fraction of Nedd8 bound to Ubc12 that was not reducible by DTT. Accordingly, all thioester reactions were carried out for 10 minutes or less. For use in binding assays, the reaction mix was quenched with the addition of EDTA to a final concentration of 50 mM and purified on a G-50 micro spin desalting column. For competition experiments, reaction conditions were identical except for the addition of a gradient of free Ubc12 to the purified

thioester reaction mix. For thioester reaction involving the competition between E1 and SCCRO for Ubc12, all components were added simultaneously and loading of Nedd8 to Ubc12 was assessed by western blotting. Reaction conditions for HeLa transfected with HA-Ubc12 or HA-Ubc12Δ1-26 was the same, except a longer incubation time (30 min) was employed for HA-Ubc12Δ1-26.

In vitro neddylation

The source of Cullin-ROC1 substrate for *in vitro* neddylation reactions was either HeLa lysates or bacterially derived (see above). For reactions using HeLa derived Cullin-ROC1 complexes, 100 µg of lysates (estimated Cul1 concentration is 20 fmol) were added to reactions containing 0.2–2 pmol of APPBP1/Uba3, 1–12.5 pmol Ubc12, and 150 pmol of cold Nedd8 or ^{32}P-Nedd8, in neddylation buffer (100 mM Tris-HCl, pH 7.8, 150 mM NaCl, 2.5 mM DTT, and 5 mM $MgCl_2$). Reactions were incubated at 30°C and stopped with the addition of 6x Lamelli buffer. Reactions with bacterially derived substrate were performed at 30°C in neddylation buffer containing 20 nM Cul1-ROC1, 4 mM ATP, 10 nM of APPBP1/Uba3, 20 nM Ubc12, and 0.9 µM of Nedd8. In reactions containing CAND1, Cul1-ROC1 was preincubated with the indicated amounts of CAND1 for 15 min at room temperature. Proteins were resolved on an SDS-PAGE and subjected to autoradiography and/or western blot analysis. For quantification, western blots were imaged using MultiImage Light Cabinet and quantified using AlphaEaseFC v3.2.1 (Alpha Innotech Corp., CA).

Assay for binding to neddylated and unneddylated cullins

Neddylation reactions were performed on purified Cul1-ROC1 at 30°C for the indicated time. The reactions were stopped by the addition of EDTA to a final concentration of 50 mM and the products purified on a G-50 micro spin desalting column. A small aliquot of the flow-through was subjected to western blot analysis for Cul1 to establish the level of cullin neddylation. The remaining flow-through was incubated with GST-SCCRO and/or GST-CAND1 (at limiting concentrations) at room temperature for 20 minutes, followed by the addition of Glutathione Sepharose beads and incubation with gentle rocking at 4°C for 45 minutes. After three 20x bead volume washes with EBC wash buffer, 6x Lamelli buffer was added to the beads and bound proteins were resolved on an SDS-PAGE and analyzed by western blot for Cul1. To assess the effects of lysate on release of cullins from CAND1, neddylated or unneddylated Cul1-ROC1 was incubated with GST-CAND1 at room temperature for 20 minutes and rocked at 4°C for 30 minutes. SCCRO, SCCRO-D241N and/or testis lysate from *SCCRO*$^{+/+}$ or *SCCRO*$^{-/-}$ mice was added onto the beads and rotated at 4°C for 1 hour, followed by three 20x bead volume washes with EBC buffer. 6x Lamelli buffer was added to the beads and bound proteins were analyzed by western blot for Cul1.

Results

SCCRO interacts with components of the neddylation pathway

We identified SCCRO by fluorescent in situ hybridization (FISH)-based fine resolution mapping of a recurrent amplification at 3q26.3 that is present in multiple human cancers (18,20-22). As a step towards understanding the molecular function of SCCRO, we sought to identify interacting proteins. GST-SCCRO pull down from HeLa lysates identified two unique bands relative to GST alone (Fig. 1A). These bands were excised and subjected to mass spectrometric analysis (MALDI-ReTOF) identifying CAND1 and members of the cullin family of proteins (Cul1, Cul2, Cul3, and Cul4) as putative binding partners (Fig. 1A). We confirmed these interactions by GST-SCCRO pull down from HeLa lysates followed by western blot for each of the identified proteins. In addition, we found that SCCRO also binds to Cul5 and ROC1 (Fig. 1B). GST pulldown assays using purified proteins showed that SCCRO directly binds to ROC1 consistent with findings in yeast (data not shown) (23). Since they are soluble only as a complex with ROC1, we could not assess if SCCRO can also bind to cullins directly.

Given the established role of CAND1 and the cullin family of proteins in neddylation, we assessed for binding to other proteins in the neddylation pathway, including Nedd8, APPBP1/Uba3, and Ubc12 and found that SCCRO interacts with Ubc12 (Fig. 1B, lane 2). The co-immunoprecipitation of SCCRO with each of its putative binding partners in HA-SCCRO transfected HeLa cells confirmed that the observed interactions occur in cells (Fig.1C, lane 2). SCCRO does not bind to Ubc9 (an E2 for sumolation), SKP1 or SKP2, suggesting that its interactions are specific to the components of the neddylation pathway (data not shown). To confirm these interactions occur in vivo, we performed immunoprecipitation experiments using a SCCRO monoclonal antibody that is highly sensitive and specific for SCCRO. Western blots on the immunoprecipitates showed that SCCRO binds to Cul1, ROC1, and CAND1 (Fig.1D, left panel). Similarly, reciprocal immunoprecipitation for ROC1 followed by Western blotting confirmed the interaction with SCCRO as well as CAND1, Cul1 and SKP2 (Fig. 1D, right panel). While SCCRO did not interact with SKP2, ROC1 bound, as expected.

To map binding domains we created a series of SCCRO deletions and point mutants as GST fusions, including those involving the N-terminal UBA (aa 8-45) and C-terminal DCUN1 domain (aa 60-259) (Fig. 1B,C, and E, and supplemental Fig.2). Whereas the N-terminal deletions (SCCROΔ1-33, SCCROΔ1-45, and SCCROΔ1-82) retained binding, C-terminal deletions (SCCROΔ151-259 and SCCROΔ210-259) lost detectable binding to CAND1, Cul-ROC1 and Ubc12, suggesting that these proteins interact with the C-terminal 49 amino acids within the DCUN1 domain of SCCRO (Fig. 1B and C, lane 3 and 4, and E). Point mutations were generated in highly conserved residues within the C-terminal region of SCCRO and tested for binding to cullins, CAND1 and Ubc12. SCCRO-D241N lost detectable binding to CAND1 and Cul-ROC1 complex, but not to Ubc12 suggesting that Ubc12 and CAND1/Cul-ROC1 bind to different regions within the C-terminus of SCCRO (Fig. 1B, lane 6). Our findings using a biochemical approach are consistent with results from structure based analyses of C. elegans and S.cerevisiae DCN-1/Dcn1p where mutations in a similar residue (D259) also resulted in loss of binding to cullin-ROC1 (23-25).

Figure 1. SCCRO Interacts with Cullins, CAND1 and Ubc12.

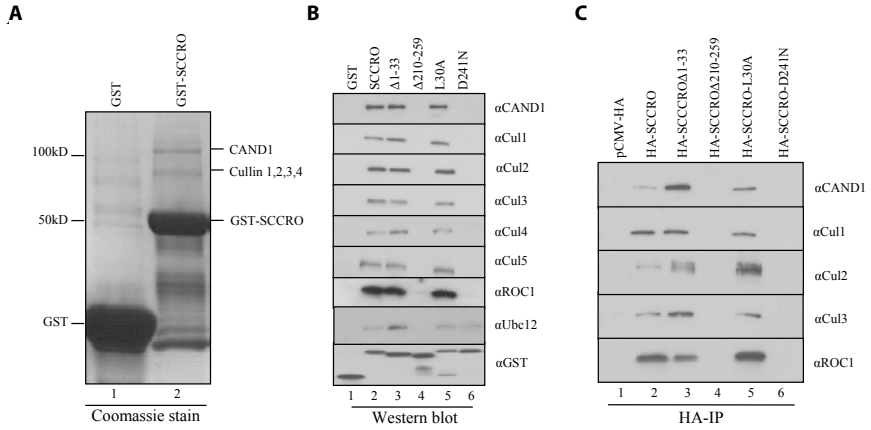

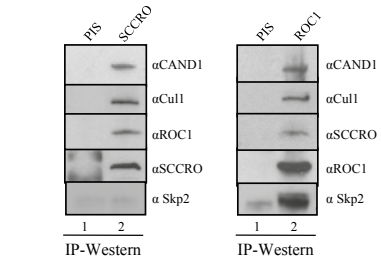

E

SCCRO Mutants	Cul-ROC1	Ubc12	CAND1
Wild type	+	+	+
Δ1-33	+	+	+
Δ1-45	+	+	+
Δ1-82	+	+	+
Δ151-259	-	-	-
Δ210-259	-	-	-
L30A	+	+	+
D218N	+	+	+
D231N	+	+	+
E232Q	+	+	+
D231N, E232Q	+	+	+
G234E	+	+	+
V238A	+	+	+
I240F	+	+	+
D241N	-	+	-
D242A	+	+	+

(**A**), Coomassie-stained SDS-PAGE gel showing GST (*lane 1*) and GST-SCCRO (*lane 2*) pulldown products from HeLa extracts. Unique bands from GST-SCCRO pulldown assays were excised and subjected to tandem mass spectroscopy analysis (MALDI-ReTOF) revealing the 120-kDa band as CAND1 and the 80–90-kDa bands as cullins 1–4. (**B**), Western blot on the pulldown products of GST-SCCRO and GST-SCCRO mutants from HeLa extracts probed with indicated antibodies showing SCCRO binds to CAND1, cullins 1–5, ROC1, and Ubc12 (*lane 2*). The C-terminal (SCCROΔ210–259; *lane 4*) but not the N-terminal deletion of SCCRO (SCCROΔ1–33; *lane 3*) or the N-terminal point mutant of SCCRO (SCCRO_L30A; *lane 5)* lost interaction with the Cullin-ROC1, CAND1, and Ubc12. SCCRO-D241N lost interaction with the Cullin-ROC1 and CAND1 while retaining binding to Ubc12 (*lane 6*). The level of the various GST-tagged proteins used in the pulldown experiment was confirmed by probing a Western blot with anti-GST antibody (*bottom panel*). (**C**), Western blot showing products from an HA immunoprecipitation (*IP*) of lysates from HeLa cells transfected pCMV-HA-SCCRO or selected SCCRO deletions/mutants probed with indicated antibodies showing SCCRO maintains binding to neddylation components *in vivo* (*lane 2*). SCCROΔ210–259 (*lane 4*) and SCCRO-D241N (*lane 6*) lose binding to cullins, ROC1, and CAND1. (**D**), Western blot on immunoprecipitates from HeLa extract prepared with anti- SCCRO (*left panel*; *lane 2*) anti-ROC1 (*right panel*; *lane 2*) or preimmune serum (*PIS*; *lane 1*) probed with indicated antibodies showing *in vivo* interaction between native SCCRO and CAND1, Cul1, and ROC1 but not SKP2 (*left panel*), whereas ROC1 binds to CAND1, Cul1, SCCRO, and SKP2 (*right panel*). (**E**), summary of results from pulldown assays using GST-SCCRO or SCCRO deletions/mutations showing binding of CAND1, Cul-ROC1, and Ubc12 requires C-terminal 50 amino acids. SCCRO-D241N loses binding to CAND1 and Cul1-ROC1 but retains binding to Ubc12.

SCCRO augments cullin neddylation

Recently it was reported that DCN-1/Dcn1p, the C. elegans and S.cerevisiae orthologs of SCCRO, facilitate cullin neddylation (23-25). To test if the human ortholog also promotes cullin neddylation, we performed *in vitro* neddylation assays in the presence of varying concentrations of SCCRO. Reactions containing Nedd8, recombinant APPBP/Uba3 (E1), Ubc12 (E2), ATP and whole cell lysate from HeLa cells (as a source of cullin-ROC1 substrate) showed a dose dependent increase in cullin neddylation with SCCRO (Fig. 2A and B). A time course reaction showed that SCCRO also enhances the rate of cullin neddylation (Fig. 2C and D).

To determine if binding is required for the observed functional effects, we supplemented neddylation reactions with SCCRO or selected SCCRO deletions. Whereas the N-terminal deletion (SCCROΔ1-33) enhanced the rate of Cul3 neddylation to levels similar to SCCRO, the C-terminal deletion (SCCROΔ210-259) that loses binding to Ubc12 and Cul-ROC1 failed to augment cullin neddylation beyond basal levels (Fig. 2C and D). These findings suggest that the effects of SCCRO on cullin neddylation require its interaction with Cul-ROC1 and/or Ubc12 and implicate it is a component of the neddylation E3.

Furthermore, cullin neddylation increased with transient expression of HA-SCCRO and decreased with knockdown of SCCRO by RNAi (Fig. 3B and D). The decrease in cullin neddylation as a result of SCCRO protein knockdown by RNAi was rescued by the addition of recombinant SCCRO to the lysate (Fig. 3D).

SCCRO is not required for neddylation *in vitro*

Several *in vitro* studies suggest that ROC1 functions as an E3 ligase and is sufficient to promote neddylation by itself (26-29). To determine the effect of SCCRO on cullin neddylation, we performed a time course reaction using recombinant purified components (E1, E2, ATP, Nedd8 and Cul1-ROC1). Although Cul1 neddylation occurred in its absence (Fig. 2F, lanes 2,3,4), addition of SCCRO enhanced the rate of cullin neddylation (Fig. 2F, compare lanes 2,3,4 with 6,7,8). This is consistent with published reports showing cullin neddylation occurs in the absence of SCCRO *in vitro* (26,28). However, neddylation is absent in testis lysates from SCCRO knockout mice (Fig. 3E, right panel) (Kaufman et al., unpublished data). Similar findings are also reported in C. elegans and S. cerevisiae where DCN-1/Dcn1p knockouts also lose neddylation activity (24). Combined these findings suggest that although SCCRO is not required for neddylation *in vitro*, it is essential *in vivo*.

Figure 2. SCCRO augments Cullin neddylation *in vitro*.

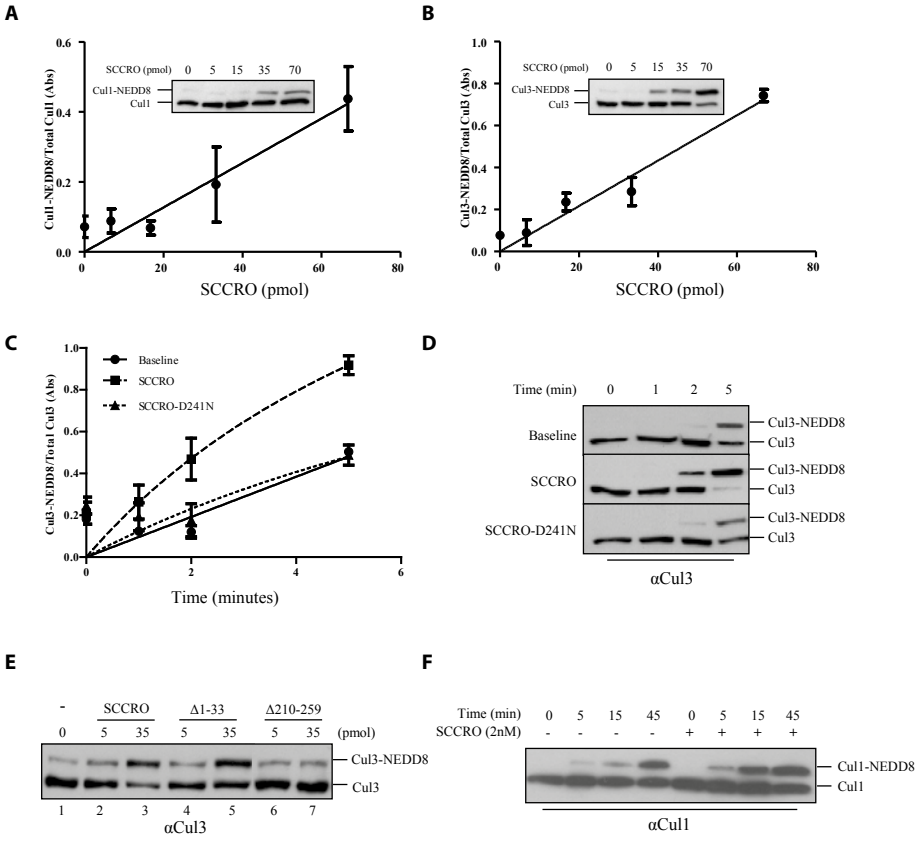

(**A**) and (**B**), plot showing levels of Cul1 (**A**) and Cul3 (**B**) (mean ± S.E.) neddylation quantified by densitometry of Western blots from three independent *in vitro* neddylation reactions containing HeLa extract (as a source of cullin substrate), E1, E2, ATP, Nedd8, and a concentration gradient of SCCRO. The fraction of neddylated Cul1 (**A**) and Cul3 (**B**) increased with increasing SCCRO concentration. Representative Western blots from *in vitro* neddylation reactions are shown as *insets*. (**C**), a plot showing the fraction of neddylated Cul3 (means ± S.E.) against time in minutes from three independent neddylation assays. SCCRO but not SCCRO-D241N enhances neddylation efficiency. (**D**), representative Western blot from C showing Cul3 neddylation in presence of SCCRO or SCCRO-D241N. (**E**), results from *in vitro* neddylation reaction supplemented with SCCRO (*lanes 2* and *3*) or SCCRO deletions showing SCCROΔ1–33 (*lanes 4* and *5*) but not the C-terminal deletion SCCROΔ210–259 (*lanes 6* and *7*) retained neddylation activity. (**F**), Western blot for Cul1 from a time course *in vitro* reaction containing purified, bacterially expressed Cul1-ROC1 showing SCCRO enhances efficiency but is not required for neddylation.

Figure 3. SCCRO augments cullin neddylation *in vivo*.

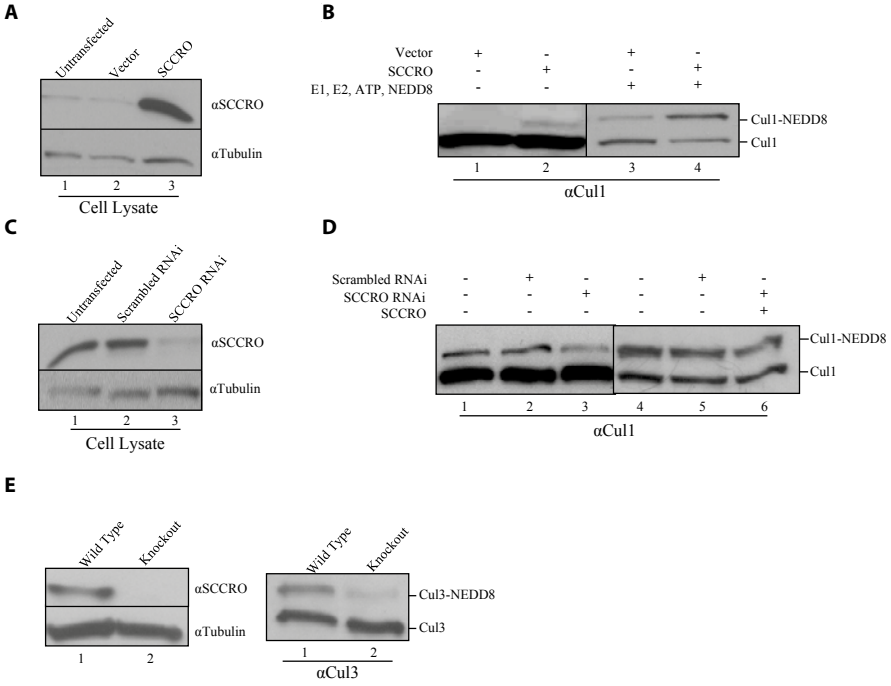

(**A**), Western blot on HeLa lysates showing elevated SCCRO protein levels in *SCCRO* transfected (*lane 3*) relative to untransfected (*lane 1*) or vector-transfected (*lane2*) cells. (**B**), Western blot showing a higher level of neddylated cullins in lysates from *SCCRO* transfected (*lane 2*) relative to vector-transfected cells (*lane 1*). Western blot on HeLa lysates from B after addition of neddylation components (E1, E2, Nedd8, and ATP) showing increased neddylated Cul1 levels in *SCCRO*-transfected (*lane 4*) relative to empty vector (*lane 3*)-transfected cells. (**C**), Western blot on lysates from SCC15 cells showing a decrease in SCCRO protein levels in cells transfected with specific RNAi against *SCCRO* (*lane 3*) relative to untransfected (*lane 1*) or scrambled RNAi-transfected cells (*lane 2*). (**D**), *in vitro* neddylation reaction of the same lysates showing decreased Cul1 neddylation in *SCCRO*-RNAi transfected (*lane 3*) compared with untransfected (*lane 1*) or scrambled RNAi (*lane 2*)-transfected cells. The addition of recombinant SCCRO to the lysate from SCCRO RNAi-transfected SCC15 cells (*lane 6*) recovers Cul1 neddylation to levels observed in controls (*lanes 4* and *5*). (**E**), Western blot showing the absence of detectable SCCRO protein in testis lysates from *SCCRO-/-* mice (*left panel*, *lane 2*) in contrast to a *SCCRO-/-* (*left panel*, *lane 1*) litter mate control. The same lysates were subjected to neddylation assays (*right panel*) showing a significant decrease in neddylated Cul3 levels in *SCCRO-/-* mice (*lane 2*).

SCCRO preferentially interacts with Ubc12 thioester intermediate

The mechanisms and reaction processivity involved in the conjugation of Ub and Ublp are highly conserved. A mutually exclusive interaction between E1 and E3 with E2 is a key aspect in maintaining reaction processivity. Accordingly, an E2 conjugating enzyme must dissociate from its cognate E1 before binding to E3 (30). One way this is achieved is the differential affinity of E1 and E3 for free and conjugated E2. Several studies show that the affinity of E2 for E1 (and E3 to E2)

is higher when the latter is loaded with Ub or Ublp (13,31,32). If SCCRO functions as a component of the neddylation E3, it should have greater affinity for Ubc12~Nedd8 thioester over free Ubc12. GST-SCCRO pull down from a Ubc12 thioester reaction followed by western blot for Ubc12 showed that SCCRO preferentially binds to Ubc12~Nedd8 thioester even in the presence of large excess of free Ubc12 (Fig. 4A, lane1,3). To quantify the differences in binding affinity of SCCRO for Ubc12 and Ubc12~Nedd8, competition experiments were performed. GST-SCCRO pull downs from a mixture containing Ubc12~Nedd8 (generated and purified as discussed in the experimental procedures section) and a gradient of free Ubc12 followed by westernblot showed that SCCRO preferentially binds to Ubc12~Nedd8 even in the presence of ≥ 20-fold excess of free Ubc12 (Fig. 4B, lane 3). Similarly, when lysates from HA-SCCRO transfected HeLa cells that were subjected to *in vitro* thioester reaction (Fig. 4C, top and middle panel) were immunoprecipitated with anti-HA antibody and probed for Ubc12, preferential binding of SCCRO to Ubc12~Nedd8 was detected (Fig. 4C, bottom panel). The preferential interaction with Ubc12~Nedd8 thioester over free Ubc12 suggests that SCCRO conforms to the conserved processivity paradigm of Ub and Ublp pathway and supports its role as a component of the E3 complex for neddylation.

SCCRO interacts with the unique N-terminus of Ubc12

A second mechanism ensuring processivity in Ub and Ublp conjugation results from the presence of overlapping binding sites on E2 for E1 and E3, making their interactions mutually exclusive (30). Like all E2s, Ubc12 contains a ~150 residue catalytic core domain. However, it is distinguished from other E2s by the presence of a unique N-terminal extension (33). Studies have shown that both the N-terminal extension and the catalytic core domain of Ubc12 are involved in its interaction with the Nedd8~E1 (33). ROC1 binds to the catalytic core domain of Ubc12, with no known role for the N-terminal extension in the Ubc12-ROC1 interaction (11,34). To determine if SCCRO binds to the unique N-terminal region of Ubc12 or to the catalytic core domain, we performed HA-immunoprecipitation on lysates from HeLa cells transfected with either HA-Ubc12 or HA-Ubc12Δ1-26 (N-terminal deleted Ubc12) and probed for SCCRO on a western blot. Since SCCRO preferentially interacts with the Ubc12~Nedd8 thioester, we performed a thioester reaction on the lysate to generate Nedd8 loaded HA-Ubc12 and HA-Ubc12Δ1-26 prior to immunoprecipitation (Fig. 4D, top). As the efficiency of thioester formation is lower for Ubc12Δ1-26 deletion, we allowed the reaction adequate time to run to completion so as to generate an equivalent amount of the Nedd8 thioester. Even though longer incubation time was required to generate HA-Ubc12Δ1-26~Nedd8, this interaction was reducible with DTT, suggesting the presence of a thioester bond (data not shown). Despite equal loading of Nedd8 to Ubc12 and Ubc12Δ1-26 (Fig. 4D, top), only HA-Ubc12 pulled down SCCRO (Fig. 4D, middle). However, ROC1, which is known to interact with the conserved core domain of Ubc12, bound to both HA-Ubc12 and HA-Ubc12Δ1-26 (Fig. 4D, bottom). These observations suggest that the binding site of SCCRO on Ubc12 (E2) overlaps with the Nedd8~E1. Moreover, unlike ROC1 which interacts with the conserved core domain of Ubc12

(E2), SCCRO interacts with its unique N-terminal extension, raising the possibility that SCCRO-Ubc12 interaction is specific to the neddylation pathway. This is further strengthened by lack of interaction between SCCRO and other E2s (Ubc9) in GST pull down assays (data not shown). Taken together, these observations suggest that SCCRO conforms to the conserved reaction processivity paradigms, further supporting its candidacy as a component of the E3 complex.

Figure 4. SCCRO interacts with the unique N terminus of Ubc12~Nedd8.

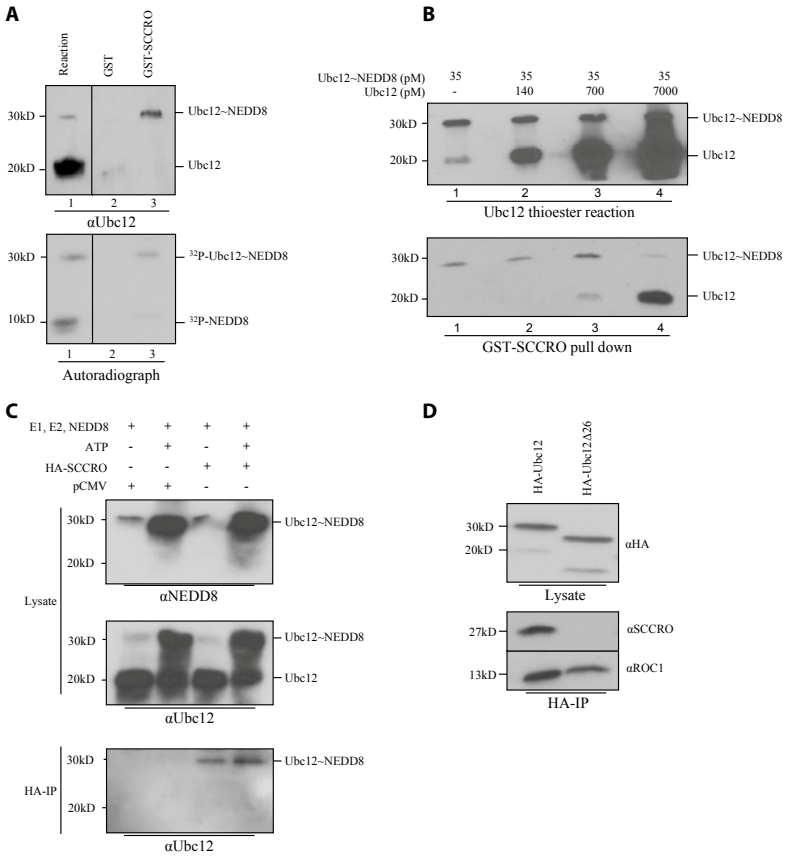

(**A**), Western blot for Ubc12 after a thioester reaction showing generation of Ubc12~Nedd8 thioester (*top panel*, *lane 1*, *upper band*). GST (*lane 2*) and GST-SCCRO (*lane 3*) pulldown on the same reaction products showing preferential interaction of SCCRO with Ubc12~Nedd8 despite a large excess of free Ubc12 (*top panel*, *lane 3*). Autoradiograph of products from a thioester reaction containing E1, E2, ATP, and 32P-labeled PK-Nedd8 showing Ubc12~Nedd8 (*bottom panel*, *lane 1*, *upper band*) and free Nedd8 (*bottom panel*, *lane 1*, *lower band*). GST (*lane 2*) or GST-SCCRO (*lane 3*) pulldown assays on thioester reaction components showing SCCRO binds to Ubc12~Nedd8 but not to free Nedd8 (*bottom panel*, *lane 3*) (**B**), Western blot showing levels of Ubc12~Nedd8 and Ubc12 from a thioester reaction supplemented with varying concentrations of free Ubc12 after quenching with EDTA (see "Experimental Procedures"; *top panel*). The same reactions were subjected to pulldown assays using limiting amounts of GST-SCCRO (70 pM) showing preferential binding to Ubc12~Nedd8 even in the presence of 20-fold excess of free Ubc12 (*bottom panel*).

(**C**), Western blots for Nedd8 (*top panel*) and Ubc12 (*middle panel*) on thioester reactions with and without ATP in lysates from HeLa cells transfected with pCMV or pCMV-SCCRO showing lower levels of Ubc12~Nedd8 in reactions not containing ATP (compare *first* and *third lanes* with the *second* and *fourth lanes*).HAimmunoprecipitation of the same reaction mix showing preferential binding of SCCRO (in limiting concentrations) to Ubc12~Nedd8 (*bottom panel*, *third* and *fourth lanes*), even in the presence of a large excess of free Ubc12 (*bottom panel*, *third lane*).(**D**), Western blot forHAafter thioester reactions on HeLa cell lysates transfected with HA-Ubc12 or HA-Ubc12Δ26 showing equal amounts of Nedd8 thioester formation after 10 and 30 min of incubation, respectively. HA immunoprecipitation on the same reaction products followed by Western blot with the indicated antibody showing SCCRO interacts with full-length Ubc12~Nedd8 but not with Ubc12Δ26~Nedd8, whereas ROC1 interacts with both (*bottom right*).

SCCRO binds CAND1 only when it is in complex with Cul1-ROC1

Reflecting the increasing complexity of protein regulation, the neddylation pathway is also more complex in higher organisms. For example, in contrast to S. cerevisiae where CAND1 is absent, in higher organisms unneddylated cullin-ROC1 exists almost exclusively in complex with CAND1 (11,35,36). Binding to CAND1 inhibits cullin neddylation and subsequent ubiquitination E3 complex assembly. Once neddylated, cullin-ROC1 is released from CAND1 and forms active E3 ubiquitination complexes. Analysis of the crystal structure shows that CAND1 binds to Cul1-ROC1 in a head to tail arrangement burying the otherwise solvent exposed lysine residue on Cul1, making it inaccessible to the neddylation machinery. In contrast, a β-hairpin motif from CAND1 directly binds to two helices in Cul1 that are involved in its interaction with SKP1. In this arrangement, it is possible for neddylation of cullins to proceed if modifications expose the target lysine, while binding to SKP1 would require dissociation of CAND1.

Given that SCCRO interacts with Cul-ROC1 and CAND1, we aimed to determine if SCCRO binds to CAND1 directly or indirectly through its interaction with Cul-ROC1. To begin to define the steric interactions, we looked for the presence of SCCRO in exclusive complexes with either Cul1-ROC1 or CAND1 in cellular systems using gel filtration analyses. SCCRO was not found in fractions containing significant amounts of CAND1, Cul1 or ROC1, suggesting that the majority of endogenous cellular SCCRO is not stably associated with CAND1 or cullin-containing complexes, thereby limiting our ability to draw conclusions about the individual protein interactions (data not shown). GST-SCCRO pull down assays using purified proteins showed that CAND1 only interacts with SCCRO when in complex with Cul1-ROC1 (Fig. 5A, compare lanes 1 and 3). A deletion of CAND1 (CAND1Δ604-1230), which loses binding to Cul1-ROC1, does not interact with SCCRO (Fig. 5A, lane 4 and 5). In a reciprocal pull down assay, GST-CAND1 only pulls down SCCRO when the latter is in complex with Cul1-ROC1 (Fig. 5B, lane 3 and 4). These findings suggest that the interaction of SCCRO with CAND1 is mediated by Cul1-ROC1. Moreover, the binding stoichiometry between SCCRO and Cul1-ROC1 was not altered by the presence of CAND1 (data not shown). Given that, in cells, unneddylated cullins exist exclusively as ternary complexes with CAND1 and ROC1, and that SCCRO preferentially interacts with unneddylated cullins (see below), it is likely that SCCRO binds to the cullin-ROC1 complexes before they are released by CAND1. These observations raised the possibility that SCCRO may be involved in overcoming CAND1 inhibition of cullin neddylation.

Figure 5. SCCRO does not overcome the inhibitory effects of CAND1 on neddylation.

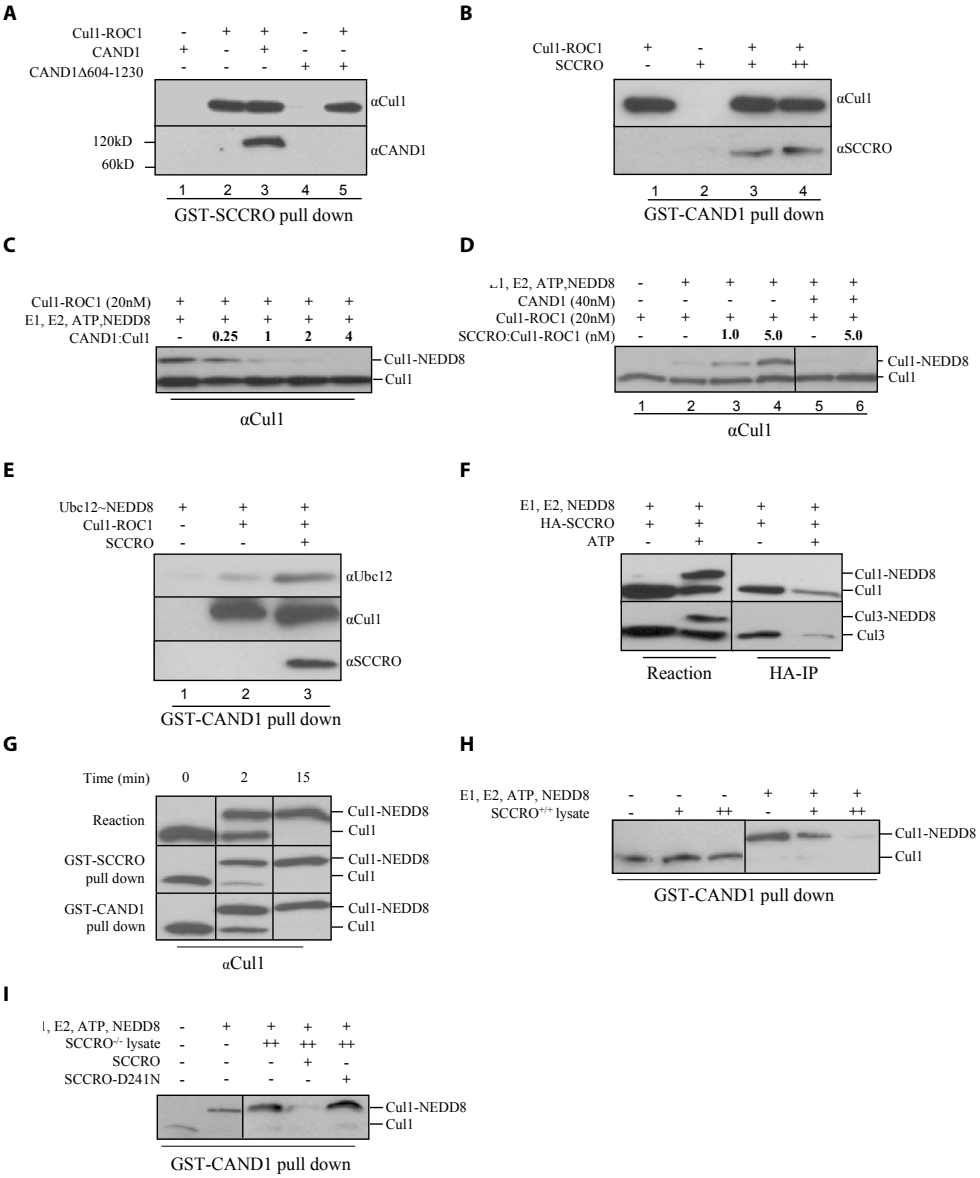

(**A**), Western blot on GST-SCCRO pulldown products after incubation with purified, bacterially expressed Cul1-ROC1 and CAND1 showing CAND1 is pulled down by SCCRO only when it is complexed with Cul1-ROC1 (*lanes 1* and *3*). A CAND1 deletion (CAND1Δ604–1230) that loses binding to cullins is not pulled down by SCCRO (*lane 4* and *5*). (**B**), Western blot from reciprocal GST-CAND1 pulldown assay showing interaction of CAND1 with SCCRO requires Cul1-ROC1 (*lanes 2–4*). (**C**), Western blot for Cul1 following *in vitro* neddylation reaction using

purified recombinant components showing complete inhibition of neddylation in the presence of 2-fold or higher molar excess of CAND1. (**D**), Western blot on products from an *in vitro* neddylation reaction confirming increasing Cul1 neddylation with increasing amounts of SCCRO (*lanes 2–4*). The addition of CAND1 inhibits Cul1 neddylation (*lane 5*), which is not rescued even by 5-fold molar excess of SCCRO (*lane 6*; same blot, excess lanes removed). (**E**), Western blot showing GST-CAND1 pulldown products after incubation with purified, bacterially expressed Cul1-ROC1, Ubc12~Nedd8, and SCCRO. CAND1 interacts with Ubc12~Nedd8 only when Cul1-ROC1 is present (*lanes 1* and *2*), and this interaction is enhanced by the presence of SCCRO (*lane 3*). (**F**), Western blot on lysates from HA-SCCRO-transfected HeLa cells subjected to neddylation reaction showing an increase in cullin neddylation with the addition of ATP (*lanes 1* and *2*). HA immunoprecipitation (*IP*) of the same reaction products showed SCCRO preferentially interacts with unneddylated cullins (*lanes 3* and *4*). (**G**), Western blot on products from an *in vitro* neddylation reaction using purified recombinant components showing an increase in the fraction of neddylated Cul1 with increasing reaction time (*top panel*). Western blot on the same reaction after GST-SCCRO (*middle panel*) and GST-CAND1 (*bottom panel*) pulldown assays showing that SCCRO and CAND1 interact with both free and neddylated cullins (same blot, excess lanes removed). (**H**), Western blot on products from pulldown assays after GST-CAND1 complexed with either Nedd8-Cul1-ROC1 or free Cul1-ROC1 was incubated with increasing amounts of testis lysate from SCCRO-/- mice showing release of Nedd8-Cul1-ROC1 but not unneddylated Cul1-ROC1. (**I**), Western blot on products from pulldown assays after GST-CAND1 complexed with either Nedd8-Cul1-ROC1 or free Cul1-ROC1 was incubated with increasing amounts of testis lysate from *SCCRO-/-* mice showing release of Cul1-ROC1-Nedd8 only with addition of SCCRO and not SCCRO-D241N (same blot, excess lanes removed).

SCCRO does not overcome inhibition of cullin neddylation by CAND1

Given the observed binding interactions, we wanted to determine if SCCRO can overcome the inhibitory effects of CAND1 on cullin neddylation. We confirmed previous findings that CAND1 inhibits cullin neddylation in an in vitro purified recombinant system (Fig. 5C) (12,35). To assess the ability of SCCRO to overcome CAND1 inhibition, we preincubated Cul1-ROC1 with the minimal concentration of CAND1 required to completely inhibit cullin neddylation. Addition of up to five-fold molar excess of SCCRO failed to overcome the inhibitory effects of CAND1 on cullin neddylation (Fig. 5D). To determine if the effects of CAND1 on cullin neddylation were related to recruitment of Ubc12~Nedd8, we performed pull down assays. We found CAND1-Cul1-ROC1 is able to bind to Ubc12~Nedd8. This binding is enhanced by the addition of SCCRO (Fig 5E, lane 3). However, assembly of these proteins was not sufficient to overcome CAND1 inhibition. As expected, this complex was not detected in HeLa lysates where its assembly should lead to efficient transfer of the Nedd8 to cullins and dissociation of CAND1 (data not shown). These observations suggest that SCCRO is not sufficient to overcome the inhibitory effects of CAND1 and raise the possibility of additional factors involved in CAND1 release.

Neddylated Cul1 can bind to CAND1 and SCCRO in vitro

To assess if SCCRO binding to Cul1-ROC1 is affected by neddylation, lysates from HeLa cells transfected with HA-SCCRO were subjected to *in vitro* neddylation reaction with and without ATP (Fig. 5F, left panel). Western blot analysis showed increased cullin neddylation in reactions containing ATP. When HA-immunoprecipitation was performed on these lysates, only unneddylated cullins were pulled down (Fig. 5F, right panel). In contrast, binding assays using purified proteins showed that both neddylated and unneddylated Cul1-ROC1 were pulled down by GST-SCCRO and GST-CAND1 (Fig. 5G). These results suggest that neddylation of cullins may not be sufficient by itself to dissociate CAND1. Since we could not detect any binding between neddylated cullins and CAND1 in lysates, a factor in the lysate may be required to release neddylated cullins. To address this issue, GST-CAND1 complexed with either neddylated or unneddylated Cul1-ROC1 was incubated with lysate. Incubation with HeLa lysate or $SCCRO^{+/+}$ mice testis lysate resulted in the dissociation of neddylated but not un-neddylated cullins from CAND1 (Fig. 5H). This dissociation was not due to competition with native cullin complexes, as these complexes were not detected on the GST-CAND1 pull down assays. In contrast, incubation with testis lysate from $SCCRO^{-/-}$ mice failed to dissociate GST-CAND1 from neddylated Cul1-ROC1. Addition of recombinant SCCRO but not SCCRO-D241N to the $SCCRO^{-/-}$ lysate allowed dissociation of neddylated Cul1-ROC1 from CAND1 (Fig. 5I). These data suggest that neddylated cullins are dissociated from CAND1 by a factor in lysate and that SCCRO may be required for this dissociation.

Discussion

Hershko and Ciechanover define ubiquitin ligases as enzymes that bind, directly or indirectly, to specific protein substrates and promote the transfer of Ub, directly or indirectly, from a thioester intermediate to amide linkages with proteins or poly-ubiquitin chains (1). Our data suggest that SCCRO is part of a complex that functions as the E3 for neddylation. The neddylation E3 ligase complex (Cul-ROC1-SCCRO) shares a modular architecture similar to CRL-containing ubiquitin ligases. CRL complexes have a constant catalytic module (ROC1 bound to E2 thioester) that is conserved in the neddylation E3 complex. SCCRO has a unique regulatory role by helping to recruit the Ubc12~Nedd8 thioester to the neddylation E3 complex. Since SCCRO promotes cullin neddylation, which serves as a signal for assembly of ubiquitination E3 complexes, factors controlling SCCRO likely regulate ubiquitination by CRL-containing E3 complexes. Given the diversity of proteins regulated by CRL-containing E3s, it is not surprising that dysregulation of Dcn1p/DCN-1 results in severe developmental defects in *S. cerevisiae* and *C. elegans* and that SCCRO appears to be a key target activated by amplification in a vast array of human cancers (18).

Assembly of E3 complexes is a key regulatory mechanism. CAND1 affects the assembly of both the neddylation E3 complex as well as the CRL complexes. Several studies, as well as our own

findings, suggest that unneddylated cullins exist almost exclusively in complexes with CAND1, while neddylated cullins are predominantly in active ubiquitination E3 complexes (10-12). Although it is accepted that neddylation serves as a signal for CAND1 dissociation from Cul1-ROC1 and subsequent assembly of ubiquitination E3 complexes, the precise mechanisms leading to the release remain ill defined. The finding that only endogenous Cul1-ROC1 (immunoprecipitated from cells) and not the recombinant protein bound to CAND1 can undergo neddylation leads to speculation that (a) factor(s) in lysate allow(s) release of CAND1 inhibition (10,12). Several experimental observations from our studies may begin to help explain the mechanisms involved in CAND1 release. First, we found that the entire E3 neddylation complex (including Ubc12~Nedd8 and SCCRO) can assemble onto purified Cul1-ROC1 while it is in complex with CAND1. However, this is neither sufficient to promote cullin neddylation nor to induce CAND1 dissociation, suggesting that the assembly of the neddylation E3 complex by itself is not sufficient to overcome the inhibitory effects of CAND1 and the subsequent CRL assembly. However, the CAND1-Cul1-ROC1-Ubc12~Nedd8 complex is not detectable in lysates, consistent with the fact that the assembly of SCCRO and Ubc12 onto the CAND1-Cul1-ROC1 results in rapid neddylation and dissociation of the complex. This is consistent with the increase in neddylation of endogenous cullins with the addition of Ubc12 and/or SCCRO to lysates. Given that SCCRO is not required for neddylation in purified systems, but is essential in *SCCRO*$^{-/-}$ mice (Kaufman, et al., manuscript in preparation) and DCN-1/Dcn1p knockouts in *C. elegans* and *S. cerevisiae*, raises the possibility that SCCRO may be required to overcome CAND1 associated inhibition of cullin neddylation in lysates where unneddylated cullins are in complex with CAND1. Consistent with this hypothesis, the addition of recombinant SCCRO, but not Ubc12~Nedd8 can rescue neddylation in lysates from both DCN-1/Dcn1p and SCCRO knockouts in *C. elegans*, *S. cerevisiae* and mice (Kaufman A, et. al., manuscript in preparation), respectively.

The prevailing theory has been that neddylation makes the binding between CAND1 and cullins unfavorable. This led to speculation that either neddylation serves as a signal for the release or occurs after dissociation from CAND1. We found that in contrast to cellular lysates where they exist in exclusive complex with unneddylated cullins, CAND1 and SCCRO can bind to both neddylated and unneddylated cullins in assays using recombinant proteins. This raises the possibility that neddylation by itself, although required, may not be sufficient for CAND1 dissociation. When incubated with HeLa or *SCCRO*$^{+/+}$ mouse testis lysates, CAND1 is dissociated from neddylated Cul1-ROC1, but not unneddylated Cul1-ROC1, suggesting that cellular factors are involved in the release of neddylated cullins from CAND1. In contrast, neddylated Cul1 was not released by CAND1 when incubated in lysates from *SCCRO*$^{-/-}$ mice unless supplemented with recombinant SCCRO (but not SCCRO-D241N). Factors that compete for binding of neddylated cullins (i.e. SKP1/SKP2) dissociate CAND1 from Cul1-ROC1 only in lysates (which contains wild type SCCRO), but not in purified protein systems, suggesting that SCCRO is required for release. The combined results from these experiments suggest that SCCRO plays a critical role in both cullin neddylation and CAND1 release. Our findings suggest that SCCRO by itself is not sufficient for cullin neddylation and CAND1

release and factor(s) in lysate are required in these processes. Goldberg and colleagues suggest that this factor may be a small molecule that binds the CAND1-Cul1-ROC1 complex to modify its structure, exposing the neddylation site on Cul1 (12). Because CAND1 binds to both neddylated and unneddylated cullins with equal affinity, neddylation in itself, although required, may not be sufficient for CAND1 release. We propose that neddylation occurs through the assembly of the competent neddylation E3 complex onto cullin-ROC1-CAND1, including SCCRO, Ubc12~Nedd8 and an unidentified CAND1 opening factor present in lysate. In this model, neddylation serves as a signal for recruitment of release factors required to dissociate CAND1. The release factor remains to be defined but can include a novel binding protein or posttranslational modifications in reaction components. Although provocative, further studies are required to validate this model.

The other critical question that remains is what is downstream of SCCRO. Katanin is a key target in *C.elegans* and yeast, as its levels are altered in DCN1/DCN1p knockouts. The identification of CRL target downstream of SCCRO is more complex given the presence of multiple paralogs that retain neddylation activity and the complex phenotype in SCCRO knockout mice.

Supplemental figure 1.

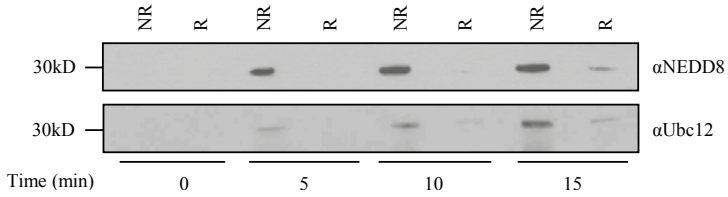

In vitro thioester reactions containing E1 (APPBP1/Uba3), E2 (Ubc12), Nedd8 and ATP were stopped at the indicated time by the addition of Lamelli buffer with (R) or without (NR) 50mM DTT. Western blots showing reduction of the reaction products by DTT in reactions up to 10 minutes (compare R to NR), suggesting that Ubc12~Nedd8 thioester was generated. Longer incubation (15 min) resulted in products resistant to reduction by DTT, suggesting the formation of Ubc12-Nedd8 isopeptide.

Supplemental figure 2.

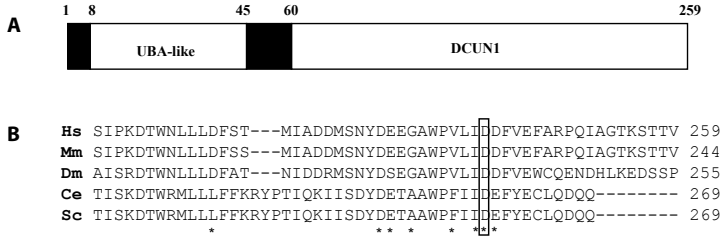

(**A**), figure showing the two functional domains in SCCRO: a UBA-like domain and a DCUN1 domain. (**B**), sequence alignment showing SCCRO has a high degree of sequence conservation in the C-terminal region (shown). Conserved residues mutated for binding studies (see Fig.1E) are indicated by an asterisk. Residue D241, which is important for SCCRO's interaction with Cul-ROC1 and CAND1, is boxed.

References

1. Hershko, A., and Ciechanover, A. (1998) *Annu Rev Biochem* 67, 425-479
2. Hicke, L. (2001) *Nat Rev Mol Cell Biol* 2, 195-201
3. Kerscher, O., Felberbaum, R., and Hochstrasser, M. (2006) *Annu Rev Cell Dev Biol* 22, 159-180
4. Mukhopadhyay, D., and Riezman, H. (2007) *Science* 315, 201-205
5. Aguilar, R. C., and Wendland, B. (2003) *Curr Opin Cell Biol* 15, 184-190
6. Pickart, C. M., and Eddins, M. J. (2004) *Biochim Biophys Acta* 1695, 55-72
7. Petroski, M. D., and Deshaies, R. J. (2005) *Nat Rev Mol Cell Biol* 6, 9-20
8. Hotton, S. K., and Callis, J. (2008) *Annu Rev Plant Biol* 59, 467-489
9. Wu, K., Chen, A., and Pan, Z. Q. (2000) *J Biol Chem* 275, 32317-32324
10. Liu, J., Furukawa, M., Matsumoto, T., and Xiong, Y. (2002) *Mol Cell* 10, 1511-1518
11. Zheng, J., Yang, X., Harrell, J. M., Ryzhikov, S., Shim, E. H., Lykke-Andersen, K., Wei, N., Sun, H., Kobayashi, R., and Zhang, H. (2002) *Mol Cell* 10, 1519-1526
12. Goldenberg, S. J., Cascio, T. C., Shumway, S. D., Garbutt, K. C., Liu, J., Xiong, Y., and Zheng, N. (2004) *Cell* 119, 517-528
13. Kawakami, T., Chiba, T., Suzuki, T., Iwai, K., Yamanaka, K., Minato, N., Suzuki, H., Shimbara, N., Hidaka, Y., Osaka, F., Omata, M., and Tanaka, K. (2001) *EMBO J* 20, 4003-4012
14. Sakata, E., Yamaguchi, Y., Miyauchi, Y., Iwai, K., Chiba, T., Saeki, Y., Matsuda, N., Tanaka, K., and Kato, K. (2007) *Nat Struct Mol Biol* 14, 167-168
15. Wimuttisuk, W., and Singer, J. D. (2007) *Mol Biol Cell* 18, 899-909
16. Lyapina, S., Cope, G., Shevchenko, A., Serino, G., Tsuge, T., Zhou, C., Wolf, D. A., Wei, N., and Deshaies, R. J. (2001) *Science* 292, 1382-1385
17. Wei, N., and Deng, X. W. (2003) *Annu Rev Cell Dev Biol* 19, 261-286
18. Sarkaria, I., P, O. c., Talbot, S. G., Reddy, P. G., Ngai, I., Maghami, E., Patel, K. N., Lee, B., Yonekawa, Y., Dudas, M., Kaufman, A., Ryan, R., Ghossein, R., Rao, P. H., Stoffel, A., Ramanathan, Y., and Singh, B. (2006) *Cancer Res* 66, 9437-9444
19. Zheng, N., Schulman, B. A., Song, L., Miller, J. J., Jeffrey, P. D., Wang, P., Chu, C., Koepp, D. M., Elledge, S. J., Pagano, M., Conaway, R. C., Conaway, J. W., Harper, J. W., and Pavletich, N. P. (2002) *Nature* 416, 703-709
20. Singh, B., Gogineni, S. K., Sacks, P. G., Shaha, A. R., Shah, J. P., Stoffel, A., and Rao, P. H. (2001) *Cancer Res* 61, 4506-4513
21. Singh, B., Reddy, P. G., Goberdhan, A., Walsh, C., Dao, S., Ngai, I., Chou, T. C., P, O. C., Levine, A. J., Rao, P. H., and Stoffel, A. (2002) *Genes Dev* 16, 984-993
22. Singh, B., Stoffel, A., Gogineni, S., Poluri, A., Pfister, D. G., Shaha, A. R., Pathak, A., Bosl, G., Cordon-Cardo, C., Shah, J. P., and Rao, P. H. (2002) *Am J Pathol* 161, 365-371
23. Yang, X., Zhou, J., Sun, L., Wei, Z., Gao, J., Gong, W., Xu, R. M., Rao, Z., and Liu, Y. (2007) *J Biol Chem* 282, 24490-24494
24. Kurz, T., Ozlu, N., Rudolf, F., O'Rourke, S. M., Luke, B., Hofmann, K., Hyman, A. A., Bowerman, B., and Peter, M. (2005) *Nature* 435, 1257-1261
25. Kurz, T., Chou, Y. C., Willems, A. R., Meyer-Schaller, N., Hecht, M. L., Tyers, M., Peter, M., and Sicheri, F. (2008) *Mol Cell* 29, 23-35
26. Kamura, T., Conrad, M. N., Yan, Q., Conaway, R. C., and Conaway, J. W. (1999) *Genes Dev* 13, 2928-2933
27. Dharmasiri, S., Dharmasiri, N., Hellmann, H., and Estelle, M. (2003) *EMBO J* 22, 1762-1770
28. Morimoto, M., Nishida, T., Nagayama, Y., and Yasuda, H. (2003) *Biochem Biophys Res Commun* 301, 392-398
29. Sufan, R. I., and Ohh, M. (2006) *Neoplasia* 8, 956-963
30. Eletr, Z. M., Huang, D. T., Duda, D. M., Schulman, B. A., and Kuhlman, B. (2005) *Nat Struct Mol Biol* 12, 933-934
31. Huang, D. T., Paydar, A., Zhuang, M., Waddell, M. B., Holton, J. M., and Schulman, B. A. (2005) *Mol Cell* 17, 341-350
32. Siepmann, T. J., Bohnsack, R. N., Tokgoz, Z., Baboshina, O. V., and Haas, A. L. (2003) *J Biol Chem* 278, 9448-9457
33. Huang, D. T., Miller, D. W., Mathew, R., Cassell, R., Holton, J. M., Roussel, M. F., and Schulman, B. A. (2004) *Nat Struct Mol Biol* 11, 927-935
34. Zheng, N., Wang, P., Jeffrey, P. D., and Pavletich, N. P. (2000) *Cell* 102, 533-539
35. Hwang, J. W., Min, K. W., Tamura, T. A., and Yoon, J. B. (2003) *FEBS Lett* 541, 102-108
36. Oshikawa, K., Matsumoto, M., Yada, M., Kamura, T., Hatakeyama, S., and Nakayama, K. I. (2003) *Biochem Biophys Res Commun* 303, 1209-1216

Chapter 3

The ubiquitin-associated (UBA) domain of SCCRO (DCUN1D1) protein serves as a feedback regulator of biochemical and oncogenic activity

G. Huang, C. Towe, L. Choi, Y. Yonekawa, C.C. Bommeljé, S. Bains, W. Rechler, B. Hao, Y. Ramanathan, B. Singh

J. Biol. Chem, 2015 Jan 2; 290(1):296-309

Abstract

Amplification of *SCCRO* activates its function as an oncogene in a wide range of human cancers. SCCRO's oncogenic activity requires its PONY domain, which regulates its E3 activity for neddylation. Contribution of the N-terminal ubiquitin-associated (UBA) domain to SCCRO's function remains to be defined. We found that the UBA domain of SCCRO preferentially binds to polyubiquitin chains in a linkage-independent manner. Binding of polyubiquitin chains to the UBA domain inhibits SCCRO's neddylation activity *in vivo* by inhibiting SCCRO-promoted nuclear translocation of neddylation components and results in a corresponding decrease in cullin-RING-ligase promoted ubiquitination. The results of colony-formation and xenograft assays showed mutation in UBA domain of SCCRO that reduces binding to polyubiquitin chains significantly enhances its oncogenic activity. Analysis of 47 lung and head and neck squamous cell carcinomas identified a case with a frame-shift mutation in SCCRO that putatively codes for a protein that lacks a UBA domain. Analysis of data from The Cancer Genome Atlas (TCGA) showed that recurrent mutations cluster in the UBA domains of SCCRO, lose binding to polyubiquitinated proteins, and have increased neddylation and transformation activities. Combined, these data suggest that the UBA domain functions as a negative regulator of SCCRO function. Mutations in the UBA domain lead to loss of inhibitory control, which results in increased biochemical and oncogenic activity. The clustering of mutations in the UBA domain of SCCRO suggests that mutations may be a mechanism of oncogene activation in human cancers.

Introduction

Posttranslational modification by ubiquitin regulates the activity of proteins involved in a wide range of essential cellular processes. Although ubiquitin modifications primarily target proteins for degradation by the 26S proteasome, they can also signal for nonproteolytic effects on protein function. The pleiotropic effects of the ubiquitin signal are encoded for by variations in length and linkage of the ubiquitin chain. In general, Lys48-linked polyubiquitin chains signal for protein degradation, whereas monoubiquitin and non–Lys48-linked polyubiquitin chains signal for nonproteolytic effects (Lys6, Lys11, Lys27, Lys29, Lys33, Lys63) (1-5). However, the same ubiquitin linkage can have varying consequences: for example Lys11-linked chains can promote degradation of the targeted proteins by either the proteasome or the endoplasmic reticulum, as well as promote endocytosis and nondegradative activities that lead to NF-κB activation (6). The diversity of effects imparted by the ubiquitin signal are mediated by motifs that bind to ubiquitin and/or ubiquitin chains and transduce their effects, analogous to the role played by binding of phosphorylated proteins to phospho-binding domains (7-10). Collectively known as ubiquitin-binding domains (UBDs), these motifs comprise more than 20 different families. The ubiquitin-associated (UBA) domain, the prototypic and most common type of UBD, is composed of a motif of 40 residues that are arranged in three tightly packed α-helices that share structural homology with coupling of ubiquitin conjugation to ER degradation (CUE)-type UBDs (9,11-14). It is estimated that more than 79 proteins contain UBA domains. The majority of UBA domains recognize a canonical Ile44/Val70-binding patch on ubiquitin and preferentially bind to polyubiquitin chains (15,16). However, the affinities of individual UBA domains vary considerably, binding to ubiquitin chains of different lengths and linkages (10). UBA domains are thought to limit ubiquitin chain elongation and to help with localization of the bound ubiquitinated proteins to the 26S proteasome for degradation. Recent studies show that UBA domains can also transduce for a variety of other consequences, including modulation of protein interactions and subcellular localization, as well as nonproteasomal turnover of the ubiquitinated proteins and/or the UBA domain-containing proteins (9,17,18).

The presence of a UBA domain in SCCRO (aka DCUN1D1), a protein that functions as an E3 in neddylation (conjugation of the ubiquitin-like protein Nedd8), raises several intriguing possibilities about its function. In contrast to ubiquitination, only a limited number of proteins are subject to neddylation, with the cullin protein family (Cul1, Cul2, Cul3, Cul4, Cul5, and Cul7) being the best-characterized targets (19). Cullins serve as the scaffold for assembly of cullin-RING-ligase (CRL) type E3 ligases, the most common type of ubiquitination E3s (20,21). Neddylation of cullins promotes assembly of the CRL complex and optimizes its conformation to allow efficient transfer of ubiquitin from the E2 to the substrate protein. In its role in promoting neddylation, SCCRO activity regulates levels of ubiquitination activity in cells: an increase in SCCRO activity increases levels of ubiquitinated proteins by promoting CRL activity, whereas a decrease in SCCRO activity has the opposite effect (22-27).

So what is the role of the UBA domain in SCCRO? The high degree of conservation and the existence of splice forms of the SCCRO orthologue DCN1 in lower organisms and SCCRO paralogs in higher organisms that lack a UBA domain suggest that, although it is not required, the UBA domain plays an important role in SCCRO's function. *In vitro* studies confirm that the UBA domain is not required for SCCRO's neddylation activity (26). Our finding that SCCRO regulates neddylation *in vivo* by promoting nuclear translocation of the neddylation components (27)—combined with recent reports that the UBA domain promotes monoubiquitination of SCCRO, leading to its nuclear export (28)—suggests that the UBA domain may regulate SCCRO's neddylation activity *in vivo*. In this report, we show that binding of polyubiquitin chains to the UBA domain inhibits the activity of SCCRO, a core protein in the ubiquitin-proteasome pathway. In this role, the UBA domain serves as a feedback regulator of SCCRO's *in vivo* neddylation and oncogenic activity. Moreover, clustering of mutations in the UBA domain of SCCRO that mitigate binding to polyubiquitinated proteins suggests that it is a mechanism for oncogene activation. Moreover, the presence of mutations in the UBA domain of many other proteins suggests this may be an underappreciated mechanism of oncogene activation in human cancers. Given the conserved binding characteristics of the UBA domain, targeting it may have therapeutic benefit in the treatment of human cancer.

Experimental procedures

Alignment and sequence analyses

Database and BLAST searches were performed at the National Center for Biotechnology Information. Sequence alignments were performed using the ClustalW program.

Reagents

All mutants were generated by PCR mutagenesis and verified by sequencing. Proteins were expressed as GST fusions in *Escherichia coli* using the pGEX4T3 vector. The proteins were purified using glutathione-Sepharose 4B beads (Amersham Biosciences, Piscataway, NJ), followed by thrombin cleavage, where required. Cul1-ROC1 was expressed and purified from *E. coli* as described previously (29). APPBP1/Uba3, Ubc12, Nedd8, and all ubiquitin chains were obtained from a commercial source (Boston Biochem, Cambridge, MA). The proteasome inhibitor Z-Leu-Leu-Leu-al (here referred to as MG132) was purchased from Sigma-Aldrich (St. Louis, MO). The following antibodies were used in this study: anti-Cul1 (Zymed Laboratories, South San Francisco, CA); anti-Cul3 (BD Biosciences, San Jose, CA); anti-Ubc12 (Rockland Immunochemicals, Gilbertsville, PA); anti-Nedd8 (Invitrogen); anti-CAND1 (BD Biosciences); anti-αTubulin (Calbiochem, Billerica, MA); anti-HA, anti-6xHis, and anti-ROC1 (Abcam, Cambridge, MA); and anti-Myc and anti-Ubiquitin (Santa Cruz Biotechnology, Dallas, TX). Anti-SCCRO (rabbit polyclonal) antibody was produced and used as described previously (30). Anti-SCCRO monoclonal antibody was raised against an N-terminal

region of the protein in *SCCRO*$^{-/-}$ mice. This antibody was found to be highly sensitive and specific (data not shown). All cell lines used in this study were obtained from American Type Culture Collection (Manassas, VA) and maintained as recommended.

cDNAs for mammalian transfection were cloned into the pBABE-puro vector (Addgene, Cambridge, MA) or pUSE-amp (Clontech, Mountain View, CA). NIH 3T3 cells were doubly exposed to virus in the presence of 7 ug/mL Polybrene (Sigma-Aldrich) for 24 h each. Infected cells were selected for by use of puromycin (Sigma-Aldrich). pUSE-amp transfection was performed using Lipofectamine 2000 reagent (Invitrogen, Grand Island, NY), in accordance with the manufacturer's specifications.

In vitro neddylation

Cullin-ROC1 substrate for *in vitro* neddylation reactions was derived from either HeLa cell lysates or bacteria (see above). For reactions using HeLa-derived Cullin-ROC1 complexes, 50 µg of lysate (Cul1 concentration, ~20 fmol) was added to reactions containing 10 nM APPBP1/Uba3, 4 nM Ubc12, and 0.9 µM Nedd8 in neddylation buffer (50 mM Tris-HCl [pH 7.5], 55 mM NaCl, and 5 mM $MgCl_2$). Reactions were incubated at 30°C and stopped with the addition of 6x Laemmli buffer. Reactions with bacterially derived substrate were performed at 30°C in neddylation buffer containing 27 nM Cul1-ROC1, 4 mM ATP, 10 nM APPBP1/Uba3, 20 nM Ubc12, and 0.9 µM Nedd8. Proteins were resolved on SDS-PAGE gels and subjected to Western blot analysis. For quantification, Western blots were imaged using ImageJ software (NIH).

GST pull-down assay and immunoprecipitation

GST-tagged proteins were bound to glutathione-Sepharose beads by gentle rotation at 4°C for 45 min. The beads were washed 5 times with EBC buffer (50 mM Tris-HCl [pH 7.5], 2.5 mM $MgCl_2$, 150 mM NaCl, and 0.5% Nonidet P-40) at 20x bead volume. The beads were incubated with HeLa cell lysate or purified proteins, as indicated, at 4°C for 1 h, followed by 5 washes with EBC buffer at 20x bead volume. Bound proteins were eluted by the addition of 6x Laemmli buffer, were resolved on SDS-PAGE gels, and were analyzed by Western blot. GST-tagged proteins were visualized by use of Coomassie R250 staining (Sigma-Aldrich). Immunoprecipitations were performed essentially as described previously (30). In brief, 1 mg of whole-cell lysate was incubated with antibody bound to agarose beads by gentle rocking at 4°C for 2 h. The wash and detection were the same as described above for the GST pull-down assay.

Immunofluorescence

Rhodamine-conjugated anti-Myc and FITC-conjugated anti-HA antibodies were obtained from a commercial source (Jackson ImmunoResearch Laboratories, West Grove, PA). Cells transfected with plasmid(s) were seeded in 6-well plates with cover glass. Forty-eight hours after transfection, cells

were washed with PBS and fixed in 4% formaldehyde for 10 min. The fixed cells were permeabilized with 0.5% Triton X-100 for 5 min, incubated in blocking buffer (PBS containing 10% FCS) for 30 min, and stained overnight at 4°C with fluorochrome-conjugated antibodies. The cells were washed 3 times with PBS, counterstained with DAPI, covered with ProLong Gold Antifade Reagent (Invitrogen, Carlsbad, CA), and examined with a Leica inverted confocal microscope fitted with appropriate fluorescence filters.

Colony formation and xenograft assays

Soft agar assay was performed essentially as described previously (30). Xenograft assays were performed as described previously and in accordance with Institutional Animal Care and Use Committee guidelines. In brief, NIH 3T3 cells (5 x 10^6) were implanted into the flanks of 8-week-old female BALB/c SCID (severe combined immunodeficiency) mice (Taconic, Hudson, NY). Tumor size was measured every 3 days by a single observer and analyzed using Microsoft Excel and GraphPad Prism 5 software. According to institutional guidelines, mice were sacrificed when tumor burden impeded normal feeding and movement.

UBA mutation analysis

Sixty-four human UBA domain–containing proteins from SMART (http://smart.embl.de/smart/do_annotation.pl?DOMAIN=SM00165) and 15 UBA domain–containing proteins from the literature were analyzed. Of these proteins, 28 were included in the TCGA data set. These 28 proteins were assessed for presence and location of mutations against 29 cancer types by use of the cBioPortal for Cancer Genomics (http://www.cbioportal.org/public-portal/).

Statistical analysis

Paired *t* tests were used to compare the means ± SD of soft agar colony formation counts by use of SPSS 19 software (IBM, Armonk, NY). Survival curves were generated using the Kaplan-Meier method and were compared using the log-rank test, by use of Graphpad Prism (Graphpad Software, La Jolla, CA). Disease-free survival was defined as the time from primary treatment of cancer to development of recurrence. Survival outcomes were censored for patients who died of intercurrent disease or who survived to the end of the study. A two-tailed $P \leq 0.05$ was considered to indicate statistical significance.

Results

The UBA domain of SCCRO binds polyubiquitin chains in a linkage-independent manner

Results of sequence and structural analyses show that the UBA domain of SCCRO is composed of a three-helical bundle architecture that shares homology with several other UBA and CUE

Figure 1. The UBA domain of SCCRO binds polyubiquitin chains in a linkage-independent manner.

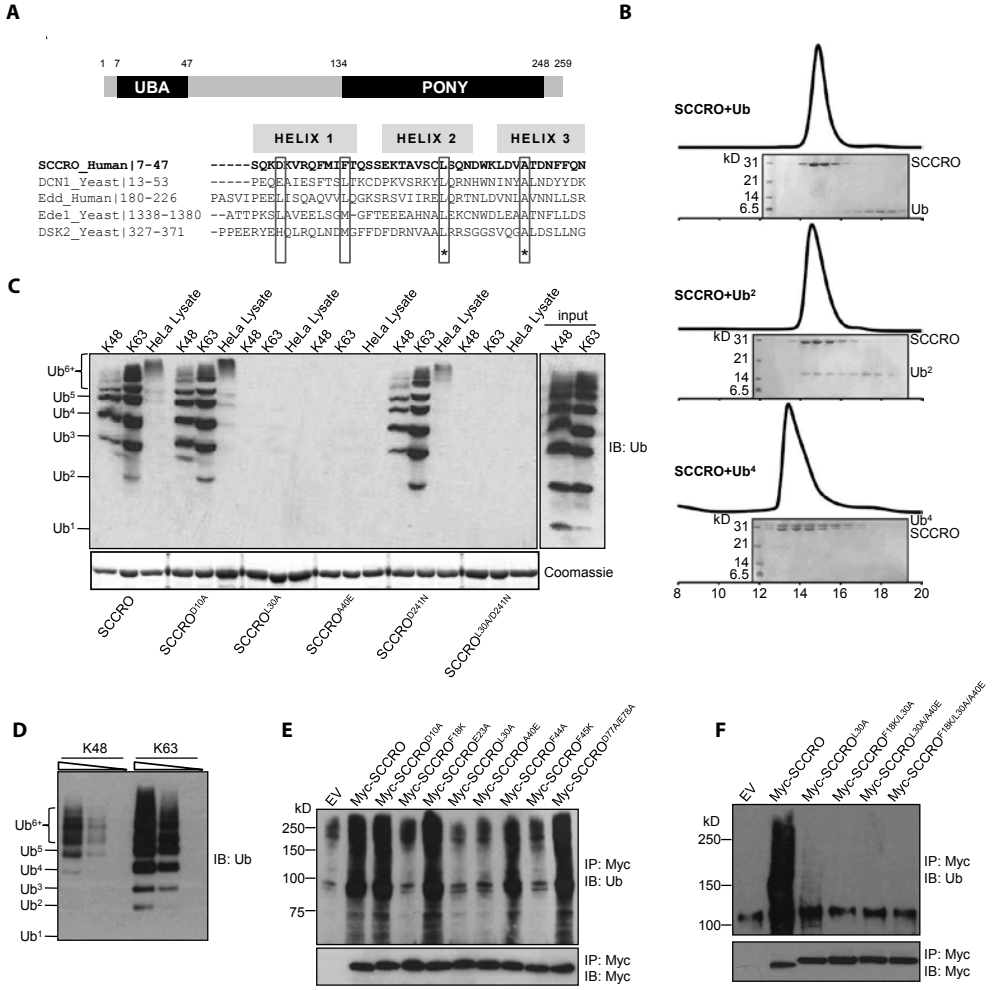

(**A**) Schematic depiction of the domain structure of SCCRO (top panel) and sequence analysis of the UBA domain of SCCRO with several other UBA and CUE domains (bottom panel). Highlighted are conserved hydrophobic residues critical for binding to ubiquitinated proteins. (**B**) SCCRO preferentially binds Ub^4 over Ub or Ub^2. K48-linked ubiquitin chains (Ub^2 and Ub^4) were synthesized *in vitro*. Pictured is a size-exclusion chromatogram showing that SCCRO was co-eluted with Ub^4 but not with Ub or Ub^2. (**C**) Pull-down assay using GST-SCCRO and its mutants on K48 or K63 ubiquitin chains or HeLa cell lysates, followed by Western blot analysis for ubiquitin, showing that SCCRO binds to the ubiquitin chain in a linkage-independent manner. (**D**) Pull-down assay using GST-SCCRO on serially diluted K48 or K63 ubiquitin chains, showing SCCRO has preferential binding toward K63-linked ubiquitin chains. (**E**) and (**F**) Immunoblot analysis of lysates from U2OS cells transfected with *Myc-SCCRO* and selected mutants probed with antibody against ubiquitinated proteins following immunoprecipitation for Myc showing that conserved hydrophobic residues in the UBA domain of SCCRO are critical for binding to ubiquitin chains. EV, empty vector.

domains (26,31). Hydrophobic residues that are critical for interactions with ubiquitin chains in structurally related domains are highly conserved in the UBA domain of SCCRO (Figure 1A). Whereas previous studies have shown that the UBA domain of the yeast orthologue of SCCRO (DCN1) binds to monoubiquitin, structurally related domains preferentially bind to polyubiquitin chains and have a low affinity for monoubiquitin (16,22). To define the binding preferences, we used *in vitro* synthesized K48-linked ubiquitin chains (Ub^2 and Ub^4) and assessed their binding to SCCRO by size-exclusion chromatography. The results showed a preferential 1:1 co-elution of the Ub^4-SCCRO complex, even in the presence of excess Ub or Ub^2 (Figure 1B). To validate these binding preferences and precisely map the residues involved, glutathione-S-transferase (GST)–SCCRO and selected UBA and PONY domain mutants were used in a pull-down assay containing ubiquitin chains of varying lengths and linkages (K48 or K63). The results showed that SCCRO bound to both K48- and K63-linked Ub^4 or great length chains with higher affinity than Ub or Ub^2 chains (Figure 1C). Pull down assays were repeated using serial dilutions of equal concentrations of K48- and K63-linked polyubiquitin chains showing a higher affinity for binding to K63-linked chains (Figure 1D). Mutations in conserved hydrophobic residues in the UBA domain of SCCRO (L30A and A40E) reduced binding, whereas mutations of nonconserved residues in the UBA domain or of residues in the PONY domain did not affect binding to polyubiquitin chains (Figure 1C). Immunoprecipitation for Myc in lysates from U2OS cells expressing Myc-tagged SCCRO or SCCRO mutants, followed by Western blot analysis for ubiquitin, showed that SCCRO binds to polyubiquitinated proteins *in vivo* and that this interaction requires conserved hydrophobic residues (F18, L30, A40, and F45) but not other residues in the UBA domain (Figure 1E). Mutations in two ($SCCRO^{F18K/L30A}$ and $SCCRO^{L30A/A40E}$) or three conserved residues ($SCCRO^{F18K/L30A/A40E}$) in SCCRO's UBA domain result in complete loss of binding to polyubiquitinated proteins (Figure 1F). These findings confirm the requirement of the UBA domain in binding to polyubiquitinated proteins. Previous studies have suggested that UBA domain–containing proteins can be sub-classified on the basis of the length and linkage of the ubiquitin chains to which they bind (32). Our results show that the UBA domain of SCCRO is best included in the class 4 subgroup, although it does not bind to monoubiquitin.

The UBA domain of SCCRO binds to polyubiquitinated CRL substrates

To determine if SCCRO binds to proteins that are ubiquitinated by CRL complexes activated by neddylation, we performed tandem affinity purification to assess for binding to known Cul1 and Cul3 anchored CRL substrates. GST-SCCRO pull-downs on whole cell lysate from HeLa cells pretreated with MG132 were performed to enrich for SCCRO-binding proteins. After thrombin cleavage to release these proteins from the glutathione beads, immunoprecipitation was performed using anti-ubiquitin antibody to enrich for ubiquitinated proteins. Immunoblotting showed that SCCRO bound to polyubiquitinated Aurora B and RhoA, established substrates of Cul3 anchored CRL complexes, but not to cyclin E or p21, substrates of Cul1 anchored CRL complexes (Figure 2A). However, as there is a limited amount of ubiquitinated Aurora B and RhoA in cellular lysates,

extended exposure of the Western blot was required to detect binding. To verify these results, we repeated binding experiments on HeLa cells transfected with Aurora B or RhoA. Transfected cells were treated with MG132 and subjected to tandem affinity purification following the approach described above. As an additional control, we also included pull-downs with GST-SCCRO^{L30A} on the same lysates. We found clear binding of polyubiquitinated Aurora B and RhoA to GST-SCCRO but not to GST or GST-SCCRO^{L30A} (Figure 2B). Combined, these findings suggest that SCCRO binds to Cul3-anchored CRL targets.

Figure 2. The UBA domain of SCCRO binds to polyubiquitinated CRL substrates.

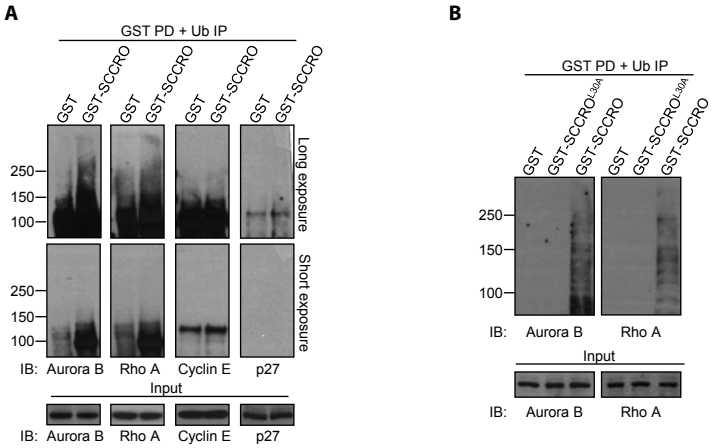

(**A**) GST-SCCRO pull-down products from HeLa cell lysate pretreated with MG132 were released by thrombin cleavage. SCCRO and SCCRO interacting proteins were further immunoprecipitated with antibody against polyubiquitinated proteins and analyzed by Western blotting with antibodies against Aurora B and RhoA (Cul3 substrates) and Cyclin E and p27 (Cul1 substrates), which showed SCCRO selectively bound to polyubiquitinated Aurora B and RhoA. (**B**) Experiments were performed as described for panel A except that HeLa cells were transfected with Aurora B or RhoA before MG132 treatment. Note that GST-SCCRO, but not GST or GST-SCCRO^{L30A}, bound to polyubiquitinated Aurora B and RhoA. IP, immunoprecipitation; IB, immunoblotting; PD, pulldown.

The UBA domain does not affect SCCRO's neddylation activity in vitro

To determine whether the UBA domain modulates SCCRO's neddylation activity, we performed structure-function studies to investigate its effect in *in vitro* assays. *In vitro* reactions contained recombinant Nedd8, APPBP1/Uba3 (E1), Ubc12 (E2), ATP, and whole-cell lysate from HeLa cells (as a source of Cul-ROC1 substrate), in the presence of varying concentrations of SCCRO or selected SCCRO mutants. As expected, the addition of SCCRO increased cullin neddylation in a dose-dependent manner. Deletion or mutation of the UBA domain (SCCRO$^{\Delta N}$ or SCCRO^{L30A}) did not alter SCCRO's neddylation-promoting activity, whereas deletion or mutation of the PONY domain

(SCCRO$^{\Delta C}$ or SCCRO^{D241N}) abrogated its activity (Figure 3A) (23). Moreover, the addition of a 20-fold molar excess of K48-linked Ub^4 did not affect the efficiency with which SCCRO and SCCRO^{L30A} increased levels of neddylated Cul1 or Cul3 (Figure 3B). These findings are consistent with those reported previously for DCN1 in *Caenorhabditis elegans* and yeast (26), confirming that binding of ubiquitin chains to the UBA domain does not affect SCCRO's neddylation activity *in vitro*.

Figure 3. SCCRO's UBA domain does not affect neddylation activity *in vitro*.

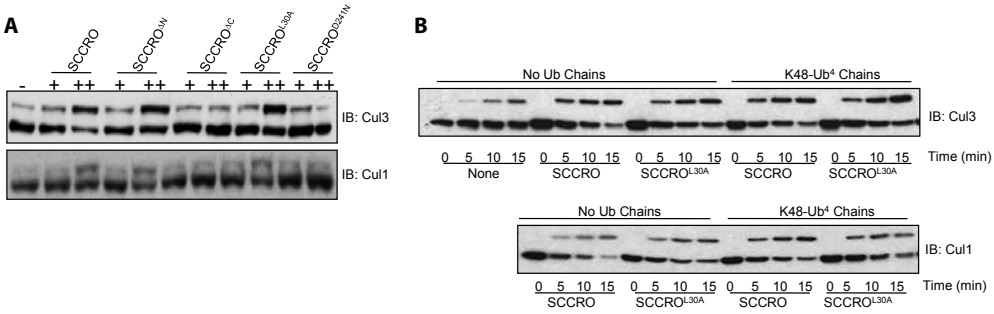

(**A**) *In vitro* neddylation reaction with concentration gradients of SCCRO or SCCRO mutants. Mutations in the PONY domain, but not the UBA domain, blocked the neddylation activity of SCCRO (ΔN: SCCRO with N-terminal 1-45 amino acids deleted; ΔC: SCCRO with C-terminal 151-259 amino acids deleted). (**B**) *In vitro* neddylation reaction with purified recombinant SCCRO or SCCRO^{L30A}, followed by Western blot analysis for Cul1 and Cul3, showing that the presence of a 20-fold molar excess of K48-linked tetraubiquitin failed to inhibit effect of SCCRO or SCCRO^{L30A} on neddylation. IB, immunoblotting.

The UBA domain affects SCCRO's neddylation activity in vivo

Given our recent findings showing differential requirements for SCCRO in neddylation *in vitro* and *in vivo* (27), we next assessed the requirement of the UBA domain for SCCRO's neddylation activity *in vivo*. To determine whether these effects were caused by binding of polyubiquitinated proteins to the UBA domain, HeLa cells were treated with sublethal doses of proteasome inhibitor (MG132), which resulted in accumulation of polyubiquitinated proteins, relative to DMSO-treated controls. Whereas transfection of either *SCCRO* or *SCCRO^{L30A}* increased levels of neddylated Cul1 and Cul3 in DMSO-treated cells, levels of neddylated Cul1 and Cul3 increased only in *SCCRO^{L30A}* transfected HeLa cells treated with MG132 (Figure 4A).

To validate these findings, we expressed Myc-tagged SCCRO, SCCRO^{L30A}, SCCRO$^{\Delta 210\text{-}259}$, a neddylation-deficient mutant that retains binding to polyubiquitinated proteins, or SCCRO$^{L30A/\Delta 210\text{-}259}$, a neddylation-deficient mutant with reduced binding to polyubiquitinated proteins in U2OS cells and confirmed effects of UBA mutations on binding to polyubiquitinated proteins by immunoprecipitation and Western blotting for Ub (Figure 4B). Immunoprecipitation using anti-HA antibody on lysates co-transfected with *HA-SCCRO* and *Myc-SCCRO$^{\Delta 210\text{-}259}$* or *Myc-SCCRO$^{L30A/\Delta 210\text{-}259}$* followed by Western blotting for Ub showed reduced binding of polyubiquitinated proteins to HA-

SCCRO when it was co-transfected with *Myc-SCCRO*$^{\Delta 210\text{-}259}$ but not with *Myc-SCCRO*$^{L30A/\Delta 210\text{-}259}$ (Figure 4C; compare lanes 1-3), even though HA-SCCRO was expressed at equal levels (Figure 4C; see IB: HA). This is likely due to sequestration of polyubiquitinated proteins by Myc-SCCRO$^{\Delta 210\text{-}259}$, reducing the pool available to bind HA-SCCRO. Co-expression of *Myc-SCCRO* with *Myc-SCCRO*$^{\Delta 210\text{-}259}$ increased the levels of neddylated Cul3 relative to cell transfected with *Myc-SCCRO* alone (Figure 4D; lanes 1-2). Neither co-transfection of *Myc-SCCRO*$^{\Delta 210\text{-}259}$ or *Myc-SCCRO*$^{L30A/\Delta 210\text{-}259}$ affected levels neddylated Cul3 in *Myc-SCCRO*^{L30A} transfected U2OS cells (Figure 4D; lanes 4-6). Combined, our observations suggest that binding of polyubiquitinated proteins to the UBA domain of SCCRO inhibits its neddylation activity *in vivo*. These findings suggest that the UBA domain may serve as a sensor and inhibitor of SCCRO's neddylation activity in response to increased levels of polyubiquitinated proteins.

Figure 4. Mutations in the UBA domain augment the neddylation activity of SCCRO *in vivo*.

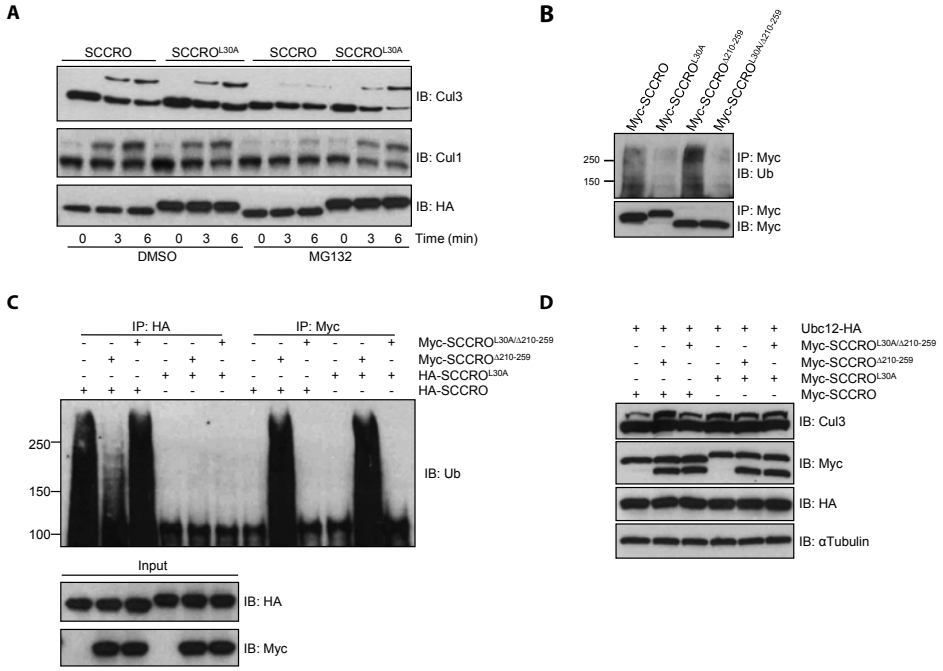

(**A**) Neddylation reaction on HeLa cell lysates, with and without pretreatment with MG132, showing that the level of neddylated Cul1 and Cul3 was reduced in cells transfected with *HA-SCCRO*, but not with *HA-SCCRO*^{L30A}, when pretreated with MG132. (**B**) Immunoblot analysis with antibody against polyubiquitinated proteins following immunoprecipitation for Myc on lysates from U2OS cells transfected with *Myc-SCCRO* mutants, showing SCCRO$^{\Delta 210\text{-}259}$, but not SCCRO^{L30A} or SCCRO$^{L30A/\Delta 210\text{-}259}$, retains binding to ubiquitinated proteins. (**C**) Immunoblot analysis with antibody against polyubiquitinated proteins following immunoprecipitation for either HA or Myc on lysates from U2OS cells transfected as indicated, showing SCCRO$^{\Delta 210\text{-}259}$, but not SCCRO$^{L30A/\Delta 210\text{-}259}$, competes with SCCRO for polyubiquitinated proteins. (**D**) Western blot analysis of neddylated Cul3 in U2OS cells transfected as indicated, showing that coexpression of *SCCRO* with *SCCROΔ210-259*, but not with *SCCRO*$^{L30A/\Delta 210\text{-}259}$, resulted in increased levels of neddylated Cul3 (lanes 1-3). In contrast, neither of the SCCRO mutants affected neddylation of Cul3 promoted by SCCRO^{L30A} (lanes 4-6).

The UBA domain affects SCCRO's compartmentalization activity

To determine the mechanisms by which the UBA domain modulates SCCRO's neddylation activity, we first investigated whether binding of polyubiquitinated proteins to the UBA domain affects interactions between SCCRO and other neddylation components (27). Lysates from HeLa cells transfected with *HA-Ubc12*, *HA-Cul1*, and *Myc-SCCRO* or *Myc-SCCRO^{L30A}* were subjected to immunoprecipitation using anti-Myc antibody, followed by Western blotting for neddylation components. We found no differences between the binding of Myc-SCCRO and Myc-SCCRO^{L30A} to neddylation components (HA-Cul1 or HA-Ubc12) (Figure 5A). Similar results were obtained from GST pull-down assays with no detectable differences in binding to neddylation E3 components between GST-SCCRO and GST-SCCRO^{L30A} in HeLa cell lysates treated with DMSO or MG132 (Figure 5B).

Given the importance of nuclear localization to SCCRO's function (27), we next investigated the effects of MG132 pretreatment on the subcellular localization of Myc-SCCRO or Myc-SCCRO^{L30A} in U2OS cells. Treatment of U2OS cells with MG132 resulted in increased cytoplasmic localization of Myc-SCCRO, compared with treatment with DMSO cells (Figure 5C). In contrast, treatment with MG132 had no effect on localization of Myc-SCCRO^{L30A}, which remained primarily nuclear. Next, we cotransfected U2OS cells with *Myc-SCCRO* or *Myc-SCCRO^{L30A}* and *HA-Cul1$^{\Delta 610-615}$*, a mutant that depends on SCCRO for nuclear translocation and neddylation *in vivo* (27). Both Myc-SCCRO and Myc-SCCRO^{L30A} promoted nuclear translocation of HA-Cul1$^{\Delta 610-615}$ in U2OS cells treated with DMSO. However, treatment with MG132 blocked Myc-SCCRO, but not Myc-SCCRO^{L30A}, promoted nuclear translocation of HA-Cul1$^{\Delta 610-615}$ (Figure 5C). These observations suggest that the subcellular localization of SCCRO is regulated by binding of polyubiquitinated proteins to the UBA domain. Combined with our previous work showing the importance of SCCRO-promoted nuclear translocation of CRL complexes for the neddylation of cullins, these results provide an explanation for why the UBA domain of SCCRO differentially affects cullin neddylation *in vitro* and *in vivo*.

Binding of polyubiquitinated proteins to the UBA domain promotes monoubiquitination and nuclear export of SCCRO

Previous studies have shown that the UBA domain is required for monoubiquitination of SCCRO, which promotes its nuclear export (28). We therefore sought to determine whether cytoplasmic localization of SCCRO in MG132 treated cells is due to increased monoubiquitination of SCCRO. We expressed HA-SCCRO or HA-SCCRO^{L30A} in U2OS cells. Whole cell lysates from cells treated with either MG132 or DMSO were fractionated and immunoblotted for HA. HA-SCCRO, but not HA-SCCRO^{L30A}, was monoubiqutinated and was present only in the cytoplasmic fraction of MG132 treated cells (Figure 5D). Consistent with previous findings (28), SCCRO^{L30A} was not monoubiquitinated under any conditions tested (Figure 5D).

To determine if monoubiquitination is required for nuclear export promoted by binding

Figure 5. Binding of ubiquitinated proteins affects SCCRO-promoted nuclear translocation of cullins.

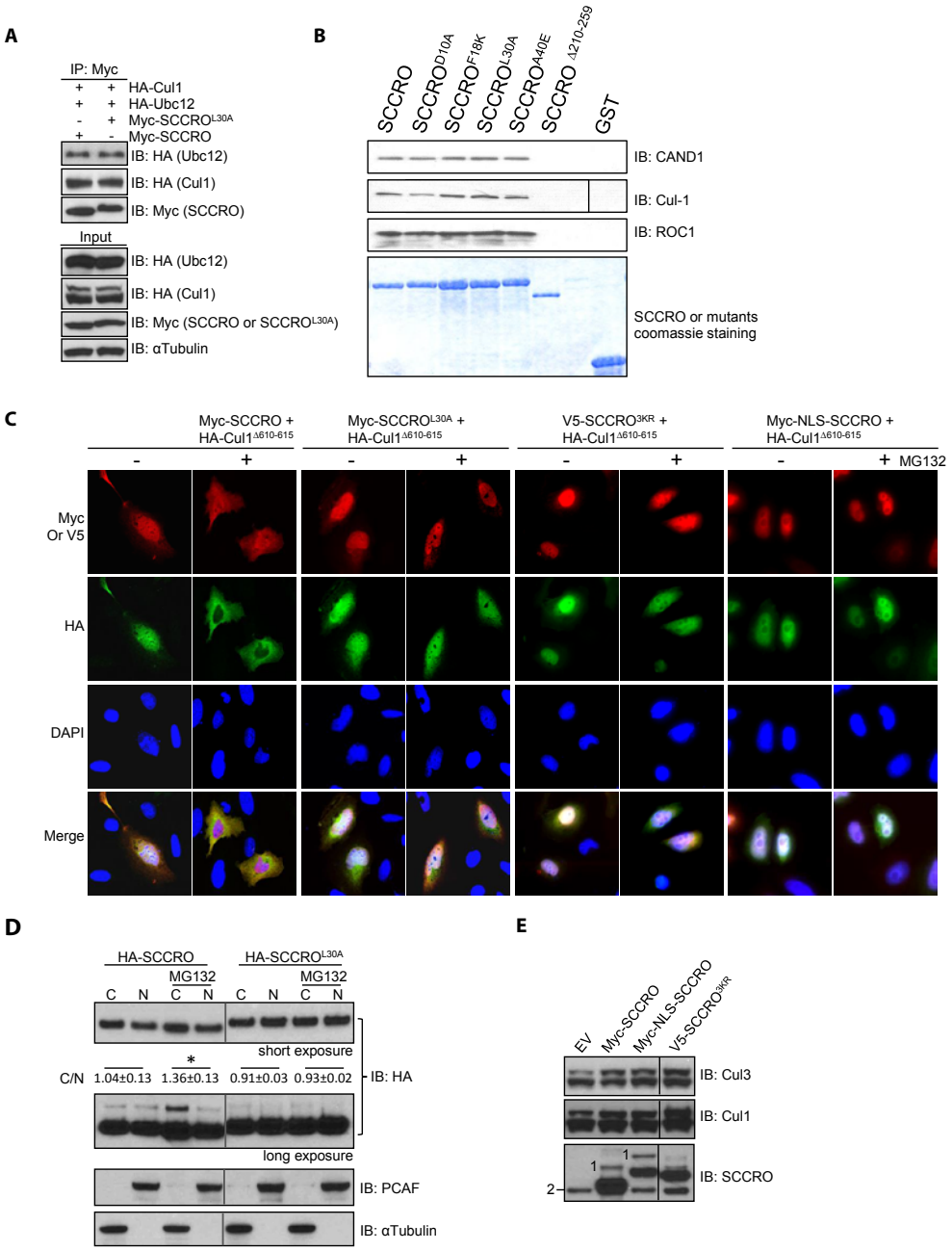

(**A**) Immunoblot analysis of lysates from U2OS cells transfected with indicated constructs, following immunoprecipitation for Myc, showing no differences between the binding of SCCRO and SCCRO^{L30A} to neddylation components. (**B**) Western blot analysis of the pull-down products of GST-SCCRO and SCCRO mutants from HeLa cell extracts probed with indicated antibodies, showing that SCCRO binds to CAND1, Cul1, and ROC1. The cullin-binding mutant SCCRO$^{\Delta 210\text{-}259}$ loses binding to CAND1, Cul1, and ROC1; in contrast, UBA mutants do not. (**C**) Immunofluorescence analysis using rhodamine-conjugated anti-Myc or anti-V5 and FITC-conjugated anti-HA on U2OS cells transfected with *Myc-SCCRO*, *Myc-SCCRO^{L30A}*, *V5-SCCRO^{3KR}* or *Myc-NLS-SCCRO* and *HA-Cul1$^{\Delta 610\text{-}615}$* in the presence or absence of MG132. Pretreatment with MG132 caused translocation of a significant proportion of Myc-SCCRO, but not Myc-SCCRO^{L30A}, V5-SCCRO^{3KR}, or Myc-NLS-SCCRO, from the nucleus to the cytoplasm (first row). In addition, pretreatment with MG132 blocked nuclear translocation of HA-Cul1$^{\Delta 610\text{-}615}$ promoted by SCCRO, but not by SCCRO^{L30A}, V5-SCCRO^{3KR}, or Myc-NLS-SCCRO (second row). (**D**) Fractionation analysis of U2OS cells transfected with *HA-SCCRO*, showing increased levels of cytosolic SCCRO and monoubiquitinated SCCRO, but not SCCRO^{L30A}, after treatment with MG132. Results from densitometry measurement of Western blots from three independent experiments are shown (C, cytoplasm; N, nucleus; C/N stands for ratios of the levels of cytosolic SCCRO or SCCRO^{L30A} vs the levels of nuclear SCCRO or SCCRO^{L30A}). *, P=0.043. (**E**) Western blot analysis of neddylated Cul1 and Cul3 in U2OS cells transfected as indicated, showing that expression of *NLS-SCCRO* or *SCCRO^{3KR}* resulted in increased levels of neddylated Cul1 and Cul3 to the extent similar to expression of *SCCRO*. Western blot for SCCRO on the same lysates showed that while both Myc-SCCRO and Myc-NLS-SCCRO underwent monoubiquitination, V5-SCCRO^{3KR} did not under identical conditions (1, monoubiquitinated SCCRO; 2, endogenous SCCRO).

of polyubiquitinated proteins to the UBA domain of SCCRO, we cotransfected *V5-SCCRO^{3KR}* (a monoubiquitination-deficient mutant; Figure 5E) and *HA-Cul1$^{\Delta 610\text{-}615}$* into U2OS cells. In contrast to cells expressing SCCRO, treatment with MG132 had no effect on localization of V5-SCCRO^{3KR} or V5-SCCRO^{3KR} promoted nuclear translocation of HA-Cul1$^{\Delta 610\text{-}615}$ (Figure 5C), suggesting monoubiquitination is important for nuclear export. We next questioned if the nuclear export of SCCRO is important for the inhibitory effects exerted by binding of polyubiquitinated proteins to the UBA of SCCRO. Myc-NLS-SCCRO and HA-Cul1$^{\Delta 610\text{-}615}$, when cotransfected into U2OS cells, did not translocate to the cytoplasm upon treatment with MG132 in U2OS cells (Figure 5C). Combined with the observed changes in localization and neddylation activity of SCCRO that resulted from treatment with MG132, these data suggest that binding of polyubiquitinated proteins to the UBA domain promotes monoubiquitination and nuclear export of SCCRO, thereby inhibiting its neddylation activity.

Mutation of the UBA domain increases SCCRO's oncogenic activity

We previously reported that overexpression of SCCRO increases cullin neddylation, which promotes malignant transformation *in vivo*. To determine whether the UBA domain affects SCCRO's function *in vivo*, we assessed the effects of stable expression of *HA-SCCRO*, *HA-SCCRO^{L30A}*, or *HA-SCCRO^{F44Y}* on transformation of NIH 3T3 cells. Independent stable clones, with relatively equal levels of transgene expression, were selected for each construct. We first confirmed functional effects of SCCRO and SCCRO UBA mutants. Levels of neddylated Cul1 or Cul3 were assessed by immunoblot analysis on lysates from at least two independent stable clones for each construct. We found that levels of neddylated Cul1 and Cul3 were higher in cells transfected with *SCCRO^{L30A}* than

in cells transfected with *SCCRO* or *SCCRO*^{F44Y} (Figure 6A; compare lanes 5, 6, and 7 with the other lanes). These observations suggest that the UBA domain modulate SCCRO's neddylation activity in these cells. Next we assessed oncogenicity in stably transfected NIH 3T3 clones by soft agar assay, which showed that clones expressing SCCRO^{L30A} formed significantly more colonies than NIH 3T3 clones expressing SCCRO (Figure 6B and 6C). In contrast, no differences in colony formation were seen between clones expressing SCCRO^{F44Y} (which retains binding to polyubiquitinated proteins) and those expressing SCCRO. To confirm that the increase in anchorage-independent growth in UBA domain mutants depends on SCCRO's neddylation activity, we investigated the transforming activity of the neddylation-dead mutant (SCCRO^{D241N}) and a double mutant (in both the UBA domain and the PONY domain: SCCRO$^{L30A/D241N}$). Neither the SCCRO^{D241N} mutant nor the SCCRO$^{L30A/D241N}$ double mutant was able to form colonies in soft agar, which suggests that the neddylation activity of SCCRO plays an essential role in its oncogenic activity (Figure 6B and 6C). To validate these findings, we performed *in vivo* xenograft assays in BALB/c nude mice using *SCCRO*- or *SCCRO*^{L30A}-transfected NIH 3T3 clones. We found that there was shortened latency and significantly higher growth for *SCCRO*^{L30A}-transfected than *SCCRO*-transfected NIH 3T3 cells (Figure 6D-F). Necropsy of mice and histopathologic analyses showed that tumor xenografts resulting from injection of SCCRO^{L30A}-expressing NIH 3T3 cells were poorly differentiated and metastasized to pelvic lymph nodes in all mice (data not shown). Conversely, tumor xenografts resulting from injection of SCCRO-expressing NIH 3T3 cells were more differentiated and rarely metastasized to lymph nodes. These results suggest that SCCRO's oncogenic activity is modulated by its UBA domain. To determine the relevance of these findings to human tumors, we screened 47 lung and head and neck squamous cell carcinomas for mutations, using the Sequenom method, and identified one with a frame-shift mutation that putatively produces a truncated SCCRO protein with an alternate start site downstream of the mutation and without a UBA domain (Figure 7A). However, because of a lack of tumor tissue, we could not confirm the effect of this mutation on the production of SCCRO protein. We further screened available whole-genome sequencing results from TCGA projects for different human cancers. This analysis showed that, although they are rare, mutations in SCCRO cluster in the UBA domain (Figure 7B). To assess whether TCGA identified UBA domain mutants bind to ubiquitin chains, we carried out an immunoprecipitation assay to assess for their binding to ubiquitin chains of varying lengths and linkages (Lys48 or Lys63). In contrast to wild-type SCCRO, we found that none of tumor-derived UBA mutants bound to ubiquitin chains (Figure 7C). Moreover, immunoprecipitation for Myc in lysates from U2OS cells expressing Myc-tagged SCCRO or UBA mutants identified in TCGA, followed by Western blot analysis for ubiquitin, showed that all TCGA mutants lost ability to bind to polyubiquitinated proteins *in vivo* (Figure 7D).

To determine if UBA mutants identified in the TCGA dataset affect SCCRO's biochemical and oncogenic functions, we assessed their effect on cullin neddylation and transformation. Whereas transfection of *SCCRO*, *SCCRO*^{R13H}, or *SCCRO*^{Q20A} increased levels of neddylated Cul1 and Cul3 in DMSO treated HeLa cells, neddylated Cul1 and Cul3 only increased in *SCCRO*^{R13H} or *SCCRO*^{Q20A}

transfected cells after MG132 treatment (Figure 8A). Next, to assess the transforming activities of tumor-derived SCCRO UBA mutants, we stably transfected NIH 3T3 cells and selected stable clones with similar transgene expression levels (Figure 8B). These cells were subjected to soft agar assays, which showed significantly higher colony formation in NIH 3T3 cells expressing TCGA-identified SCCRO UBA mutants relative to those expressing wild-type SCCRO (Figure 8C and 8D). Combined, these findings suggest that SCCRO's UBA domain modulates its neddylation activity and that this has functional relevance to tumorigenesis.

Figure 6. Disruption of ubiquitin binding increases SCCRO's transforming activity.

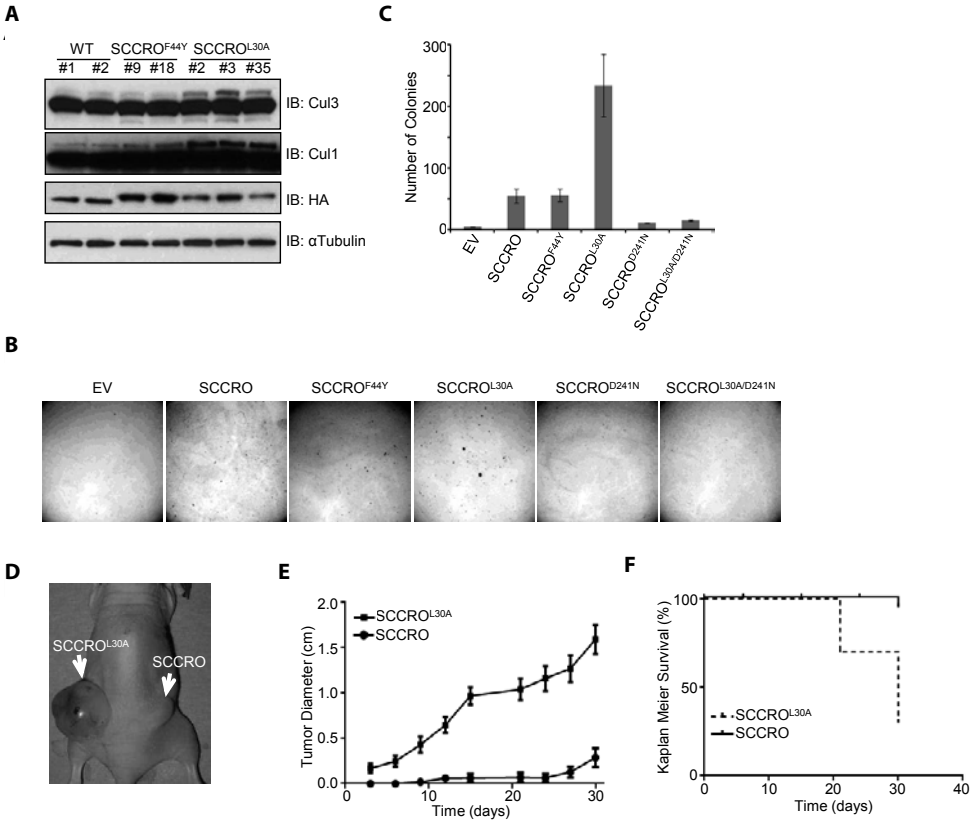

(**A**) Western blot analysis showing that levels of neddylated Cul1 and Cul3 are higher in NIH 3T3 cells transfected with *HA-SCCRO*^{L30A} than in those transfected with *HA-SCCRO* (*WT*) or *HA-SCCRO*^{F44Y}. (**B**) Representative results from soft agar assay showing that, in NIH 3T3 cells, stable expression of SCCRO^{L30A} resulted in increased colony formation, compared with expression of SCCRO. Note that NIH 3T3-expressing PONY domain mutants (SCCRO^{D241N} and SCCRO$^{L30A/D241N}$) had a similar number of colonies as empty vector (EV) controls did. (**C**) Graph quantification of colonies for panel B. (**D**) and (**E**), *In vivo* xenograft assays in nude mice with NIH 3T3 clones expressing SCCRO or SCCRO^{L30A}, showing more aggressive tumor growth (*D*) with a larger tumor diameter (*E*) for SCCRO^{L30A} than for SCCRO. (**F**) Kaplan-Meier survival curves showing that mice transplanted with NIH 3T3 clones expressing SCCRO^{L30A} had shorter survival than those transplanted with NIH 3T3 clones expressing SCCRO. IB, immunoblotting.

Figure 7. Mutations in the UBA domain of SCCRO are present in human cancers.

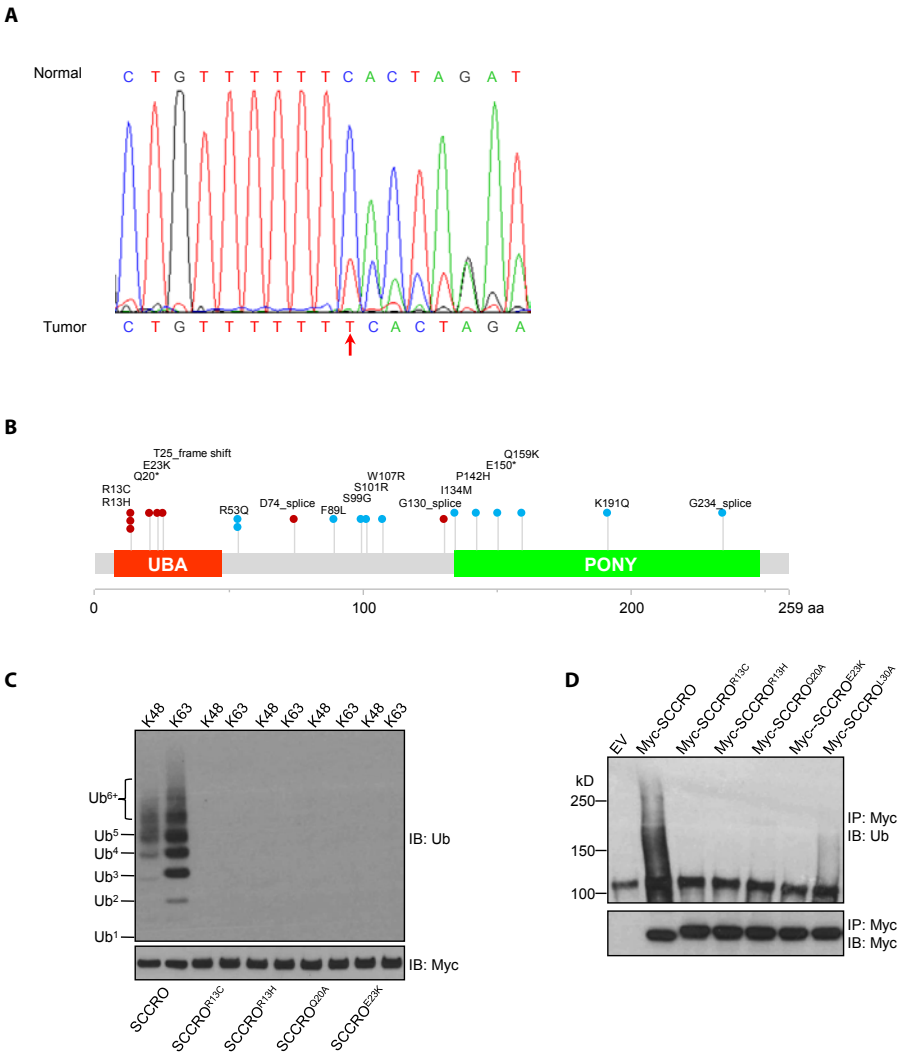

(**A**) Frame-shift mutation in the UBA domain identified in 1 case out of 47 lung and head and neck squamous cell carcinomas assessed by the use of the Sequenom method. A truncated SCCRO mutant without a UBA domain is predicted. (**B**) Mutations in SCCRO identified in TCGA projects. Red dots represent UBA domain point mutations or splice mutations putatively producing truncated SCCRO without a UBA domain; light blue dots represent non–UBA domain mutations. Each dot represents a separate cancer. The asterisk (*) indicates nonsense mutation. (**C**) Immunoprecipitation assay using Myc-SCCRO and its TCGA UBA mutants on K48- or K63-linked ubiquitin chains, followed by Western blot analysis for ubiquitin, showing that TCGA-identified UBA domain mutants do not bind ubiquitin chains. (**D**) Immunoblot analysis of lysates from U2OS cells transfected with *Myc-SCCRO* or TCGA UBA mutants probed with antibody against ubiquitinated proteins following immunoprecipitation for Myc showing all mutants lose the ability to bind to polyubiquitinated proteins.

Figure 8. Tumor-derived UBA mutations increase SCCRO's transforming activity.

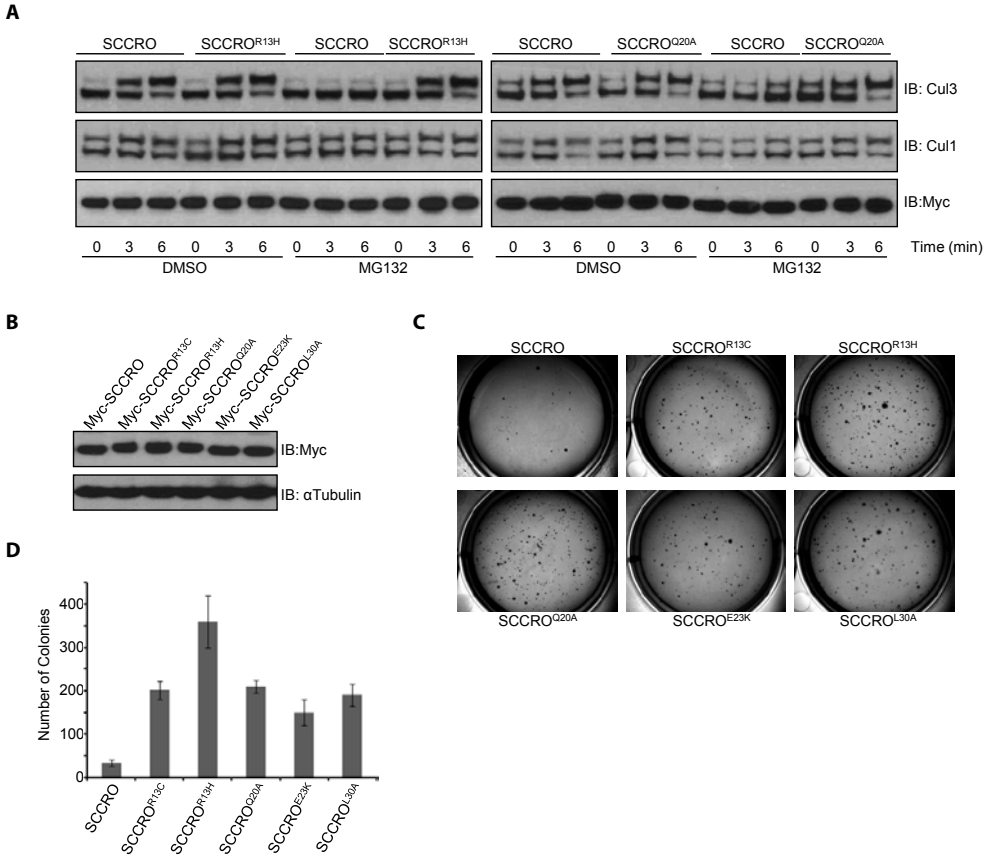

(**A**) TCGA-identified mutations in the UBA domain augment the neddylation activity of SCCRO *in vivo*. Neddylation reaction on lysates derived from HeLa cells with and without pretreatment with MG132, showing that the levels of neddylated Cul1 and Cul3 are reduced by pretreatment with MG132 in *Myc-SCCRO* transfected but not *Myc-SCCRO^{R13H}* or *Myc-SCCRO^{Q20A}* transfected cells. Results were confirmed by densitometry measurement. (**B**) Western blot analysis of lysates from NIH 3T3 cells stably transfected with the indicated *SCCRO* constructs, probed with anti-Myc antibody, showing equivalent expression. (**C**) Representative results from soft agar assay showing that stable expression of TCGA-identified UBA domain mutants in NIH 3T3 cells results in increased colony formation in soft agar relative to expression of SCCRO. (**D**) Graph showing average number of colonies for each NIH 3T3 clone from panel B.

Discussion

Through its role as an E3 in neddylation, SCCRO promotes CRL activity, which results in an increase in cellular levels of polyubiquitinated proteins (27). We found that binding of polyubiquitinated proteins to the N-terminal UBA domain of SCCRO inhibits its neddylation activity, suggesting the presence of a classical negative-feedback loop that regulates CRL-promoted ubiquitination activity (Figure 9).

Figure 9. Proposed model of UBA domain–mediated regulation of SCCRO.

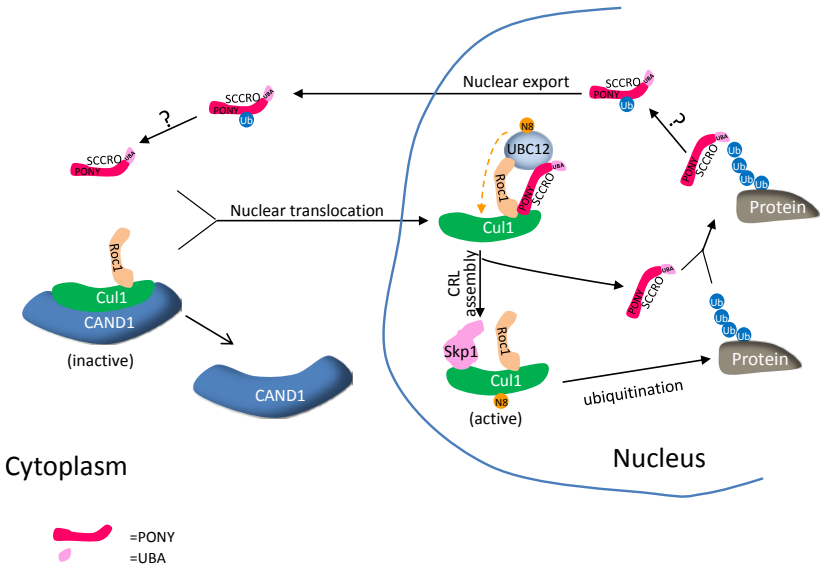

In this model, SCCRO's N-terminal UBA domain serves as a sensor of polyubiquitinated proteins, as well as an effector by promoting the auto-ubiquitination of SCCRO. The effects of the UBA domain do not appear to be allosteric, as the addition of polyubiquitin chains or mutation of the UBA domain has no effect on SCCRO's neddylation function *in vitro*, whereas accumulation of polyubiquitinated proteins shows classical negative-feedback dynamics *in vivo*. Interestingly, the requirement for SCCRO in neddylation is also different *in vitro* and *in vivo*, with its essential effects *in vivo* involving compartmentalization of neddylation components. As Ubc12, the E2 for neddylation, is primarily located in the nucleus, SCCRO-promoted nuclear translocation of Cullin-ROC1 complexes is required for neddylation. Consistent with this, we found that the effect that binding of polyubiquitinated proteins to the UBA domain had on SCCRO's function was imparted by cytoplasmic translocation of SCCRO: increase in levels of polyubiquitinated proteins increased cytoplasmic localization of SCCRO and inhibited nuclear localization of neddylation components, whereas mutation in the UBA domain abrogated these effects.

These findings raise obvious questions about how binding of polyubiquitinated proteins to the UBA domain affects the subcellular localization and function of SCCRO. Recent work by Wu et al. shows that the UBA domain of SCCRO is required for its monoubiquitination and that monoubiquitination promotes nuclear export of SCCRO. Conversely, mutations in the UBA domain block monoubiquitination of SCCRO and, consequently, its nuclear export (Figure 5C and 5D) (28). These findings suggest that the binding of polyubiquitinated proteins to the UBA domain serves as a signal for the monoubiquitination of SCCRO. A limitation of this work is reliance on SCCRO mutants to assess structure-function relationships. It remains possible that the generated mutants affect protein function in unanticipated ways. Mitigating this issue, at least in part, we found that blocking the monoubiquitination of SCCRO by mutation of ubiquitination residues in SCCRO or restricting SCCRO's nuclear export by NLS tag had identical effects on SCCRO localization and function as UBA domain mutants expressed in cells exposed to MG132.

UBD-coupled auto-ubiquitination has been reported for several other proteins, including Sts1, Sts2, Eps15, Eps15R, Vps27p/Hrs, Vps9p, and Rabex-5 (9). Although the precise underlying mechanisms remain to be defined, a range of functional consequences are known to accompany UBD-coupled auto-ubiquitination, including effects on inter- and intra-protein interactions and subcellular localization. Various UBDs have been implicated in coupled auto-ubiquitination, including UIM, CUE, MIU, and A20 ZnF domains; however, this has not been previously reported for UBA domain–containing proteins. In the case of SCCRO, coupled auto-ubiquitination leads to its cytoplasmic translocation and functional inhibition *in vivo*. What remains to be defined is how monoubiquitinated SCCRO is translocated and sequestered in the cytoplasm. Given the relatively low affinity of the UBA domain in SCCRO for monoubiquitin, it is unlikely that intra-protein interaction is the cause of changes in SCCRO's localization. These effects are also unlikely to be caused by changes in interactions with neddylation components, as the presence of polyubiquitin chains and/or mutations in the UBA domain does not affect binding between SCCRO and Cul1 or Ubc12. Given that SCCRO and other neddylation E3 components lack a canonical nuclear localization sequence, one possibility for nuclear export is that monoubiquitination of SCCRO inhibits interactions with NLS-containing protein partners involved in nuclear import.

In the broader context, the principal presence of the UBA domain in E2s and E3s (33) raises the question of whether UBA domains serve as general feedback regulators of the ubiquitination pathway. In a related model, the auto-ubiquitination and ubiquitin binding of the UBD in Rabex-5 affected its ubiquitin ligase activity (34). It remains to be determined whether UBA domains play similar roles in other proteins.

Although specific mechanisms require definition, it is quite clear that mutations in the UBA domain that inhibit interactions with ubiquitinated proteins increase SCCRO's neddylation activity *in vivo*. We have previously shown that increased neddylation activity resulting from overexpression of SCCRO promotes oncogenesis *in vitro* and *in vivo* (30). In primary tumors, SCCRO's oncogenic activity is promoted by amplification that is present in many types of cancers, including lung,

ovarian, head and neck and esophageal cancers (35-37). Interestingly, we found that transgenic expression of UBA domain mutants of SCCRO was more oncogenic than wild-type SCCRO. Moreover, we found that, although they are rare, somatic mutations cluster in the UBA domain of SCCRO. As the spontaneously occurring somatic UBA domain mutations lose binding to polyubiquitinated proteins and have increased neddylation and transforming activity, they represent an alternate mechanism for activation of SCCRO's oncogenic activity in human cancers.

The role of the UBA domain in cancer pathogenesis has been well-established. For example, germline mutations in the UBA domain of SQSTM1 are associated with the development of Paget's disease of bone. These mutations impair the ability of SQSTM1 to bind to ubiquitin chains, altering proteasome- and/or autophagy-based turnover of the bound ubiquitinated proteins (38-42). Although the specific polyubiquitinated proteins involved remain to be identified, the carcinogenic effects that result from loss of binding due to mutation in the UBA domain of SQSTM1 are achieved through activation of NF-κB signaling (39,40). Moreover, the identification of mutation clusters in the UBA domains of other proteins suggests that these domains may play a larger and more direct role in oncogenesis than previously appreciated (Supplemental Table 1). In the broader context, functional domains typically have similar activities, even when present in different proteins. As such, functionally related mutations in cancers may cluster in domains, rather than in individual genes or gene families. Domain-based analysis of genome-wide sequencing data may identify novel targets for anticancer therapies. For example, the activity of an oncogene may be mitigated by agents that bind to or mimic the oncoprotein's UBA domain. In one such instance, overexpression of the UBA domain of hFAF1 significantly promotes cell death by increasing the degradation of polyubiquitinated proteins (43).

References

1. Hershko, A., and Ciechanover, A. (1998) The ubiquitin system. Annu Rev Biochem 67, 425-479
2. Hicke, L. (2001) Protein regulation by monoubiquitin. Nat Rev Mol Cell Biol 2, 195-201
3. Kerscher, O., Felberbaum, R., and Hochstrasser, M. (2006) Modification of proteins by ubiquitin and ubiquitin-like proteins. Annu Rev Cell Dev Biol 22, 159-180
4. Mukhopadhyay, D., and Riezman, H. (2007) Proteasome-independent functions of ubiquitin in endocytosis and signaling. Science 315, 201-205
5. Aguilar, R. C., and Wendland, B. (2003) Ubiquitin: not just for proteasomes anymore. Curr Opin Cell Biol 15, 184-190
6. Kulathu, Y., and Komander, D. (2012) Atypical ubiquitylation—the unexplored world of polyubiquitin beyond Lys48 and Lys63 linkages. Nat Rev Mol Cell Biol 13, 508-523
7. Madura, K. (2002) The ubiquitin-associated (UBA) domain: on the path from prudence to prurience. Cell Cycle 1, 235-244
8. Buchberger, A. (2002) From UBA to UBX: new words in the ubiquitin vocabulary. Trends Cell Biol 12, 216-221
9. Hurley, J. H., Lee, S., and Prag, G. (2006) Ubiquitin-binding domains. Biochem J 399, 361-372
10. Su, V., and Lau, A. F. (2009) Ubiquitin-like and ubiquitin-associated domain proteins: significance in proteasomal degradation. Cell Mol Life Sci 66, 2819-2833
11. Trempe, J. F., Brown, N. R., Lowe, E. D., Gordon, C., Campbell, I. D., Noble, M. E., and Endicott, J. A. (2005) Mechanism of Lys48-linked polyubiquitin chain recognition by the Mud1 UBA domain. EMBO J 24, 3178-3189
12. Ohno, A., Jee, J., Fujiwara, K., Tenno, T., Goda, N., Tochio, H., Kobayashi, H., Hiroaki, H., and Shirakawa, M. (2005) Structure of the UBA domain of Dsk2p in complex with ubiquitin molecular determinants for ubiquitin recognition. Structure 13, 521-532
13. Swanson, K. A., Hicke, L., and Radhakrishnan, I. (2006) Structural basis for monoubiquitin recognition by the Ede1 UBA domain. J Mol Biol 358, 713-724
14. Lowe, E. D., Hasan, N., Trempe, J. F., Fonso, L., Noble, M. E., Endicott, J. A., Johnson, L. N., and Brown, N. R. (2006) Structures of the Dsk2 UBL and UBA domains and their complex. Acta Crystallogr D Biol Crystallogr 62, 177-188
15. Searle, M. S., Garner, T. P., Strachan, J., Long, J., Adlington, J., Cavey, J. R., Shaw, B., and Layfield, R. (2012) Structural insights into specificity and diversity in mechanisms of ubiquitin recognition by ubiquitin-binding domains. Biochem Soc Trans 40, 404-408
16. Wilkinson, C. R., Seeger, M., Hartmann-Petersen, R., Stone, M., Wallace, M., Semple, C., and Gordon, C. (2001) Proteins containing the UBA domain are able to bind to multi-ubiquitin chains. Nat Cell Biol 3, 939-943
17. Husnjak, K., and Dikic, I. (2012) Ubiquitin-binding proteins: decoders of ubiquitin-mediated cellular functions. Annu Rev Biochem 81, 291-322
18. Trempe, J. F. (2011) Reading the ubiquitin postal code. Curr Opin Struct Biol 21, 792-801
19. Xirodimas, D. P. (2008) Novel substrates and functions for the ubiquitin-like molecule Nedd8. Biochem Soc Trans 36, 802-806
20. Cardozo, T., and Pagano, M. (2004) The SCF ubiquitin ligase: insights into a molecular machine. Nat Rev Mol Cell Biol 5, 739-751
21. Petroski, M. D., and Deshaies, R. J. (2005) Function and regulation of cullin-RING ubiquitin ligases. Nat Rev Mol Cell Biol 6, 9-20
22. Kurz, T., Ozlu, N., Rudolf, F., O'Rourke, S. M., Luke, B., Hofmann, K., Hyman, A. A., Bowerman, B., and Peter, M. (2005) The conserved protein DCN-1/Dcn1p is required for cullin neddylation in C. elegans and S. cerevisiae. Nature 435, 1257-1261
23. Kim, A. Y., Bommeljé, C. C., Lee, B. E., Yonekawa, Y., Choi, L., Morris, L. G., Huang, G., Kaufman, A., Ryan, R. J., Hao, B., Ramanathan, Y., and Singh, B. (2008) SCCRO (DCUN1D1) is an essential component of the E3 complex for neddylation. J Biol Chem 283, 33211-33220
24. Scott, D. C., Monda, J. K., Grace, C. R., Duda, D. M., Kriwacki, R. W., Kurz, T., and Schulman, B. A. (2010) A dual E3 mechanism for Rub1 ligation to Cdc53. Mol Cell 39, 784-796
25. Heir, P., Sufan, R. I., Greer, S. N., Poon, B. P., Lee, J. E., and Ohh, M. (2013) DCNL1 functions as a substrate sensor and activator of cullin 2-RING ligase. Mol Cell Biol 33, 1621-1631
26. Kurz, T., Chou, Y. C., Willems, A. R., Meyer-Schaller, N., Hecht, M. L., Tyers, M., Peter, M., and Sicheri, F. (2008) Dcn1 functions as a scaffold-type E3 ligase for cullin neddylation. Mol Cell 29, 23-35
27. Huang, G., Kaufman, A. J., Ramanathan, Y., and Singh, B. (2011) SCCRO (DCUN1D1) promotes nuclear translocation and assembly of the neddylation E3 complex. J Biol Chem 286, 10297-10304

28. Wu, K., Yan, H., Fang, L., Wang, X., Pfleger, C., Jiang, X., Huang, L., and Pan, Z. Q. (2011) Mono-ubiquitination drives nuclear export of the human DCN1-like protein hDCNL1. J Biol Chem 286, 34060-34070
29. Zheng, N., Schulman, B. A., Song, L., Miller, J. J., Jeffrey, P. D., Wang, P., Chu, C., Koepp, D. M., Elledge, S. J., Pagano, M., Conaway, R. C., Conaway, J. W., Harper, J. W., and Pavletich, N. P. (2002) Structure of the Cul1-Rbx1-Skp1-F boxSkp2 SCF ubiquitin ligase complex. Nature 416, 703-709
30. Sarkaria, I., P, O. c., Talbot, S. G., Reddy, P. G., Ngai, I., Maghami, E., Patel, K. N., Lee, B., Yonekawa, Y., Dudas, M., Kaufman, A., Ryan, R., Ghossein, R., Rao, P. H., Stoffel, A., Ramanathan, Y., and Singh, B. (2006) Squamous cell carcinoma related oncogene/DCUN1D1 is highly conserved and activated by amplification in squamous cell carcinomas. Cancer Res 66, 9437-9444
31. Yang, X., Zhou, J., Sun, L., Wei, Z., Gao, J., Gong, W., Xu, R. M., Rao, Z., and Liu, Y. (2007) Structural basis for the function of DCN-1 in protein Neddylation. J Biol Chem 282, 24490-24494
32. Raasi, S., Varadan, R., Fushman, D., and Pickart, C. M. (2005) Diverse polyubiquitin interaction properties of ubiquitin-associated domains. Nat Struct Mol Biol 12, 708-714
33. Hofmann, K., and Bucher, P. (1996) The UBA domain: a sequence motif present in multiple enzyme classes of the ubiquitination pathway. Trends Biochem Sci 21, 172-173
34. Mattera, R., Tsai, Y. C., Weissman, A. M., and Bonifacino, J. S. (2006) The Rab5 guanine nucleotide exchange factor Rabex-5 binds ubiquitin (Ub) and functions as a Ub ligase through an atypical Ub-interacting motif and a zinc finger domain. J Biol Chem 281, 6874-6883
35. Huang, G., and Singh, B. (2013) Coamplification and cooperation: toward identifying biologically relevant oncogenes. Clin Cancer Res 19, 5549-5551
36. Wang, J., Qian, J., Hoeksema, M. D., Zou, Y., Espinosa, A. V., Rahman, S. M., Zhang, B., and Massion, P. P. (2013) Integrative genomics analysis identifies candidate drivers at 3q26-29 amplicon in squamous cell carcinoma of the lung. Clin Cancer Res 19, 5580-5590
37. Chen, Y., McGee, J., Chen, X., Doman, T. N., Gong, X., Zhang, Y., Hamm, N., Ma, X., Higgs, R. E., Bhagwat, S. V., Buchanan, S., Peng, S. B., Staschke, K. A., Yadav, V., Yue, Y., and Kouros-Mehr, H. (2014) Identification of druggable cancer driver genes amplified across TCGA datasets. PLoS One 9, e98293
38. Seibenhener, M. L., Geetha, T., and Wooten, M. W. (2007) Sequestosome 1/p62--more than just a scaffold. FEBS Lett 581, 175-179
39. Layfield, R., and Searle, M. S. (2008) Disruption of ubiquitin-mediated processes in diseases of the brain and bone. Biochem Soc Trans 36, 469-471
40. Lucas, G. J., Daroszewska, A., and Ralston, S. H. (2006) Contribution of genetic factors to the pathogenesis of Paget's disease of bone and related disorders. J Bone Miner Res 21 Suppl 2, P31-37
41. Daroszewska, A., and Ralston, S. H. (2005) Genetics of Paget's disease of bone. Clin Sci (Lond) 109, 257-263
42. Layfield, R., Ciani, B., Ralston, S. H., Hocking, L. J., Sheppard, P. W., Searle, M. S., and Cavey, J. R. (2004) Structural and functional studies of mutations affecting the UBA domain of SQSTM1 (p62) which cause Paget's disease of bone. Biochem Soc Trans 32, 728-730
43. Lee, J. J., Kim, Y. M., Jeong, J., Bae, D. S., and Lee, K. J. (2012) Ubiquitin-associated (UBA) domain in human Fas associated factor 1 inhibits tumor formation by promoting Hsp70 degradation. PLoS One 7, e40361

Chapter 4

SCCRO3 (DCUN1D3) antagonizes the neddylation and oncogenic activity of SCCRO (DCUN1D1)

G. Huang, C. Stock, C.C. Bommeljé, V.B. Weeda, K. Shah, S. Bains, E. Buss, M. Shaha, W. Rechler, Y. Ramanathan, B. Singh

J. Biol. Chem, 2014 Dec 12; 289(50):34728-42

Abstract

The activity of cullin-RING type ubiquitination E3 ligases (CRLs) is regulated by neddylation, a process analogous to ubiquitination that culminates in covalent attachment of the ubiquitin-like protein Nedd8 to cullins. As a component of the E3 for neddylation, SCCRO/DCUN1D1 plays a key regulatory role in neddylation and, consequently, CRL activity. SCCRO's essential contribution to neddylation is to promote nuclear translocation of the cullin-ROC1 complex. The presence of a myristoyl sequence in SCCRO3, one of four SCCRO paralogs present in humans, that localizes it to the membrane raises questions about its function in neddylation. We found that although SCCRO3 binds to CAND1, cullins, and ROC1, it does not efficiently bind to Ubc12, promote cullin neddylation, or conform to the reaction processivity paradigms—suggesting that SCCRO3 does not have E3 activity. Expression of SCCRO3 inhibits SCCRO-promoted neddylation by sequestering cullins to the membrane, thereby blocking its nuclear translocation. Moreover, SCCRO3 inhibits SCCRO's transforming activity. SCCRO3's inhibitory effects on SCCRO-promoted neddylation and transformation require both an intact myristoyl sequence and PONY domain, confirming that membrane localization and binding to cullins are required for *in vivo* functions. Taken together, our findings suggest that SCCRO3 functions as a tumor suppressor by antagonizing the neddylation activity of SCCRO.

Introduction

Ubiquitination regulates the activity of proteins involved in diverse and essential cellular processes, including transcription, differentiation, signal transduction, cell cycle progression, and apoptosis (1). Although ubiquitination serves as the primary signal targeting proteins for degradation at the proteasome, it can modify protein function in many other ways (2). Ubiquitination results from the sequential activity of activating (E1), conjugating (E2), and ligating (E3) enzymes (3,4), with substrate-derived signals (e.g., misfolding, mutation, and posttranslational modifications [i.e., phosphorylation]) serving as initiators of the cascade (5). E3s provide specificity and serve as the rate-limiting step in ubiquitination. Thus, factors regulating assembly of multiprotein complexes to constitute functional E3 ligases are the primary regulators of ubiquitination activity. For cullin-RING ligases (CRLs), the largest class of mammalian ubiquitination E3s, neddylation of cullin serves as the key signal for assembly of the E3 complex (6,7). Neddylation is a process analogous to ubiquitination, in which a tripartite cascade resulting in covalent modification of the cullin family of proteins by the ubiquitin-like protein Nedd8 is regulated by activity of the neddylation E3 (8-10). We and others identified SCCRO/DCUN1D1 and showed that it functions as a regulatory component in the neddylation E3 (11-15). SCCRO promotes neddylation in three ways: (1) it binds to cullin-ROC1 complexes in the cytoplasm and promotes their nuclear translocation; (2) it enhances recruitment of E2~Nedd8 (Ubc12~Nedd8) thioester to the complex; and (3) it optimizes the orientation of proteins in the complex to allow efficient transfer of Nedd8 from the E2 to the cullin substrates.

SCCRO is not required for neddylation in *in vitro* assays (14), but studies in yeast and *Caenorhabditis elegans* suggest that SCCRO's activity is essential for neddylation, as targeted inactivation of SCCRO results in lethality (12). In contrast, SCCRO knockout mice are viable, likely due to compensation by the SCCRO paralogs, which are exclusively present in higher organisms (14) (unpublished data). Bioinformatics analysis shows that SCCRO has four paralogs in mammals, which can be classified into three subgroups on the basis of their phylogeny and N-terminal sequences: SCCRO and SCCRO2 (DCUN1D2) contain an ubiquitin-associated (UBA) domain, SCCRO3 (DCUN1D3) contains a myristoyl sequence, and SCCRO4 (DCUN1D4) and SCCRO5 (DCUN1D5) contain a nuclear localization signal in the N-terminus. Although it has been suggested that each of the SCCRO family members promotes neddylation, the precise *in vivo* contributions remain to be defined (11-17) (18). Interestingly, N-terminal motifs either directly or indirectly regulate subcellular localization of all SCCRO paralogs. The UBA domain of SCCRO and SCCRO2 regulates its nuclear localization (19). We recently showed that SCCRO5's function as an oncogene requires its nuclear localization signal (NLS) (16). Given the importance of nuclear localization in the neddylation function of SCCRO family members, the presence of a myristoyl sequence in SCCRO3 that localizes it to the membrane raises questions about its *in vivo* activities (17). Moreover, in contrast to the other SCCRO family members, SCCRO3 is reported to function as a tumor suppressor (20). In this study, we sought to determine the mechanisms underlying SCCRO3's contributions to neddylation and human cancer pathogenesis.

We show that, by sequestering cullins to the membrane to prevent their nuclear translocation, SCCRO3 inhibits SCCRO-promoted neddylation and, consequently, CRL-promoted ubiquitination. Its inhibitory effects on SCCRO activity endow SCCRO3 with putative tumor-suppressor function. The high prevalence of reduced SCCRO3 expression in multiple tumor types suggests that it plays a significant role in human cancer pathogenesis.

Experimental procedures

Tumor tissue, cell lines, antibodies, and plasmids

Primary tumor specimens and adjacent normal tissue from head and neck, lung, oral, ovarian, and thyroid neoplasms were collected from patients undergoing surgical resection, after informed consent was obtained and in accordance with institutional guidelines. Cell lines H1299, NIH-3T3, U2OS, and HeLa were obtained from American Type Culture Collection (Manassas, VA); 16HBE was a gift from Dr. Alan Hall (Memorial Sloan-Kettering Cancer Center [MSKCC]). The following antibodies were used: anti-DCUN1D3 (Abnova, Taipei City, Taiwan); anti-Cul1 and Alexa Fluor 488 Phalloidin (Invitrogen, Grand Island, NY); anti-Cul3 (BD Biosciences, San Jose, CA); anti-ROC1 (Spring Bioscience, Pleasanton, CA); anti-Ubc12 (Rockland, Gilbertsville, MA); anti-CAND1 and anti-GST (Upstate, Lake Placid, NY); anti-tubulin (Sigma-Aldrich, St Louis, MO); anti-HA (Covance, Princeton, NJ); anti-Aurora B (BD Biosciences); anti-actin and anti-RhoA (Santa Cruz Biotechnology, Santa Cruz, CA); Cy3-conjugated anti-Myc and FITC-conjugated anti-HA (Jackson ImmunoResearch Laboratories, West Grove, PA); anti-GAPDH (Millipore, Billerica, MA); and secondary antibodies conjugated to horseradish peroxidase (Santa Cruz Biotechnology, Santa Cruz, CA), with dilutions according to the manufacturers' specifications. Anti-SCCRO (rabbit polyclonal) antibody was produced and used as described previously (21).

All DNA constructs were generated using a standard PCR-ligation technique and verified by automated sequencing. Proteins were expressed as glutathione-S-transferase (GST) fusions in *Escherichia coli* strains BL21 (DE3) (Novagen, Madison, WI), were induced overnight at 18°C with the addition of 1 mM IPTG, and were purified by passage through Glutathione Sepharose 4B beads (GE Healthcare Life Sciences, Piscataway, NJ), followed by thrombin cleavage as required. APPBP1/Uba3, Ubc12, and Nedd8 were obtained from a commercial source (Boston Biochem, Cambridge, MA). The human SCCRO3 plasmid was obtained from a commercial source (Clontech, Mountain View, CA). The human PUM2 construct was a gift from Dr. Judith Kimble (Howard Hughes Medical Institute investigator, University of Wisconsin, Madison). SCCRO and SCCRO3 shRNA lentiviral constructs were obtained from Sigma-Aldrich through the high-throughput screening core facility at MSKCC (see Table 1 for sequences). SCCRO3 cDNAs were cloned into pGEX-4T-3 (GE Healthcare Life Sciences, Piscataway, NJ), pBABE (Addgene, Cambridge, MA), or pCMV-HA (BD Biosciences, San Jose, CA) vectors per the manufacturers' protocols. Transfections were performed

with Lipofectamine 2000 (Invitrogen, Grand Island, NY), in accordance with the manufacturer's protocols. Stable overexpression and shRNA knockdown clones were selected in the presence of puromycin. An NIH-3T3 cell line stably expressing *SCCRO* was derived as described previously (21).

Table 1. Primer sequences for SCCRO3 methylation analysis and SCCRO3 mutations and sequences for SCCRO and SCCRO3 knockdown.

Sequence type	Primer
DNA methylation primer sequences	
Methylated(s)	5 – TGGCGATGATATCGAGTCGTTTC – 3
Methylated(as)	5 – GACTCCAAACGCGAAAAACTAACG – 3
Unmethylated(as)	5 – AAAACACCAACTCCAAACACAAAAAAC – 3
Unmethylated(s)	5 – GTTGGTGGTGATGATATTGAGTTGTTTT – 3
cDNA cloning primer sequences	
DCUN1D3 G2A	5 – ATGGCCCAGTGTGTCACCAAGTGTAAG – 3
DCUN1D3 D241N	5 – CATGTTCCAAGTGTTCCGGGAGATGCCCTT – 3
DCUN1D3 A265R	5 – AAAGAGACTTGGCCACCGCTCATCTTCACT – 3
DCUN1D3 D271N	5 – CCACAAAGGTGTTAAAGAGACTTGGCC – 3
DCUN1D3 deletion 1-26	5 – CGGAATTCCGCCGCCACCATGAAGTCACAT – 3
shRNA primer sequences	
Primer shRNA1	5 – CACTTGGAACATGTTCCTTAA – 3
Target shRNA1	5 – CCGGCACTTGGAACATGTTCCTTAACTCGAGTTAAGGAACATGTTCCAAGTGTTTTTTG – 3
Primer shRNA2	5 – CCTTAACTTCACTCAGGTGAT – 3
Target shRNA2	5 – CCGGCCTTAACTTCACTCAGGTGATCTCGAGATCACCTGAGTGAAGTTAAGGTTTTTTG – 3

Real-time reverse-transcriptase PCR

Total RNA was extracted with Trizol reagent (Life Technologies, Grand Island, NY) and repurified using the RNeasy Mini spin column (Qiagen, Valencia, CA). Gene-specific primers were designed using the Primer3 program and were purchased from Operon Technologies (Alameda, CA) (for primer sequences, see Table 2). The relative quantitative analysis of SCCRO3 mRNA expression, normalized to GAPDH, was performed using the 7900HT Sequence Detector System (Applied Biosystems, Foster City, CA). PCR cycling conditions for all samples were as follows: denaturation (94°C for 5 min) and amplification repeated for 40 cycles (94°C for 15 s, Tm for 20 s, 72°C for 20 s). Real-time PCR assays were conducted in duplicate for each sample, and each PCR experiment included 2 nontemplate control wells. A standard curve for serial dilutions of cDNA of head and neck cancer cell lines MDA686 and MDA1186 was similarly generated. The comparative threshold cycle method was used to calculate the SCCRO3/DCUN1D3–like gene expression ratio in each

sample relative to the value observed in the control standard curve, using GAPDH as a control for normalization among samples. Melt curve analysis was performed after amplification. The acquisition temperature was set at 1°C to 2°C below the Tm of the specific PCR product. The relative quantification of a target gene, compared with that of a reference gene (GAPDH rRNA), was performed as described previously (21).

Table 2. Real-time RT-PCR primer sequences.

	Primer	
Gene	Forward	Reverse
SCCRO1/DCUN1D1	5 – CTGGAGGACACCAACATG – 3	3 – TTCACTAGATTGTGTGAAGATC – 5
SCCRO2/DCUN1D2	5 – GTTCACCTCCATTTCTCAATGTG – 3	3 – CTTAGAAATGGCTGTTGCGT – 5
SCCRO3/DCUN1D3	5 – CACAGAATTTCGAGTGCTG – 3	3 – TGCACTTATTGCTTTGCAG – 5
SCCRO4/DCUN1D4	5 – CTGGCAAATATTCATAAGATCTACC – 3	3 – AAGACCGCAGACTTCCTG – 5
SCCRO5/DCUN1D5	5 – TGCGCTCACAGTTGAATGATATTTCGTC – 3	3 – CAGTGGCCATGTCCTCCCAAGCAG – 5
GAPDH	5 – GCACCACCAACTGCTTAG – 3	3 – CATGGACTGTGGTCATGAG – 5

DNA sequencing and mutational analysis, DNA methylation analysis

Putative exonic regions of the *SCCRO3* gene (NCBI Human Genome Build 36.1) were broken into 61 amplicons of 500 bp or less, and specific primers were designed using Primer3. Sequence reactions were run on an ABI PRISM 3730xl sequencing apparatus (Applied Biosystems, Foster City, CA). PCR was performed in 384-well plates, in a Duncan DT-24 water bath thermal cycler, with 10 ng of whole-genome amplified DNA (Repli-G Midi; Qiagen, Valencia, CA) as template, using a touchdown PCR protocol with HotStart Taq (Kapa Biosystems, Cape Town, South Africa). Templates were purified using AMPure (Agencourt Biosciences, Beverly, MA). The purified PCR reactions were split in 2 and sequenced bidirectionally with M13 forward and reverse primer and Big Dye Terminator Kit (version 3.1; Applied Biosystems, Foster City, CA) at Agencourt Biosciences. Dye terminators were removed using the CleanSEQ kit (Agencourt Biosciences). Mutations were detected using an automated detection pipeline at the Memorial Sloan-Kettering Cancer Center Bioinformatics Core. Bidirectional reads and mapping tables (to link read names with sample identifiers, gene names, read direction, and amplicon) were subjected to a quality control filter, which excludes reads that have an average Phred score of <10 for bases 100 to 200. Passing reads were assembled against the SCCRO3 reference sequence, containing all coding and UTR exons, including 5 Kb upstream and downstream of the gene, using command line Consed 16.0 (22). Assemblies were passed on to Polyphred 6.02b (23) and Polyscan 3.0 (24), generating lists of putative mutations. Putative mutation calls were normalized to "+" genomic coordinates and annotated using the Genomic Mutation Consequence Calculator (25). The resulting list was loaded into a Postgres database, along with select assembly details for each mutation call. To reduce the number of false-positives generated by the mutation detection software packages, only point mutations supported by at

least 1 bidirectional read pair and at least 1 sample mutation called by Polyphred were considered, and only the putative mutations annotated as having nonsynonymous coding effects and that occurred within 11 bp of an exon boundary or had a conservation score >0.699 were included in the final candidate list. Indels called by any method were manually reviewed and included in the candidate list if found to hit an exon. All putative mutations were confirmed by a second PCR and sequencing reaction, in parallel with amplification and sequencing of matched normal-tissue DNA.

For DNA methylation analysis, genomic DNA was extracted from primary lung tumors by use of All Prep DNA/RNA (Qiagen, Valencia, CA). Bisulfite conversion of genomic DNA was performed using the EZ DNA methylation kit (Zymo Research, Irvine, CA). One microgram of genomic DNA was used. Methylation-specific PCR was performed using primers designed for methylated and unmethylated promoter sequences using the program MSPPrimer. Methylation-specific PCR was performed as previously described (26). All PCR products were analyzed by electrophoresis on a 2.5% agarose gel. Primers are listed in Table 1.

GST pull-down assay

GST-tagged proteins were bound to Glutathione Sepharose beads (GE Healthcare Life Sciences, Piscataway, NJ) by gentle rocking at 4°C for 30 min. The beads were washed 4 times with EBC buffer (50 mM Tris-HCl [pH 7.5], 2.5 mM $MgCl_2$, 150 mM NaCl, and 0.5% Nonidet P-40) at 20x bead volume. The beads were incubated with 500 µg of HeLa cell lysate or purified proteins, as indicated, at 4°C for 1 h, followed by 3 washes with EBC buffer at 20x bead volume. Bound proteins were eluted by the addition of 6x Laemmli buffer or nonreducing Laemmli buffer (when thioester bonds were involved), were resolved on SDS-PAGE gels, and were analyzed by Western blot.

Thioester reactions

Reactions were performed at room temperature in buffer (50 mM Tris-HCl [pH 7.6], 50 mM NaCl, 10 mM $MgCl_2$, and 0.5 mM DTT) with 4 mM ATP, 80 nM APPBP1/Uba3, 800 nM Ubc12, and 9 µM Nedd8. After 10 min, which was previously determined to be the optimal reaction time (15), reactions were quenched by the addition of EDTA (to a final concentration of 50 mM) and were purified on a G-50 micro spin desalting column (GE Healthcare Life Sciences, Piscataway, NJ). Next, 13.1 µL of reaction product containing 10 pmol Ubc12 was added to 1 nmol GST-SCCRO binding assay with a gradient of purified protein as indicated. The wash and detection sequences were as described above. The presence of Ubc12~Nedd8 thioester complexes was verified by Western blot analysis for Ubc12. Ponceau S stain was performed as a loading control.

In vivo and in vitro neddylation assay

For *in vivo* neddylation, cell lysates were directly subjected to immunoblotting for cullin(s). *In vitro* neddylation assays were performed, as described previously (15), using HeLa lysate (as a source of

cullin-ROC1) and purified SCCRO/SCCRO3 proteins or lysate from U2OS cells transfected with *HA-SCCRO3* and *Myc-Cul1*. The reaction mixture also contained recombinant Nedd8 (2 μM), E1 (5 nM), E2 (5 μM), and ATP (4 mM).

Cell morphologic analysis

Cells were seeded in chamber slides (Lab-Tek; Thermo-Fisher Scientific, Rochester, NY), incubated in appropriate media for 24 h at 37°C with 5% CO_2, washed with PBS, and photographed using phase-contrast microscopy at 4x and 10x magnification (Olympus IX71).

Immunofluorescence analysis

H1299 cells, 16HBE cells, and U2OS cells transfected with the indicated plasmids were seeded in chamber slides or 6-well plates with cover glass and left overnight at 37°C in 5% CO_2. Twenty-four hours after seeding or after transfection, cells were washed (PBS) and fixed in 4% formaldehyde for 10 min or were fixed with methanol acetone for 20 min at -20°C. Fixed cells were permeabilized with 0.5% Triton X-100 (Spectrum Chemicals, Gardena, CA) for 5 min, were stained with Alexa Fluor 488 Phalloidin for 30 min at room temperature or incubated in blocking buffer (1% bovine serum albumin in PBS-T) for 30 min, were washed (PBS), and were stained overnight in a humid chamber at 4°C with fluorochrome-conjugated antibodies. The cells were washed 3 times (PBS), were counterstained with DAPI (Vector Laboratories, Burlingame, CA), were washed an additional 3 times (PBS), were covered by ProLong Gold Antifade Reagent (Invitrogen, Grand Island, NY), and were examined with Leica and Olympus IX71 inverted confocal microscopes fitted with appropriate fluorescence filters at 20x or 63x magnification. For the subcellular localization assay, percentages of nuclear and nonnuclear Cul1 were calculated on the basis of 200 transfected cells for each condition.

Cell motility and transformation assays

For scratch assays, cells were plated and grown until they formed a confluent monolayer. Cells were then starved of serum for 24 h and treated with mitomycin C for 90 min to arrest cell proliferation, using a previously published protocol (27). The monolayer was scratched in a straight line using a 20-μL pipette tip. We checked these cells at intervals to ensure that cells were migrating across the scratch, rather than broad-front advancement resulting from cell proliferation. The cells were washed with PBS and then photographed using a phase-contrast microscope (Olympus IX71) at 4x magnification. The petri dishes were placed at 37°C in humidified air with 5% CO_2 for 24 or 36 h, depending on the cell line, and were then photographed in the same location. For soft agar assays, vector, SCCRO3, or mutant DNA was stably transfected into H1299 cells, as well as into NIH-3T3 cells stably transfected with SCCRO, and the cells were plated in 0.35% agarose-coated 6-well plates, at densities of ~1000 and ~5000 cells in agarose. After incubation for 2 to 6 weeks, cells were stained

with 0.005% crystal violet (Sigma-Aldrich) and photographed using a dissecting microscope (Leica Stereoscope MZ FL-III). Colony counts were obtained using Image J software (NIH, Bethesda, MD).

Statistical analysis

Descriptive statistics were used to summarize study data. Qualitative (Fisher's exact test) and quantitative (Mann-Whitney U test) comparisons were performed using nonparametric assays. Statistical significance was defined as a two-tailed $P \leq 0.05$. All statistical analyses were performed using a commercially available statistical software package (SPSS, Chicago, IL, or SAS, Durham, NC).

Results

SCCRO3 expression is decreased in human tumors

We and others have shown that amplification and overexpression of SCCRO are common in many different types of human cancer and that they underlie its function as an oncogene (21,28-30). To determine whether SCCRO3 is also involved in cancer pathogenesis, we assessed its expression in lung, oral, ovarian, and thyroid neoplasms and matched normal tissue by real-time PCR (Fig. 1A). Expression of SCCRO mRNA was increased in many different tumor types studied, which is consistent with its known oncogenic activity (Fig. 1B). In contrast, SCCRO3 mRNA levels were decreased in a wide range of cancers, including in 58% of lung squamous cell carcinomas (n=40), 38% of lung adenocarcinomas (n=40), 85% of lung neuroendocrine tumors (n=54), 21% of oral squamous cell carcinomas (n=39), 20% of ovarian carcinomas (n=40), and 27% of thyroid tumors (n=56). We further subclassified tumors to assess those with an increase of SCCRO only, a decrease of SCCRO3 only, or both (Fig. 1B). Interestingly, there was a trend toward mutual exclusivity, with 127 cases having either an increase of SCCRO or a decrease of SCCRO3 expression and only 31 tumors having both. Co-dysregulation of SCCRO and SCCRO3 was most common among lung squamous cell carcinomas and neuroendocrine carcinomas. It remains to be determined whether co-dysregulation of SCCRO paralogs increases oncogenicity. Given that *SCCRO* and *SCCRO5* function as oncogenes, the decreased expression of SCCRO3 in human cancers is somewhat unexpected, but it is supported by previously published analyses of liver, bladder, and renal tumors (20) (16,31).

PUM2 regulates SCCRO3 levels in human tumors

To determine the cause of the decreased expression of SCCRO3 in human cancers, we assessed published genomic screening data. This did not identify any tumor types with recurrent chromosomal losses involving the SCCRO3 locus at 16p12.3 (32-34). The absence of chromosomal losses at 16p12.3 was validated by our analysis of results from array comparative genomic hybridization and/or single-nucleotide polymorphism investigations performed on thyroid, head and neck, lung, and

neuroendocrine tumors at our institution (data not shown). These findings suggest that genomic loss is not a cause of the decreased expression of SCCRO3 in human cancers. To determine whether expression of SCCRO3 is altered by mutations, we performed exon sequencing on DNA extracted from 216 thyroid, oral, and lung tumors with decreased expression of SCCRO3 mRNA, as well as on matched normal tissue. Although several single-nucleotide polymorphisms were detected (NCBI nos. rs1858901, rs34248677, rs35094690, and rs7187522), no mutations were identified in the coding region of *SCCRO3* in these tumors (data not shown). Analysis of large-scale cancer genomics data sets using the cBioPortal (www.cbioportal.org) revealed the presence of several mutations in *SCCRO3*. The prevalence of mutation (highest prevalence in melanoma [2.5% in Broad data set and 2% in TCGA data set]) was significantly lower than the prevalence of a decrease of expression of SCCRO3, suggesting that additional mechanisms may be responsible for changes in expression.

Analysis of the *SCCRO3* promoter sequence identified multiple CpG islands, prompting us to investigate DNA methylation as a mechanism of *SCCRO3* silencing (35). Methylation was assessed by PCR using the bisulfate method, with matched normal tissue serving as controls. Hypermethylation of the *SCCRO3* promoter region was not detected in any of the samples tested (Fig. 1C). These findings suggest that the decreased expression of SCCRO3 is likely not caused by changes in transcription.

We next investigated the presence of posttranscriptional factors that could affect SCCRO3 levels in human cancer. Proteins that decrease mRNA stability have emerged as key regulators of gene expression in normal and cancerous cells (36). Recent studies identified PUM2 as a *SCCRO3* mRNA–binding protein, raising the possibility that it affects translation (37). PUM2 is a member of the PUF family of proteins, which bind to sequence elements in the 3′ UTR of target mRNAs to affect stability and/or translation of the message. Immunoblotting analysis showed that PUM2 protein levels inversely correlated with levels of SCCRO3 mRNA in tumor and matched normal tissue and cancer cell lines, suggesting that an association between PUM2 levels and decreased SCCRO3 expression exists in human cancers (Fig. 1D). To determine whether PUM2 directly affects SCCRO3 levels, we expressed PUM2 in 16HBE cells, an immortalized benign human bronchial epithelial cell line that has low levels of PUM2 and high levels of endogenous SCCRO3. Western blotting analysis of lysates from 16HBE cells transiently transfected with HA-tagged *PUM2* showed a decrease in levels of SCCRO3, but not SCCRO (Fig. 1E, lane 3). Moreover, knockdown of PUM2 using shRNA in H1299 cells (a human non-small cell lung carcinoma cell line that has high levels of PUM2 and low levels of SCCRO3) resulted in an increase in levels of SCCRO3, but not SCCRO (Fig. 1F, lanes 3 and 4). To begin to elucidate how PUM2 controls SCCRO3 expression, we assessed SCCRO3 mRNA levels, using real-time PCR, in 16HBE cells overexpressing PUM2 and H1299 cells after siRNA-knockdown of PUM2. We found that overexpression of PUM2 reduced the levels of SCCRO3 mRNA, whereas knockdown of PUM2 increased its levels relative to controls (Fig. 1G). These findings suggest that PUM2 regulates SCCRO3 at the mRNA level. Next, to determine whether PUM2 regulates SCCRO3 mRNA at the level of transcription or whether it affects its stability, we treated PUM2-transfected

16HBE cells with Actinomycin D to stop transcription. Inhibition of transcription in 16HBE cells resulted in a significantly greater decrease in SCCRO3 mRNA levels in PUM2, compared with vector-transfected cells, suggesting that PUM2 affects SCCRO3 mRNA stability (Fig. 1G). Taken together, these findings suggest that SCCRO3 mRNA is a target of PUM2-mediated decay, which may explain the decreased SCCRO3 expression in at least some human tumors.

Figure 1. SCCRO3 expression in human tumors has an inverse relationship with PUM2 levels.

A

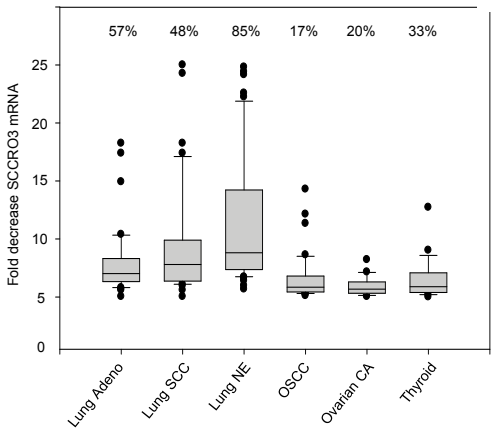

B

Tumor type	SCCRO	SCCRO3*	SCCRO only (n)	SCCRO3 only* (n)	Both (n)
Lung squamous cell carcinoma (n=40)	55%	58%	9	10	13
Lung adenocarcinoma (n=40)	5%	38%	2	15	0
Lung neuroendocrine carcinoma (n=54)	35%	85%	3	30	16
Oral squamous cell carcinoma (n=39)	38%	21%	13	6	2
Oligodendroma (n=10)	60%	0%	6	0	0
Ovarian Carcinoma (n=40)	18%	20%	7	8	0
Thyroid benign nodular hyperplasia (n=9)	11%	22%	1	2	0
Thyroid adenoma (n=9)	0%	22%	0	2	0
Thyroid Hurtle Carcinoma (n=10)	10%	60%	1	6	0
Thyroid papillary carcinoma (n=18)	6%	17%	1	3	0
Thyroid tall cell carcinoma (n=10)	0%	20%	0	2	0

*% of cases with decrease in SCCRO3 expression

C

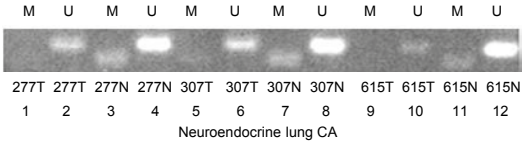

D

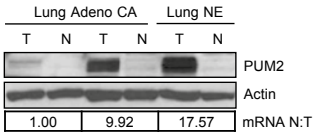

E

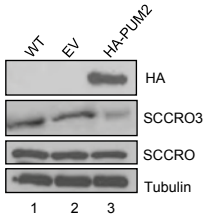

F

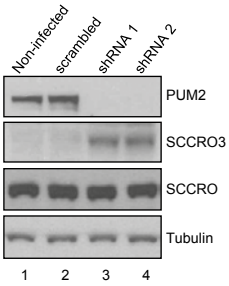

G

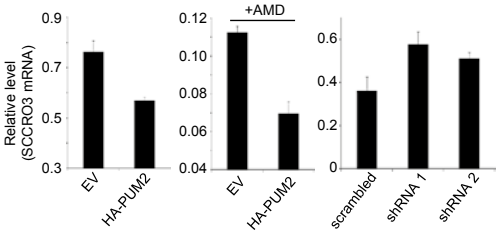

(**A**), Box plot showing fold decrease in SCCRO3 mRNA levels as measured by Real-time RT-PCR in lung adenocarcinoma (Adeno), squamous cell carcinoma (SCC), neuroendocrine carcinomas (NE), oral squamous cell carcinoma (OSCC), ovarian carcinoma (CA), and thyroid tumor samples, compared with those in matched normal tissue. (**B**), Results from quantitative real-time PCR analysis showing percentage of cases with *SCCRO* over-expression and decreased *SCCRO3* expression in the indicated tumor types. Columns 4 to 6 represent the numbers of cases with an increase of SCCRO only, of a decrease of SCCRO3 only, and of both an increase of SCCRO and a decrease of SCCRO3. (**C**), Bisulfate-treated DNA from 3 representative neuroendocrine lung tumor samples (and matched normal samples) with decreased SCCRO3 mRNA expression was PCR amplified using *SCCRO3* promoter–specific primer pairs for methylated (M) and unmethylated (U) DNA. PCR product was obtained (lanes 3, 7, and 11) only in template DNA from normal tissue, using primer pair (M). (**D**), Western blot analysis of lysates from lung adenocarcinoma or neuroendocrine carcinomas (T) and matched histologically normal tissue (N) showing inverse correlation between PUM2 protein levels and SCCRO3 mRNA expression in tumors by real-time PCR analysis (shown below the blot). (**E**), Western blot analysis of lysates from untransfected (WT), empty vector (EV) or HA-PUM2 transfected 16HBE cells probed with anti-HA (top), anti-SCCRO3 (2nd panel), anti-SCCRO (3rd panel), and anti–α-tubulin (loading control; bottom panel) antibodies, showing a decrease in SCCRO3 but no change in SCCRO levels in cells expressing HA-PUM2 (lane 3). (**F**), Western blot analysis of lysates from H1299 cells showing a decrease in PUM2 and increase in SCCRO3 levels in cells infected with virus expressing shRNA against *PUM2* (shRNA1 and shRNA2) compared with uninfected cells or those infected with a virus expressing scrambled shRNA. (**G**), Real-time RT-PCR analysis for SCCRO3 expression on RNA extracted from experiments in E (left two panels) and F (right panel). AMD (Actinomycin D) was used to inhibit transcription after transfection.

SCCRO3 interacts with CAND1, cullins, and ROC1 via its PONY domain

To begin to define the role of SCCRO3 in cancer pathogenesis, we first assessed its biochemical activities. Previous studies have shown that SCCRO interacts with proteins involved in neddylation, including CAND1, cullins, ROC1, and Ubc12, via its PONY domain (11,12,15,38). Given the presence of a highly conserved PONY domain in SCCRO3, we assessed its binding to components of the neddylation E3. Immunoblots of products from GST-SCCRO3 pull-down assays of HeLa lysates showed that SCCRO3 interacts with CAND1, Cul1, Cul3, and ROC1 (Fig. 2A, lane 3). To define the regions involved in binding, we created mutations in residues in the PONY domain of SCCRO3 (corresponding to the DAD patch) that are required for binding of SCCRO to neddylation components (SCCRO3^{D241N}, SCCRO3^{A265R}, SCCRO3^{D271N}, SCCRO3$^{A265R/D271N}$, and SCCRO3$^{D241N/A265R/D271N}$ [SCCRO3^{DAD}]), as well as in the N-terminal myristoyl sequence (SCCRO3$^{\Delta 1\text{-}26}$ and SCCRO3^{G2A}) (11). GST pull-down assays of HeLa lysates showed that the SCCRO3–DAD patch mutants (Fig. 2A, lanes 4-8), but not the N-terminal mutants (Fig. 2A, lanes 9 and 10), lost binding to CAND1, cullins, and ROC1. These findings confirm that, as with SCCRO, SCCRO3's interaction with neddylation components requires its PONY domain.

SCCRO3 does not bind to Ubc12

Unlike SCCRO, SCCRO3 had no interactions with Ubc12 detected in GST pull-down assays of HeLa lysates (Fig. 2A). These findings contrast results from Meyer-Schaller et al. (17), who found that GST-Ubc12 binds to bacterially purified His-SCCRO3. We were also able to detect binding between GST-SCCRO3 and Ubc12 using purified proteins, but only when very high concentrations of protein

were used for GST pull-down, raising the possibility that the observed interactions are nonspecific (data not shown). Selective interaction between E3s and E2s charged with ubiquitin or ubiquitin-like protein, rather than free E2s, is a key mechanism for maintenance of reaction processivity. To determine whether binding to Ubc12 is functionally relevant, we assessed whether SCCRO3 maintains the reaction processivity paradigms that are conserved in all E3s for ubiquitin and ubiquitin-like protein in their interactions with E2s. We previously showed that SCCRO binds to Ubc12~Nedd8 thioester with a much higher affinity than to free Ubc12, which is consistent with its function as an E3 (11,15) (39). GST pull-down assays of the products of thioester reactions containing roughly equal quantities of free Ubc12 and Ubc12~Nedd8 thioester, followed by immunoblotting, showed that, whereas GST-SCCRO preferentially bound to Ubc12~Nedd8 thioester, GST-SCCRO3 did not bind to either Ubc12 or Ubc12~Nedd8 under identical conditions (Fig. 2B). To confirm these differences in binding efficiency, we performed the GST-SCCRO pull-down in identical experiments, adding either bacterially derived, thrombin-cleaved SCCRO or SCCRO3 to the reaction mix before the pull-down. The addition of a 10-fold molar excess of SCCRO, but not SCCRO3, blocked pull-down of Ubc12~Nedd8 by GST-SCCRO, confirming that SCCRO binds to Ubc12~Nedd8 with much higher efficiency than SCCRO3 does (Fig. 2C). These observations suggest that SCCRO3 does not conform to the conserved processivity paradigms for E3s in the ubiquitin and ubiquitin-like protein pathway, and they raise questions about its function as an E3 in neddylation.

SCCRO3 does not augment cullin neddylation in vitro

Given the limited binding of SCCRO3 to Ubc12~Nedd8, we questioned whether SCCRO3 can augment cullin neddylation. *In vitro* neddylation reactions were performed using HeLa cell lysate (as a source of cullin-ROC1 substrate) supplemented with recombinant Nedd8, APPBP1/Uba3 (E1), Ubc12 (E2), ATP, and varying amounts of either purified SCCRO or SCCRO3 (Fig. 2D). As expected, SCCRO augmented cullin neddylation in a dose-dependent manner. Under identical conditions, SCCRO3 was associated with a minimal increase of neddylated Cul3. The changes in the levels of neddylated Cul3 were independent of the dose of SCCRO3, suggesting that the observed changes may not reflect the physiological activity of SCCRO3. Combined, these findings suggest that SCCRO3 does not promote neddylation of cullins with the same efficiency as SCCRO.

Figure 2. SCCRO3 does not function as a component of the neddylation E3.

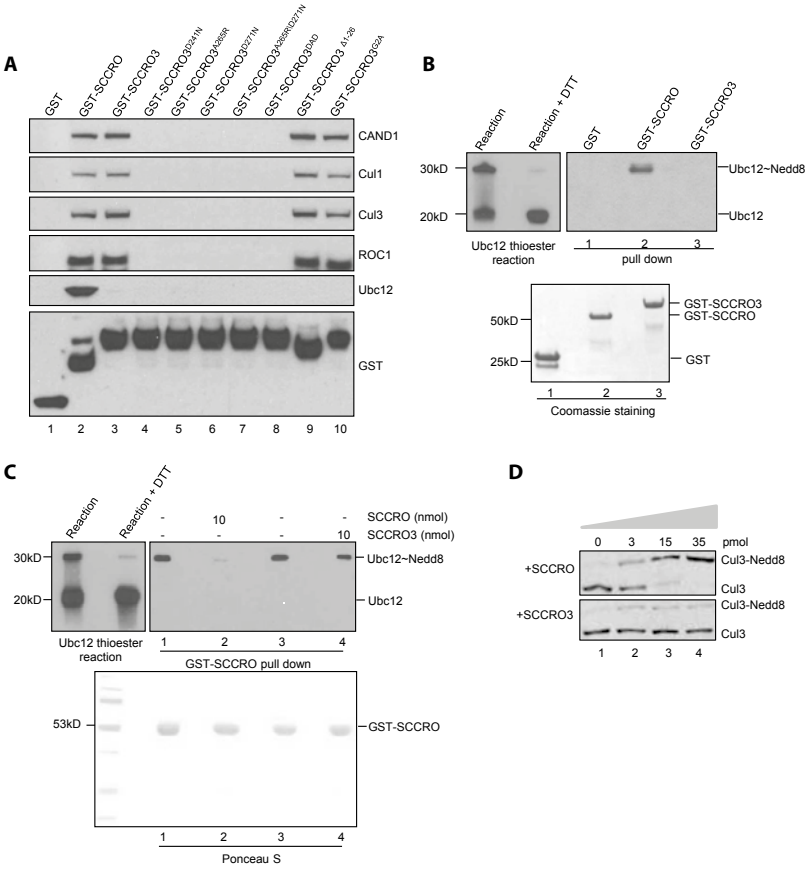

(**A**), Western blot analysis of the pull-down products of GST-SCCRO, GST-SCCRO3 or GST-SCCRO3 mutants from HeLa extracts probed with indicated antibodies, which showed GST-SCCRO (control; lane 1) binds to all the indicated proteins. SCCRO3 and its N-terminal mutants, but not its C-terminal mutants, bind to CAND1, Cul1, Cul3, and ROC1. Neither SCCRO3 nor its mutants showed binding to Ubc12. The levels of the various GST-tagged proteins used in the pull-down experiment were confirmed by probing a Western blot with anti-GST antibody (bottom panel). (**B**), Western blot analysis probing for Ubc12 on a thioester reaction, which showed generation of Ubc12~Nedd8 thioester (left panel, left lane 30kD band) and a specific reduction of thioester bonds with the addition of DTT (left panel, right lane); and Western blot analysis of the products of GST, GST-SCCRO, and GST-SCCRO3 pull-down assays from the same Ubc12 thioester reaction mixture, which showed a preferred interaction of GST-SCCRO with Ubc12~Nedd8 (right panel, lane 2) and no interaction of GST or GST-SCCRO3 with Ubc12~Nedd8 or free Ubc12 (right panel, right lane). Coomassie blue staining showing levels of GST and GST-tagged proteins (bottom panel). (**C**), Western blot analysis of a thioester reaction, showing a generation of UBC12~Nedd8 thioester (left panel, left lane, 30kD band) and its reduction with the addition of DTT (left panel, right lane); and Western blot analysis of the products of GST-SCCRO pull-down assays (1 nmol GST-SCCRO per assay) from the same Ubc12 thioester reaction (right panel) supplemented with 10 nmol of untagged SCCRO or SCCRO3 protein as indicated, which showed addition of 10x free SCCRO but not SCCRO3 blocked binding between Ubc12 and GST-SCCRO. Ponceau S staining of the blot showed equal loading. (**D**), Western blot analysis of the products of an in vitro neddylation reaction with HeLa lysate (as a source of cullin-ROC1) supplemented with a concentration gradient of either SCCRO (upper panel) or SCCRO3 (lower panel) purified proteins, which showed a dose-dependent increase in Cul3 neddylation with addition of SCCRO but not SCCRO3.

SCCRO3 competes with SCCRO for Cul1 localization

Recent work from our laboratory suggests that subcellular localization plays an important role in regulating cullin neddylation (14). To determine whether SCCRO3 affects cullin localization, HA-tagged *SCCRO*, *SCCRO3*, or selected *SCCRO3* mutants were cotransfected with Myc-tagged *Cul1* into U2OS cells. Localization of proteins expressed from transgenes was assessed by immunofluorescence with FITC-conjugated anti-HA and Cy3-conjugated anti-Myc antibodies. We found that Cul1 and SCCRO3 were colocalized to the plasma membrane (Fig. 3A, 2nd row and Fig. 3B) and SCCRO3^{DAD} was localized to the membrane without Cul1, whereas neither SCCRO3^{G2A} nor Cul1 localized to the membrane when cotransfected (Fig. 3A, 3rd and 4th rows). These findings show that SCCRO3 promotes localization of Cul1 to the membrane and that this requires both an intact myristoyl sequence and PONY domain.

Given our previous findings showing that SCCRO-promoted nuclear translocation of Cul1 is required for neddylation *in vivo*, we next questioned whether SCCRO3 competes with SCCRO for binding and localization of Cul1. To address this question, we assessed the localization of Myc-Cul1 while varying the ratio of SCCRO to SCCRO3 by shRNA knockdown or transgene expression in U2OS cells. As expected, we found that SCCRO promoted nuclear translocation, resulting in its colocalization with Cul1 in the nucleus (Fig. 3A, top row and Fig. 3B). Knockdown of SCCRO using shRNA cells led to localization of Cul1 at the cell membrane (Fig. 3C and 3D). In contrast, knockdown of SCCRO3 led to an increase of Cul1 in the nucleus (Fig. 3C and 3E). Note that shRNA knockdown of SCCRO3 did not result in removal of all Cul1 from the membrane, likely due to incomplete knockdown of SCCRO3. When SCCRO3 and SCCRO were coexpressed at equal levels in U2OS cells, Cul1 primarily localized to the membrane. Increasing the level of SCCRO expression relative to SCCRO3 expression in U2OS cells resulted in a dose-dependent increase in nuclear translocation of Cul1 (Fig. 3A, last two rows and Fig. 3B). These findings suggest that SCCRO3 antagonizes the SCCRO-promoted nuclear translocation of Cul1.

Figure 3. SCCRO3 competes with SCCRO for subcellular localization of cullins.

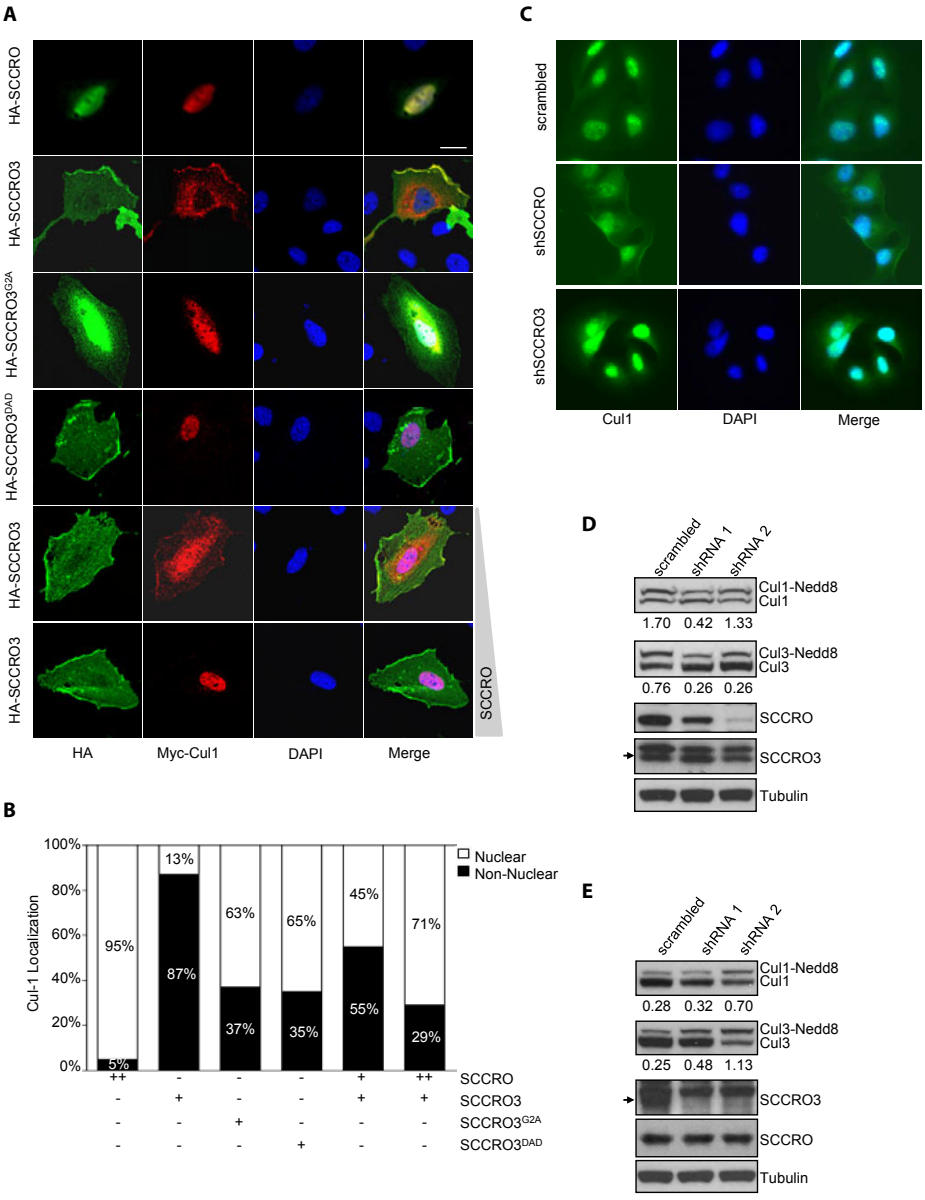

(**A**), Representative images from fluorescence microscopy (scale bar represents 20 µm) showing U2OS cells cotransfected with Myc-*Cul1*, the indicated HA-tagged constructs and varying concentrations of untagged SCCRO (rows 5 and 6) stained with FITC-conjugated anti-HA (column 1) and Cy3-conjugated anti-Myc antibody (column 2) or DAPI (Column 3). Merged images are shown (column 4). Myc-Cul1 co-localized with HA-SCCRO (row 1) in the nucleus and HA-SCCRO3 at the membrane (row 2). HA-SCCRO3^{G2A} loses membrane localization

and Myc-Cul1 is primarily nuclear in these cells (row 3). HA-SCCRO3^{DAD} retains membrane localization, but HA-Cul1 does not co-localizes with it (row 4). Co-transfection of increasing concentrations of SCCRO with HA-SCCRO3 results in progressive translocation of Myc-Cul1 from the membrane to the nucleus (rows 5 and 6). (**B**), Graph showing subcellular distribution of HA-Cul1 from experiment above at varying concentrations of SCRRO and SCCRO3. (**C**), Representative fluorescence microscopic images of U2OS cells transfected with scrambled shRNA, or shRNA against SCCRO or SCCRO3 stained for Cul1 using antibody against Cul1 (column 1) and DAPI (column 2) and merged (column 3). Knockdown of SCCRO resulted in localization of a fraction of Cul1 to the cell membrane (row 2). Knockdown of SCCRO3 increased the proportion of Cul1 in the nucleus (row 3). (**D**), Western blot analysis of lysates from U2OS cells expressing shRNA against *SCCRO* (shRNA1 and shRNA2) showing reduced levels of SCCRO (row 3), but not SCCRO3 (row 4), and a decrease in the proportion of neddylated Cul1 and Cul3. (**E**), Western blot analysis of lysates from U2OS cells expressing shRNA against *SCCRO3* (shRNA1 and shRNA2) showing decreased SCCRO3, but not SCCRO expression, and an increase in the proportion of neddylated Cul1 and Cul3. The numbers below the blots are the ratios of neddylated to nonneddylated cullins.

SCCRO3 antagonizes SCCRO-promoted cullin neddylation

Given that SCCRO3 antagonizes SCCRO-promoted nuclear translocation, we questioned whether this activity also affects cullin neddylation *in vivo*. U2OS cells were transfected with *SCCRO3*, *SCCRO3^{G2A}*, or *SCCRO3^{DAD}*, alone or in combination with varying amounts of *SCCRO*, and the levels of neddylated Cul1 *in vivo* were assessed by immunoblotting. Transfection of vector alone, *SCCRO3*, *SCCRO3^{G2A}*, or *SCCRO3^{DAD}* did not enhance Cul1 neddylation beyond basal levels (Fig. 4A, lanes 1-4). Expression of SCCRO increased levels of neddylated Cul1. Coexpression of SCCRO3, but not SCCRO3^{G2A} or SCCRO3^{DAD}, reduced the level to which SCCRO enhanced Cul1 neddylation (Fig. 4A, lanes 6 and 7; Fig. 4B). The inhibitory effects of SCCRO3 on Cul1 neddylation could be rescued by increasing SCCRO expression in a dose-dependent manner (Fig. 4A, lanes 2, 5, and 6). These results suggest that SCCRO3 antagonizes SCCRO-mediated cullin neddylation *in vivo*.

Figure 4. SCCRO3 antagonizes SCCRO-promoted cullin neddylation.

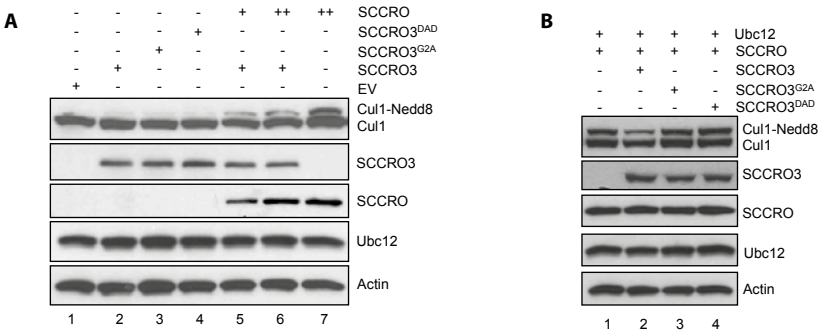

(**A**), Western blot analysis of the products of lysates of U2OS cells transfected with the *SCCRO*, *SCCRO3*, and/or *SCCRO3* mutants as indicated. Expression of SCCRO3 or its mutants had no effect on levels of neddylated Cul1 (lanes 2-4). Expression of SCCRO increased the fractions of neddylated Cul1 (lane 7). Co-expression of SCCRO3 decreased the extent to which SCCRO increased levels of neddylated Cul1 (lane 6). The effect of SCCRO3 on neddylated Cul1 levels could be partially rescued by increasing SCCRO expression levels (lanes 2, 5, and 6). (**B**), Western blot analysis on lysates from U2OS cells cotransfected with *Ubc12* and the indicated *SCCRO*/*SCCRO3* constructs. Coexpression of SCCRO3 (compare lane 1 with 2), and not SCCRO3 mutants, inhibits SCCRO-augmented Cul1 neddylation (compare lane 2 with lanes 3 and 4).

Putative tumor suppressor function of SCCRO3 requires its PONY domain and myristoyl sequence.

Because SCCRO is known to function as an oncogene, we questioned if SCCRO3's putative tumor suppressor activity involves its antagonism of SCCRO's neddylation activity. To confirm SCCRO3 functions as a tumor-suppressor, we assessed effects of its knock down in 16HBE cells. Knockdown of SCCRO3 by virally delivered shRNA resulted in a decrease in levels of SCCRO3 protein (but not SCCRO) relative to levels in 16HBE cells infected with virus expressing scrambled shRNA controls (Fig. 5A). Microscopic evaluation showed 16HBE cells in which SCCRO3 was stably knocked down changed from epitheloid to spindle shaped. These cells also showed alteration in their pattern of growth, spreading widely across the plate, rather than growing in islands, as seen in parental 16HBE cells or those infected with scrambled shRNA control (Fig. 5B). Scratch assays showed that cells in which SCCRO3 was knocked down had more directional motility than scrambled shRNA–infected cells (Fig. 5C). Staining for actin, using Alexa Fluor 488 Phalloidin, showed a reduction in stress fibers in SCCRO3 knockdown cells, compared with scrambled shRNA–infected cells (Fig. 5D).

To begin to determine the mechanisms underlying SCCRO3's effects on transformation, we performed structure-function studies in H1299 cells. We stably transfected H1299 cells with empty vector, *HA-SCCRO3*, *HA-SCCRO3*^{G2A}, or *HA-SCCRO3*^{DAD} and confirmed that transgenes were expressed at approximately equal levels by Western blot (data not shown). Microscopic analysis showed that *SCCRO3*-transfected cells acquired an epitheloid shape and grew in nests (Fig. 5E, 2nd row, first image). In contrast, vector-, *SCCRO3*^{G2A}-, and *SCCRO3*^{DAD}-transfected cells were spindle shaped and were scattered throughout the plate, resembling features seen in untransfected H1299 cells (Fig. 5E, 1st, 3rd, and 4th rows). Scratch assays showed that migration across the scratch was markedly reduced in H1299 cells expressing *SCCRO3,* compared with that in vector-, *SCCRO3*^{G2A}-, and *SCCRO3*^{DAD}-transfected cells (Fig. 5F and 5G). Staining with phalloidin showed rearrangement of the actin cytoskeleton, with stress fibers developing in *SCCRO3*-transfected cells but not in vector- or *SCCRO3* mutant-transfected cells (Fig. 5H). To determine SCCRO3's oncogenic activity, we performed soft-agar assays, which showed reduced colony formation in *SCCRO3*-transfected but not *SCCRO3*^{G2A}- or *SCCRO3*^{DAD}-transfected H1299 clones (Fig. 6A and 6B). These observations suggest that SCCRO3 functions as a putative tumor suppressor that requires membrane localization and binding to cullins.

Given the significant impact of mutation on SCCRO3's function, we critically assessed mutations occurring in human cancers. Interestingly, we found mutations in both the myristoyl sequence (SCCRO3^{G2S}) and the PONY domain, including SCCRO3^{S239F}, which occurred with a loss of the wild-type allele (www.cbioportal.org). The presence of naturally occurring mutations in human tumors that can abrogate SCCRO3's function supports the role of SCCRO3 as a putative tumor suppressor and as well as the requirement of the PONY domain and myristoyl sequence for this activity.

Figure 5. SCCRO3 has tumor suppressor activity that requires its myristoyl sequence and PONY domain.

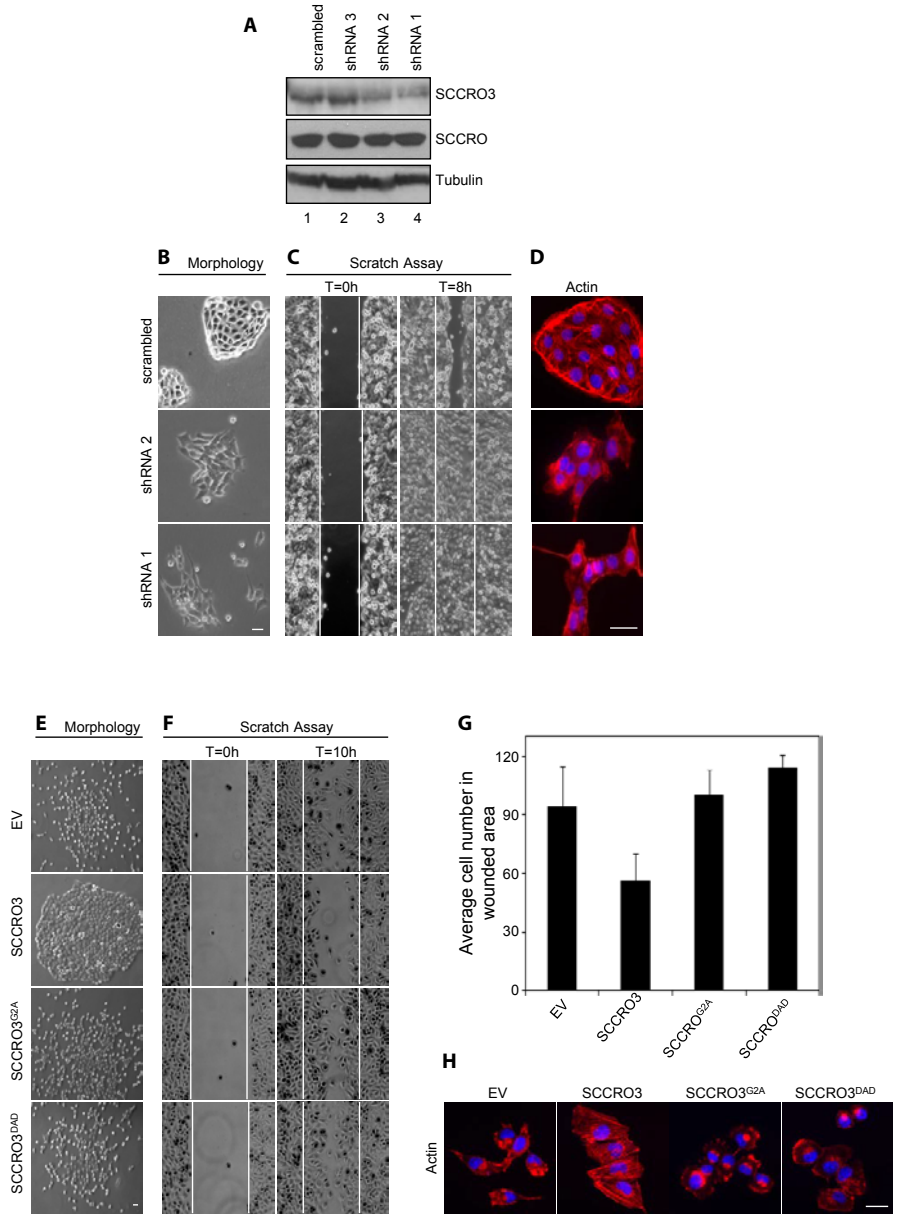

(**A**), Western blot analysis of lysates from 16HBE cells showing a decrease in SCCRO3 levels in cells infected with shRNA against *SCCRO3* (shRNA1 and shRNA2). Western blot for tubulin is shown as a loading control. (**B**), Dark field microscopic image of 16HBE cells expressing shRNA against *SCCRO3* (shRNA1, shRNA2) showing a change from epitheloid to spindle shape and decreased clumping, compared with cells expressing scrambled shRNA. (**C**), Scratch assay on the same cells showing enhanced migration in cells with SCCRO3 knocked-down relative

to those transfected with scrambled shRNA. (**D**), Indirect immunofluorescence analysis of 16HBE cells infected with shRNA against *SCCRO3* and stained with Alexa Fluor 488 Phalloidin for actin, which showed a reduction in stress fibers. (**E**), Representative images form microscopic analysis of H1299 cells stably transfected with the indicated constructs. Empty vector (EV) transected cells dispersed throughout the plate. SCCRO3 transfected cells (panel 2) shows cells maintained intercellular contact and grew in nests. Cells expressing *SCCRO3G2A* or *SCCRO3DAD* showed no change in growth characteristics relative to empty vector transfected cells. (**F**), Scratch assay on H1299 cells transfected with the indicated constructs showing decreased migration in cells transfected with SCCRO3 and no change in those transfected with *SCCRO3G2A*, *SCCRO3DAD*, or empty vector (EV). (**G**), Graph showing the average numbers of cells that migrated into wounded areas from experiments above. H, Representative images form fluorescence microscopy of H1299 cells transfected with the indicated constructs and stained with: Alexa Fluor 488 Phalloidin showing development of actin containing stress fibers in *SCCRO3* relative to empty vector transected cells, but not *SCCRO3G2A* or *SCCRO3DAD* transfected cells. All scale bars represent 20 µm.

Figure 6. SCCRO3 has tumor suppressor activity that requires its myristoyl sequence and PONY domain.

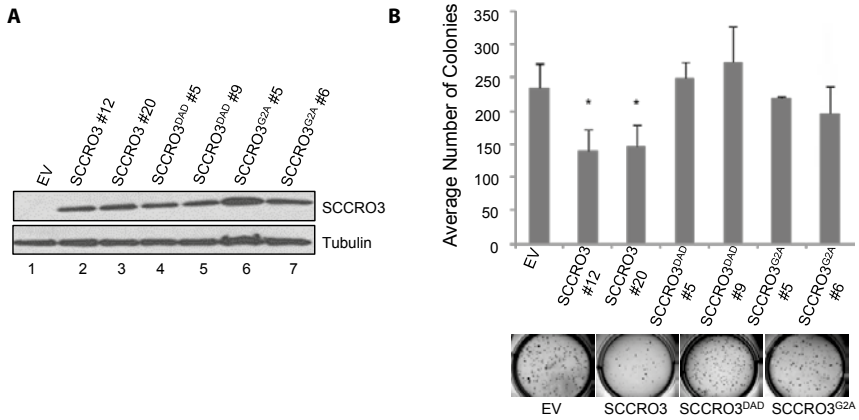

(**A**), Western blot analysis of lysates from H1299 cells stably transfected with the indicated *SCCRO3* constructs, probed with anti-SCCRO3 antibody showing equivalent expression of constructs in selected clones. (**B**), Results from soft agar assay on the same H1299 clones showing decreased colony formation in cells expressing *SCCRO3*, relative to clones expressing *SCCRO3* mutants or vector alone (average number of colonies per well of a 6-well plate ± SD; P = 0.03 for SCCRO3#12 and P = 0.03 for SCCRO3#20, compared with vector).

SCCRO3 antagonizes SCCRO's in vivo function

To determine whether SCCRO3's tumor-suppressor activity results from inhibition of SCCRO's oncogeneic activity, we assessed whether SCCRO3 inhibits SCCRO-promoted transformation *in vivo*. To do this, we established NIH-3T3 clones that stably expressed *SCCRO*. We found that in contrast to vector transected NIH-3T3 cells, SCCRO-expressing NIH-3T3 cells formed colonies in soft agar. SCCRO-expressing NIH-3T3 cells were then cotransfected with HA-tagged *SCCRO3*, *SCCRO3^{G2A}*, or *SCCRO3^{DAD}* (Fig. 7A). Cotransfection of *SCCRO3* induced morphological changes in SCCRO-expressing NIH-3T3 cells, from a spindle to an epitheloid shape. The pattern of growth was also changed, with cells growing in clusters rather than spreading throughout the plate, as seen in

the parental line. No change in shape or growth pattern was seen in SCCRO-expressing NIH-3T3 cells transfected with *SCCRO3*^{G2A} or *SCCRO3*^{DAD} (Fig. 7B). Scratch assays showed reduced directional migration of NIH-3T3 cells coexpressing SCCRO and SCCRO3 but not of cells coexpressing SCCRO and SCCRO3^{G2A} or SCCRO3^{DAD} (Fig. 7C). Moreover, colony formation in soft agar was significantly lower in SCCRO-expressing NIH-3T3 cells transfected with *SCCRO3* than in those transfected with *SCCRO3*^{G2A} or *SCCRO3*^{DAD} (Fig. 7D). Combined, these findings suggest that SCCRO3's tumor-suppressor activity involves inhibition of SCCRO-promoted oncogenesis.

Figure 7. SCCRO3 antagonizes SCCRO-induced transformation.

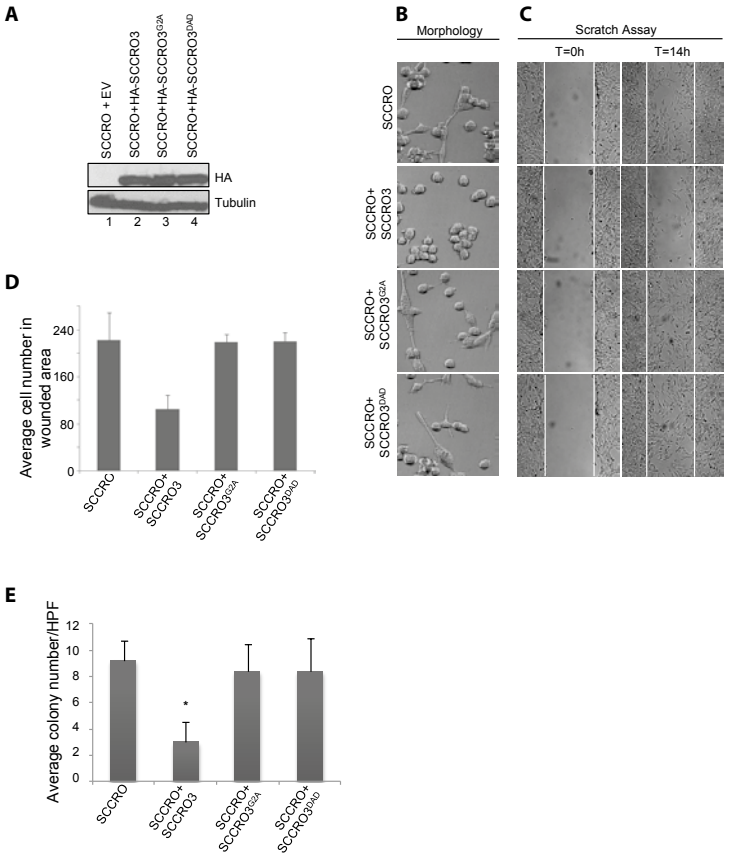

(**A**), Western blot analysis of lysates of NIH-3T3 cells stably expressing *SCCRO*, cotransfected with HA-*SCCRO3*, HA-*SCCRO3*-G2A, HA-*SCCRO3*-DAD, or vector alone and probed for the HA tag, which showed equal expression of transgenes. (**B**), Representative dark field microscopic images showing *SCCRO3* transfected cells maintaining contact and growing in nests while those stably co-expressing SCCRO with empty vector or *SCCRO3*^{G2A} or *SCCRO3*^{DAD} detached and began to disperse across the plate. (**C**), Scratch assay on the same set of cells at times 0 h and at 14 h showing a decrease in migration across the scratch for SCCRO expressing cells co-transfected with *SCCRO3* relative to empty vector, but not those co-transfected with *SCCRO3*^{G2A} or *SCCRO3*^{DAD}. (**D**), Graph

showing the average numbers of cells that migrated into wounded areas from the experiments above. (**E**), Graph showing results from soft agar assays on the same set of cells showing a decrease in colony formation in cell cotransfected with *SCCRO3* relative to those co-transfected with empty vector. No change in colony formation was seen with co-transfection of $SCCRO3^{G2A}$ or $SCCRO3^{DAD}$ (showing the average number per high-power field [HPF] ± SD; $P = 0.002$, compared with vector).

Discussion

SCCRO's role in the neddylation E3 is to promote assembly and optimize complex orientation to enhance ligase activity, which it achieves by binding to neddylation components via its PONY domain. Although the contributions of SCCRO are important, they are not required for neddylation E3 activity *in vitro*. The essential contribution of SCCRO to neddylation *in vivo* is the nuclear translocation of neddylation components, which is regulated by its UBA domain (19). To compensate for the complexities of the expanded genome, SCCRO has evolved in higher organisms to include four paralogs that have highly conserved PONY domains but variable N-terminal domains. Previous studies have suggested that all SCCRO paralogs can promote neddylation (18). However, as these studies used *in vitro* assays, they do not account for the contributions of N-terminal domains, which are all directly or indirectly involved in subcellular localization. Given the requirement of nuclear localization of cullins for neddylation, the presence of a myristoyl sequence in SCCRO3 that localizes it in the cytoplasm raises questions about its *in vivo* function. We found that, in sharp contrast to other SCCRO family members, SCCRO3 does not function as a component of the E3 or promote cullin neddylation. Although SCCRO3 binds to cullins, ROC1, and CAND1 via its PONY domain, it does not bind to Ubc12 at levels that are functionally relevant. Similar to previous reports, in the present study, we detected binding between SCCRO3 and Ubc12 only when high concentrations of purified proteins were used in *in vitro* pull-down assays (17). However, the affinity of SCCRO3 for Ubc12 is significantly lower than that of SCCRO. These findings are supported by recent work from Monda et al., who showed a K_d of 21 μM for the interaction between SCCRO3 and Ubc12, compared with 2.0 μM for SCCRO and Ubc12 (18). Moreover, unlike SCCRO, SCCRO3 does not conform to the reaction processivity paradigms for E3s, as it did not preferentially bind to Ubc12~Nedd8. Consistent with this, we found that SCCRO3 does not promote Cul1 neddylation *in vivo*. The lack of conformity with reaction processivity paradigms, combined with the absence of neddylation-promoting activity, suggests that SCCRO3 does not function as a component of the E3 for neddylation.

What then is the function of SCCRO3? Previous studies have shown that the K_d for binding to Cul1-Cul5 varies between SCCRO paralogs (18). The K_d for binding of Cul1 to SCCRO is 1.8 μM, compared with 1.1 μM for SCCRO3. Consistent with this, when SCCRO and SCCRO3 were coexpressed at relatively equal levels, HA-Cul1 predominately localized to the membrane with SCCRO3. As the transgenic expression of SCCRO is increased above that of SCCRO3, Cul1 translocates to the nucleus. Moreover, the relative levels of SCCRO and SCCRO3 expression also affected the level of cullin neddylation. SCCRO3 inhibited SCCRO-promoted Cul1 neddylation,

which could be overcome by increasing the level of SCCRO expression *in vivo*. Mutation of either the myristoyl sequence or the PONY domain in SCCRO3 abrogated colocalization and inhibition of Cul1 neddylation. These findings suggest that SCCRO and SCCRO3 compete for binding and localization of cullins. This competition affects neddylation activity and suggests that SCCRO3 functions as an antagonist of SCCRO's neddylation activity. As expected, the PONY domain mutant of SCCRO3, which loses binding to the neddylation component, also loses its *in vivo* functions. That $SCCRO3^{G2A}$, a mutant that is unable to localize to the membrane but retains the ability to bind to cullins, also loses its effects on SCCRO function suggests that membrane localization is required for SCCRO3 to impart its effects. To confirm these findings, we performed a competition assay by transecting U2OS cells with SCCRO and an increasing amount of $SCCRO3^{G2A}$. We found that, even at significantly higher expression levels, $SCCRO3^{G2A}$ had no obvious effect on SCCRO-promoted Cul3 neddylation *in vivo* (data not shown). There are several possible explanations for why the $SCCRO3^{G2A}$ mutant has no effect on SCCRO's neddylation and transformation activity. Although the $SCCRO3^{G2A}$ mutant retains binding to neddylation components in the absence of the tether to the membrane, neddylation components can still enter the nucleus (Fig. 3A). Once neddylation components are in the nucleus, the regulatory effects of compartmentalization are lost, allowing neddylation to proceed. It is also possible that co-factors present at the membrane are required for SCCRO3 to inhibit neddylation activity. Our findings need to be reconciled with previous published results, which show that SCCRO3 promotes Cul3 neddylation at the membrane. It remains possible that SCCRO3 has dual activity. Our data and those from Monda et al. clearly show that SCCRO3 has limited binding to Ubc12. As such, SCCRO3 is unlikely to be able to participate in a neddylation reaction that involves Ubc12. However, Monda et al. showed that SCCRO3 binds more efficiently to UBE2F (K_d = 1.1 μM), an alternate E2 in neddylation. Consistent with this finding, the effect of SCCRO3 on Cul5 neddylation was significantly more with the addition of UBE2F to the reaction than with addition of Ubc12. Interestingly, SCCRO3 complemented the neddylation defect of yeast *dcn1*Δ cells (SCCRO homologue), which does not contain UBE2F, suggesting that SCCRO3 may interact with yeast Ubc12. Combined, these results suggest that SCCRO3 plays a dual role: (1) antagonizing the neddylation activity of the other SCCRO paralogs and (2) promoting neddylation at the membrane by using UBE2F as the E2.

It was previously shown that overexpression of SCCRO3 in HeLa cells leads to inhibition of colony formation in soft agar. UVC irradiation increased expression of SCCRO3 in cancer cell lines, and knockdown of SCCRO3 by siRNA in HeLa cells inhibited UVC-induced cell death (20) suggesting that SCCRO3 functions as a tumor suppressor. We validated SCCRO3's function as a putative tumor suppressor by showing (1) that overexpression of SCCRO3 promotes mesenchymal-to-epithelial–like changes and is associated with a decrease in oncogenic activity in H1299 cells and (2) that knockdown of SCCRO3 by shRNA in 16HBE cells promotes epithelial-to-mesenchymal–like changes and is associated with an increase in oncogenic activity. SCCRO3's tumor-suppressor activity required both an intact myristoyl sequence and PONY domain, as mutants in these regions

abrogate its tumor-suppressor activity in 16HBE cells. Moreover, coexpression of SCCRO3 blocked SCCRO-promoted transformation, suggesting that competition between SCCRO and SCCRO3 for cullin substrate has functional implications *in vivo*.

Consistent with SCCRO3's role as a putative tumor suppressor, its expression was decreased in a large proportion of lung, oral, ovarian, and thyroid tumors. Previous reports have shown that its expression is also reduced in liver, bladder, and renal tumors (20), suggesting that SCCRO3 plays a role in the pathogenesis of a broad range of human cancers. In contrast to the other SCCRO family members, changes in SCCRO3 expression in human cancers cannot be explained by copy number changes or by promoter methylation or gene mutation. Screening for the causes of the decreased expression of SCCRO3 in human cancers led us to PUM2, an RNA-binding protein. We found that expression of PUM2 inversely correlates with levels of SCCRO3 expression in human tumors (37). PUM2 is known to bind to SCCRO3 mRNA, and we found that transgenic expression of PUM2 in cells resulted in decreased cellular levels of SCCRO3, but not SCCRO. Similarly, knockdown of PUM2 was associated with increased SCCRO3 expression, suggesting that PUM2 may be a cause of the decreased SCCRO3 expression in many human cancers. Moreover, presence of mutations in both the PONY domain and myristoyl sequence of SCCRO3 in human tumors suggests that mutation may be the cause for SCCRO3 inactivation in some cases.

Combined, our data clearly show an antagonistic relationship between SCCRO and SCCRO3 in neddylation and oncogenesis. Whether this antagonism is also attributable to competition for binding to targets downstream of CRLs remains to be elucidated. In the broader context, our results suggest that SCCRO family members play independent and overlapping roles in the regulation of cullin neddylation (13). Moreover, CRL targets that mediate the effects of SCCRO and SCCRO3 in oncogenesis have yet to be elucidated.

References

1. Hershko A and Ciechanover A (1998). The ubiquitin system. Annual review of biochemistry 67, 425-479
2. Komander D (2009). The emerging complexity of protein ubiquitination. Biochemical Society transactions 37, 937-953
3. Pickart CM (2001). Mechanisms underlying ubiquitination. Annual review of biochemistry 70, 503-533
4. Scheffner M, Nuber U and Huibregtse JM (1995). Protein ubiquitination involving an E1-E2-E3 enzyme ubiquitin thioester cascade. Nature 373, 81-83
5. Hunter T (2007). The age of crosstalk: phosphorylation, ubiquitination, and beyond. Molecular cell 28, 730-738
6. Bosu DR and Kipreos ET (2008). Cullin-RING ubiquitin ligases: global regulation and activation cycles. Cell Div 3, 7
7. Hotton SK and Callis J. (2008). Regulation of Cullin RING Ligases. Annu Rev Plant Biol 59, 467-489
8. Dye BT and Schulman BA (2007). Structural mechanisms underlying posttranslational modification by ubiquitin-like proteins. Annu Rev Biophys Biomol Struct 36, 131-150
9. Duda DM, Borg LA, Scott DC, Hunt HW, Hammel M and Schulman BA (2008). Structural insights into Nedd8 activation of cullin-RING ligases: conformational control of conjugation. Cell 134, 995-1006
10. Pan ZQ, Kentsis A, Dias DC, Yamoah K and Wu K (2004). Nedd8 on cullin: building an expressway to protein destruction. Oncogene 23, 1985-1997
11. Kurz T, Chou YC, Willems AR, Meyer-Schaller N, Hecht ML, Tyers M, Peter M and Sicheri F. (2008). Dcn1 functions as a scaffold-type E3 ligase for cullin neddylation. Molecular cell 29, 23-35
12. Kurz T, Ozlu N, Rudolf F, O'Rourke SM, Luke B, Hofmann K, Hyman AA, Bowerman B and Peter M (2005). The conserved protein DCN-1/Dcn1p is required for cullin neddylation in C. elegans and S. cerevisiae. Nature 435, 1257-1261
13. Scott DC, Monda JK, Grace CR, Duda DM, Kriwacki RW, Kurz T and Schulman B A (2010). A dual E3 mechanism for Rub1 ligation to Cdc53. Molecular cell 39, 784-796
14. Huang G, Kaufman AJ, Ramanathan Y and Singh B (2011). SCCRO (DCUN1D1) promotes nuclear translocation and assembly of the neddylation E3 complex. The Journal of biological chemistry 286, 10297-10304
15. Kim AY, Bommeljé CC, Lee BE, Yonekawa Y, Choi L, Morris LG, Huang G, Kaufman A, Ryan RJ, Hao B, Ramanathan Y and Singh B (2008). SCCRO (DCUN1D1) is an essential component of the E3 complex for neddylation. The Journal of biological chemistry 283, 33211-33220
16. Bommeljé CC, Weeda VB, Huang G, Shah K, Bains S, Buss E, Shaha M, Gonen M, Ghossein R, Ramanathan SY and Singh B (2014). Oncogenic function of SCCRO5/DCUN1D5 requires its Neddylation E3 activity and nuclear localization. Clinical cancer research : an official journal of the American Association for Cancer Research 20, 372-381
17. Meyer-Schaller N, Chou YC, Sumara I, Martin DD, Kurz T, Katheder N, Hofmann K, Berthiaume LG, Sicheri F and Peter M (2009). The human Dcn1-like protein DCNL3 promotes Cul3 neddylation at membranes. Proceedings of the National Academy of Sciences of the United States of America 106, 12365-12370
18. Monda JK, Scott DC, Miller DJ, Lydeard J, King D, Harper JW, Bennett EJ and Schulman BA (2013). Structural conservation of distinctive N-terminal acetylation-dependent interactions across a family of mammalian Nedd8 ligation enzymes. Structure 21, 42-53
19. Wu K, Yan H, Fang L, Wang X, Pfleger C, Jiang X, Huang L and Pan ZQ (2011). Mono-ubiquitination drives nuclear export of the human DCN1-like protein hDCNL1. The Journal of biological chemistry 286, 34060-34070
20. Ma T, Shi T, Huang J, Wu L, Hu F, He P, Deng W, Gao P, Zhang Y, Song Q, Ma D and Qiu X (2008). DCUN1D3, a novel UVC-responsive gene that is involved in cell cycle progression and cell growth. Cancer Sci 99, 2128-2135
21. Sarkaria I, P'ochoenrat, Talbot SG, Reddy PG, Ngai I, Maghami E, Patel KN, Lee B, Yonekawa Y, Dudas M, Kaufman A, Ryan R, Ghossein R, Rao PH, Stoffel A, Ramanathan Y and Singh B (2006). Squamous cell carcinoma related oncogene/DCUN1D1 is highly conserved and activated by amplification in squamous cell carcinomas. Cancer research 66, 9437-9444
22. Gordon D, Abajian C and Green P (1998). Consed: a graphical tool for sequence finishing. Genome research 8, 195-202
23. Nickerson DA, Tobe VO and Taylor SL (1997). PolyPhred: automating the detection and genotyping of single nucleotide substitutions using fluorescence-based resequencing. Nucleic acids research 25, 2745-2751

24. Chen K, McLellan MD, Ding L, Wendl MC, Kasai Y, Wilson RK and Mardis ER (2007). PolyScan: an automatic indel and SNP detection approach to the analysis of human resequencing data. Genome research 17, 659-666
25. Major JE (2007). Genomic mutation consequence calculator. Bioinformatics 23, 3091-3092
26. Herman JG, Graff JR, Myohanen S, Nelkin BD and Baylin SB (1996). Methylation-specific PCR: a novel PCR assay for methylation status of CpG islands. Proceedings of the National Academy of Sciences of the United States of America 93, 9821-9826
27. Ng DC, Lin BH, Lim CP, Huang G, Zhang T, Poli V and Cao X (2006). Stat3 regulates microtubules by antagonizing the depolymerization activity of stathmin. The Journal of cell biology 172, 245-257
28. Broderick SR, Golas BJ, Pham D, Towe CW, Talbot SG, Kaufman A, Bains S, Huryn LA, Yonekawa Y, Carlson D, Hambardzumyan D, Ramanathan Y and Singh B. (2010). SCCRO promotes glioma formation and malignant progression in mice. Neoplasia 12, 476-484
29. Wang J, Qian J, Hoeksema MD, Zou Y, Espinosa AV, Rahman SM, Zhang B and Massion PP (2013). Integrative genomics analysis identifies candidate drivers at 3q26-29 amplicon in squamous cell carcinoma of the lung. Clinical cancer research : an official journal of the American Association for Cancer Research 19, 5580-5590
30. Huang G and Singh B. (2013) Coamplification and cooperation: toward identifying biologically relevant oncogenes. Clinical cancer research : an official journal of the American Association for Cancer Research 19, 5549-5551
31. Estilo CL, P'Ochoenrat, Ngai I, Patel SG, Reddy PG, Dao S, Shaha AR, Kraus DH, Boyle JO, Wong RJ, Pfister DG, Huryn JM, Zlotolow IM, Shah JP and Singh B (2003). The role of novel oncogenes squamous cell carcinoma-related oncogene and phosphatidylinositol 3-kinase p110alpha in squamous cell carcinoma of the oral tongue. Clinical cancer research : an official journal of the American Association for Cancer Research 9, 2300-2306
32. Jung SH, Shin SH, Yim SH, Choi HS, Lee SH and Chung YJ (2009). Integrated analysis of copy number alteration and RNA expression profiles of cancer using a high-resolution whole-genome oligonucleotide array. Experimental & molecular medicine 41, 462-470
33. Chen M, Ye Y, Yang H, Tamboli P, Matin S, Tannir NM, Wood CG, Gu J and Wu X (2009). Genome-wide profiling of chromosomal alterations in renal cell carcinoma using high-density single nucleotide polymorphism arrays. International journal of cancer. Journal international du cancer 125, 2342-2348
34. Desouki MM, Liao S, Huang H, Conroy J, Nowak NJ, Shepherd L, Gaile DP and Geradts J (2011). Identification of metastasis-associated breast cancer genes using a high-resolution whole genome profiling approach. Journal of cancer research and clinical oncology 137, 795-809
35. Dobrovic A, Gareau JL, Ouellette G and Bradley WE (1988). DNA methylation and genetic inactivation at thymidine kinase locus: two different mechanisms for silencing autosomal genes. Somat Cell Mol Genet 14, 55-68
36. Dreyfuss G, Kim VN and Kataoka N (2002). Messenger-RNA-binding proteins and the messages they carry. Nat Rev Mol Cell Biol 3, 195-205
37. Galgano A, Forrer M, Jaskiewicz L, Kanitz A, Zavolan M and Gerber AP (2008). Comparative analysis of mRNA targets for human PUF-family proteins suggests extensive interaction with the miRNA regulatory system. PLoS One 3, e3164
38. Yang X, Zhou J, Sun L, Wei Z, Gao J, Gong W, Xu RM, Rao Z and Liu Y (2007). Structural basis for the function of DCN-1 in protein Neddylation. The Journal of biological chemistry 282, 24490-24494
39. Huang DT, Miller DW, Mathew R, Cassell R, Holton JM, Roussel MF and Schulman BA (2004). A unique E1-E2 interaction required for optimal conjugation of the ubiquitin-like protein Nedd8. Nat Struct Mol Biol 11, 927-935

Chapter 5

Oncogenic function of SCCRO5 (DCUN1D5) requires its neddylation E3 activity and nuclear localization

C.C. Bommeljé, V.B. Weeda, G. Huang, K. Shah, S. Bains, E. Buss, M. Shaha, M. Gonen, R. Ghossein, Y. Ramanathan, B. Singh

Clin Cancer Research, 2014 Jan 15;20(2):372-81

Abstract

Purpose: To determine mechanisms by which SCCRO5 (aka *DCUN1D5*) promotes oncogenesis.

Experimental Design: SCCRO5 mRNA and protein expression were assessed in 203 randomly selected primary cancer tissue samples, matched histologically normal tissues, and cell lines by use of real-time PCR and Western blot analysis. SCCRO5 overexpression was correlated with survival. The effect of SCCRO5 knockdown on viability was assessed in selected cancer cell lines. Structure-function studies were performed to determine the SCCRO5 residues required for binding to the neddylation components, for neddylation-promoting activity, and for transformation.

Results: In oral and lung squamous cell carcinomas, *SCCRO5* mRNA levels corresponded with protein levels and overexpression correlated with decreased disease-specific survival. Knockdown of *SCCRO5* by RNAi resulted in a selective decrease in the viability of cancer cells with high endogenous levels, suggesting the presence of oncogene addiction. SCCRO5 promoted cullin neddylation while maintaining conserved reaction processivity paradigms involved in ubiquitin and ubiquitin-like protein conjugation, establishing it as a component of the neddylation E3. Neddylation activities *in vitro* required the potentiating of neddylation (PONY) domain but not the nuclear localization sequence (NLS) domain. In contrast, both the NLS domain and the PONY domain were required for transformation of NIH-3T3 cells.

Conclusions: Our data suggest that *SCCRO5* has oncogenic potential and that it imparts its oncogenicity as a component of the neddylation E3. Neddylation activity and nuclear localization of SCCRO5 are important for its *in vivo* function.

Translational relevance: The importance of the ubiquitin-proteasome pathway in cancer pathogenesis is established by the therapeutic efficacy of agents that target pathway activity in treating human cancers. Neddylation, a major regulator of ubiquitin-proteasome pathway activity, is itself subject to regulation by SCCRO. SCCRO is commonly activated by amplification in many different types of cancer and its overexpression is independently associated with poor clinical outcome. Here we show that SCCRO5, a paralog of SCCRO, plays a role in cancer pathogenesis. SCCRO5 is commonly overexpressed in human cancers and its overexpression is associated with worse outcome in oral and lung squamous cell carcinomas. Establishing its role in cancer pathogenesis, we show oncogene addiction associated with SCCRO5 overexpression in cancer cell lines. Moreover, we show that SCCRO5's oncogenic activity requires it function as an E3 in neddylation, as well as, its subcellular localization. Combined our findings suggest that like SCCRO, SCCRO5 is a putative therapeutic target in oral and lung SCC, as well as, other types of cancer.

Introduction

Several important anticancer therapies have been discovered by leveraging the knowledge that changes in protein homeostasis drive human cancer pathogenesis. In this regard, the ubiquitin/proteasome system is of significance, as there is a high prevalence of aberrations among the components of this pathway (1, 2). In particular, the activity of cullin-RING type ubiquitination E3 ligases is commonly dysregulated in human cancers (3). Dysregulation often results from aberrations in the substrate recognition adaptors (ie, FBX7, SPOP, Skp2, VHL), and rarely from abnormalities in core components (eg, Cul4A amplification in breast cancer) (4-7). It has long been established that posttranslational modification of cullins by neddylation is a key regulator of cullin-RING ligase (CRL) activity (neddylation promotes assembly of the CRL complex and enhances recruitment of ubiquitin-charged E2, to facilitate ubiquitin conjugation) (8-13). As is the case with ubiquitination, neddylation results from the sequential enzymatic activity of a dedicated E1 (APPBP1-Uba3), E2 (Ubc12 [aka Ube2M] and Ube2F), and E3 (14). The link between abnormal CRL activity and dysregulation of the proteins involved in neddylation in human cancers has only recently been appreciated (15). These observations have led to the development of a small molecule inhibitor of neddylation E1, MLN4924, which has shown promise in preclinical and early human trials (3).

SCCRO (aka DCUN1D1), a key component of the E3 for neddylation, is activated by amplification in a wide range of human cancers (16, 17). The role that SCCRO plays in cancer pathogenesis has been studied in both *in vivo* and *in vitro* experimental systems, establishing its function as an oncogene (16, 18). In addition, overexpression of *SCCRO* in human tumor samples has been independently associated with poor survival outcomes (16). Of interest, SCCRO is a member of a protein family that contains four other highly conserved paralogs in higher organisms. All family members have a conserved C-terminal potentiating of neddylation (PONY) domain with a variable N-terminal region. SCCRO paralogs are subdivided into three subfamilies on the basis of the N-terminal sequence: SCCRO and SCCRO2 (aka DCUN1D2) contain a ubiquitin-associated (UBA) domain, SCCRO3 (aka DCUN1D3) contains a myristoylation sequence, and SCCRO4 (aka DCUN1D4) and SCCRO5 (aka DCUN1D5) contain a nuclear localization sequence (NLS). We have previously shown that SCCRO is oncogenic and that its oncogenic function requires its neddylation activity (16, 17). SCCRO3 has also been shown to play a role in oncogenesis (19). Recent work indicates that SCCRO5 has oncogenic activity (20). However, the precise mechanisms by which the NLS-containing SCCRO paralogs promote oncogenesis remain unknown.

Like *SCCRO* (at 3q26), its paralogs are located in chromosomal loci that are recurrently amplified in human cancers (*SCCRO2* at 13q34, *SCCRO4* at 4q12, and *SCCRO5* at 11q22) (21-23). Of these, 11q22 amplification is the second most frequent, occurring in a wide range of human cancers, with the highest prevalence in squamous cell carcinomas (SCCs) of the cervix, esophagus, head and neck, and lung (24-27). Moreover, there is an independent association between 11q22 amplification and worse clinical outcome, suggesting that this locus harbors genes that play a role in cancer pathogenesis (15, 28, 29). Although several candidate genes have been identified, including *MMP*s, *Birc2* (*cIAP1*),

Birc3 (*cIAP2*), and *Yap*, none has been clearly established as a target that drives selection for 11q22 amplification (29-31). Finemapping of 11q22.2-q22.3 in cervical, oral, and lung cancers has shown that *SCCRO5* (*MGC2714*) is located within the minimal common region of amplification (27, 30, 32). *SCCRO5* is upregulated in laryngeal SCC and putatively plays a role in its pathogenesis (20). Given the established role of SCCRO in oncogenesis, we questioned whether *SCCRO5* drives selection for 11q22 amplification in human cancers and sought to elucidate the mechanisms involved.

Here, we report the validation of *SCCRO5* as a target that drives selection for 11q22 amplification in human cancers. We found that *SCCRO5* mRNA expression is associated with a corresponding increase in protein levels and is correlated with decreased disease-specific survival in oral and lung SCCs. Specific knockdown of *SCCRO5* in cancer cell lines with high endogenous levels of *SCCRO5* expression resulted in a significantly higher decrease in viability, compared with that in cells with low expression levels, suggesting the presence of an oncogene addiction phenotype. The oncogenic potential of SCCRO5 is underscored by its ability to transform fibroblasts (NIH-3T3 cells) *in vitro*. Furthermore, we show that, like SCCRO, SCCRO5 functions as a component of the E3, promoting cullin neddylation while maintaining reaction processivity paradigms. Although only the PONY domain was required for SCCRO5's neddylation function *in vitro*, its oncogenic activity *in vivo* requires both the PONY domain and the NLS domain, suggesting that subcellular localization plays a role in its function. The precise mechanism involved in SCCRO5's *in vivo* neddylation activity remains to be defined.

Materials and Methods

Bioinformatic analyses

The ClustalW program (Conway Institute UCD, Dublin, Ireland) was used for multiple sequence alignments. Data from The Cancer Genome Atlas (TCGA) projects were accessed and analyzed using the cBio Cancer Genomics Portal (http://www.cbioportal.org).

Human tissues, cell lines, and antibodies

A total of 203 randomly selected primary cancer tissue and adjacent matched histologically normal tissue samples were obtained from patients undergoing surgical treatment at Memorial Sloan-Kettering Cancer Center between January 1, 2004, and October 1, 2007. All patients undergoing surgical resection of primary cancers were offered an opportunity to participate in the study. Only previously untreated patients with adequate tissue stored in our tissue bank were included in the study. Informed consent was obtained from all patients, in accordance with the guidelines established by the institutional review board, and use of patient samples was approved by the institutional Human Biospecimen Utilization Committee. Histopathologic confirmation of all specimens was established by an experienced pathologist. Tissues were frozen in liquid nitrogen immediately after resection and stored at -80°C until use. Demographic and tumor data for the

oral SCC, lung SCC, thyroid cancer, and lung neuroendocrine carcinoma patients are described in Supplemental Tables S1-S4.

The origins, cytogenetic characteristics, maintenance, and growth of the cell lines used in this study were as previously described (16, 33). The following antibodies were used in this study: anti-SCCRO (developed and validated as previously described [16]), anti-SCCRO5 (developed and validated in our laboratory [data not shown]), anti-Cul1 (Invitrogen, Grand Island, NY), anti-Cul2 (Abcam, Cambridge, MA), anti-Cul3 (BD Biosciences, San Jose, CA), anti-ROC1 (Abcam), anti-Ubc12 (Rockland, Gilbertsville, PA), anti-CAND1 (BD Biosciences, San Jose, CA), anti-α-tubulin and anti-GAPDH (Millipore, Billerica, MA), and anti-actin and secondary antibodies conjugated to horseradish peroxidase (Santa Cruz Biotechnology, Santa Cruz, CA).

RNA isolation, cDNA synthesis, and quantitative real-time PCR (qRT-PCR)

Total RNA was extracted from cell lines and tissue by use of Trizol reagent (Life Technologies, Grand Island, NY), repurified using RNeasy Mini spin columns (Qiagen, Valencia, CA), and treated with DNase I to eliminate residual genomic DNA. One microgram of total RNA was reverse-transcribed using MultiScribe Reverse Transcriptase (Applied Biosystems, Foster City, CA). Primers were designed for *SCCRO5* and *GAPDH* (Supplemental Table S5), by use of the Primer3 program (Howard Hughes Medical Institute, Chevy Chase, MD), to generate PCR products 75–300 bp in length and were obtained from a commercial source (Operon Technologies, Alameda, CA). To confirm specificity for *SCCRO5*, the *SCCRO5* primer set was tested on plasmids for all *SCCRO* paralogs. qRT-PCR for *SCCRO5* was performed, at least in duplicate, in two separate experiments, on the 203 tumor and paired normal samples and on appropriate controls by use of a Sequence Detector System 7900HT device (Applied Biosystems, Foster City, CA), as previously described (16). To ensure the presence of a single PCR product, melting curve analysis was performed after each experiment. A standard curve was generated using serial dilutions of cDNA from MDA686 and MDA1186 cell lines. The comparative threshold cycle method was used to calculate the *SCCRO5* expression ratio in each sample relative to the value observed in the control standard curve, with *GAPDH* used as a control for normalization among samples (34). *GAPDH* was determined to be the most stable housekeeping gene in the tissues studied, on the basis of geNorm analysis ($M < 0.298$) (35, 36). Overexpression was defined as at least 2-fold higher levels of mRNA expression in the tumor sample relative to the matched normal sample and the mean of all normal tissue samples for each cancer type.

Mutation profiling

Primers were designed, using Primer3, to cover putative exon regions of *SCCRO5* (National Center for Biotechnology Information Human Genome Build 36.1), yielding products ≤500 bp in length (Supplemental Table S6) (37). Tumor DNA was extracted using the DNeasy kit (Qiagen, Valencia, CA) and was subjected to whole-genome amplification, as previously described (38). High-throughput bidirectional dideoxynucleotide sequencing of PCR-amplified gene products was performed using

the Sanger sequencing platform, as previously described (39). PolyPhred and PolyScan software were used to generate an initial automated report of sequence variations (39). For each respective exon, tumor sequences were compared against reference sequences listed in the National Center for Biotechnology Information (RefSeq) database. After visual inspection of the individual forward and reverse chromograms, for confirmation of nonsynonymous sequence variations and insertions or deletions (including duplications), a manual review list of potential nucleotide changes was produced. Synonymous variants and those with corresponding entries in the Single Nucleotide Polymorphism Database (http://www.ncbi.nlm.nih.gov/projects/SNP/) were excluded from analysis.

cDNA cloning, mutagenesis, and short hairpin RNA (shRNA) knockdown

Human *SCCRO5* cDNA was obtained from Clontech Laboratories (Clontech, Mountain View, CA). Mutations were generated in *SCCRO5* by standard PCR mutagenesis, as previously described (17). Primers were designed using Primer3 (Supplemental Table S7). *SCCRO5* and its mutated forms were cloned into pEGFP-N2 (Clontech, Mountain View, CA), pBABE (BD Biosciences, San Jose, CA), and pGEX-4T-3 (GE Healthcare Life Sciences, Piscataway, NJ) vectors. Plasmid and protein purifications were performed as previously described (16, 17). shRNA against human *SCCRO5* (obtained from the Genome Sequencing Center at Memorial Sloan-Kettering Cancer Center) or *lacZ* shRNA (negative control) was transfected – along with packaging plasmids pLP1, pLP2, and pVSVG – into HEK293 cells by use of Lipofectamine 2000, in accordance with the manufacturer's protocol (Invitrogen, Grand Island, NY). Lentiviral particles were harvested 48 h and 72 h after transfection and were filtered, pelleted, and resuspended in media for retroviral delivery in the presence of polybrene (Millipore, Billerica, MA). Twenty-four hours after infection, cells were cultured in media containing puromycin, to select for infected cells.

Molecular and biochemical assays

Glutathione S-transferase (GST) pull-down assays, *in vitro* neddylation assays, *in vitro* thioester reactions, transfections, and immunoblotting were performed as previously described (16, 17).

Proliferation and colony formation assays

MTS proliferation assays and colony formation assays were performed as previously described (16, 17). For the soft agar assay, colonies were counted using ImageJ software (National Institutes of Health, Bethesda, MD), to analyze images captured from four 6-well plate wells per construct, from two independent experiments.

Statistical analysis

Descriptive statistics were used to summarize study day. Continuous variables were compared across groups using Student's t-test or Mann-Whitney U-test. Categorical comparisons were performed using the Fisher's exact test. Survival curves were generated using the Kaplan-Meier method and compared using the log-rank test. Time to recurrence was defined as the time between completion of primary treatment of cancer and the development of recurrent cancer at any site (local, regional, or distant). Survival outcomes were censored for patients who died of causes other than cancer, were lost to follow-up or survived to the end of the study. Statistical significance was defined as a two tailed p-value less than or equal to 0.05. All statistical analyses were performed using state-of-the-art statistical packages (SPSS, Chicago, IL; or SAS, Durham, NC).

Results

SCCRO5 binds to neddylation components

In silico analysis showed that SCCRO has four paralogs in higher organisms, all with a highly conserved C-terminal PONY domain with variable N-terminal domains (Supplemental Fig. S1A). The established role of the PONY domain in neddylation raised the possibility that, like SCCRO, SCCRO's paralogs participate in neddylation E3 activity. To determine the role that SCCRO5 plays in neddylation, we assessed the binding of SCCRO5 to neddylation components. GST pull-down assays using HeLa cell extracts, followed by Western blot analysis for neddylation components, showed that, like SCCRO, SCCRO5 binds to CAND1, Ubc12, Cul1, Cul2, Cul3, and ROC1 (Table 1 and Fig. 1A). Previous biochemical and structural studies have established that SCCRO binds to its neddylation components through its PONY domain, which contains four residues that are critical for binding interactions (Supplemental Fig. S1B) (17, 40, 41). To map the binding domains, we created a series of SCCRO5 deletions and point mutants as GST fusions, including those involving the N-terminal NLS and C-terminal PONY domains, and used them in pull-down assays on HeLa lysates. Deletion of the PONY domain (SCCRO5_Δ189-237) or mutation in critical residues (SCCRO5_D195N, SCCRO5_A219R, SCCRO5_D225N, SCCRO5_E226A, SCCRO5_A219R/D225N, and SCCRO5_D195N/A219R/D225N) resulted in loss of binding to CAND1 and Cul1-ROC1 (Table 1). Binding to Ubc12 was lost only with larger deletion of the C-terminal region of SCCRO5 (SCCRO5_Δ189-237), which is consistent with the location of the binding site of Ubc12 in SCCRO (17). Previous studies have shown that the UBA domain in SCCRO is not required for binding to neddylation components (17, 40, 41). SCCRO5 contains an NLS in its N-terminus. We found that the NLS is functional, as transiently expressed GFP-SCCRO5 was exclusively present in the nucleus, whereas NLS-deletion mutant GFP-SCCRO5 (SCCRO5_Δ1-10 and SCCRO5_Δ1-46) had a pan-cellular distribution on fluorescence microscopy (data not shown).

As with the UBA domain of SCCRO, deletion of the NLS or the entire N-terminus in SCCRO5

(SCCRO5_Δ1-10 and SCCRO5_Δ1-46, respectively) had no effect on binding to Cullin-ROC1, Ubc12, or CAND1 (Table 1). These results show that binding with the neddylation components and residues involved in the interactions are conserved between SCCRO and SCCRO5.

Table 1. Results from GST pull-downs.

SCCRO5 Mutants	Cul1-ROC1	CAND1	Ubc12
WT	+	+	+
Δ1-10	+	+	+
Δ1-46	+	+	+
Δ189-237	-	-	-
A219R	-	-	+
D195N	-	-	+
D225N	-	-	+
E226A	-	-	+
A219R/ D225N	-	-	+
D195N/ A219R/ D225N	-	-	+

SCCRO5 interacts with components of the neddylation pathway.
NOTE: The table shows a summary of results from pull-down assays using GST-SCCRO5 and selected mutants to recombinant Cul1-ROC1, Ubc12, and CAND1, which confirmed that binding to Cul1-ROC1 and CAND1 requires an intact PONY domain but not the NLS domain. In contrast, binding to Ubc12 was only lost with deletion of the C-terminus (SCCRO5_ Δ189–237).

SCCRO5 preferentially binds to Ubc12~Nedd8 thioester

The mechanisms that maintain the processivity of the reactions that result in the conjugation of ubiquitin and ubiquitin-like proteins are highly conserved. Central to maintenance of processivity is a differential affinity between E1 and E3 for free and conjugated E2, respectively. Differences in affinity ensures that an E2 must dissociate from its cognate E1 after it accepts transfer of ubiquitin or ubiquitin-like proteins and before it can bind to the E3. SCCRO has greater affinity for E2~Nedd8 thioester than for free E2, which is consistent with its role as a component of the E3 for neddylation (17). To determine whether SCCRO5 also conforms to the established processivity paradigm for E3s, we performed GST pull-down assays on products from a Ubc12 thioester reaction, followed by Western blot analysis for Ubc12. Even in the presence of molar-excess free Ubc12, SCCRO5 preferentially bound to Ubc12~Nedd8 thioester (Fig. 1B; compare lanes 1 and 3). Moreover, the results of GST pull-down assays showed that, as with SCCRO, critical residues involved in binding of SCCRO5 to Cul1-ROC1 (lanes 3 and 4) and the N-terminal region (lane 5) were not involved in binding to Ubc12~Nedd8 (Fig. 1C). These findings confirm that, in its interactions with Ubc12, SCCRO5 maintains reaction processivity paradigms.

Figure 1. SCCRO5 interacts with components of the neddylation pathway.

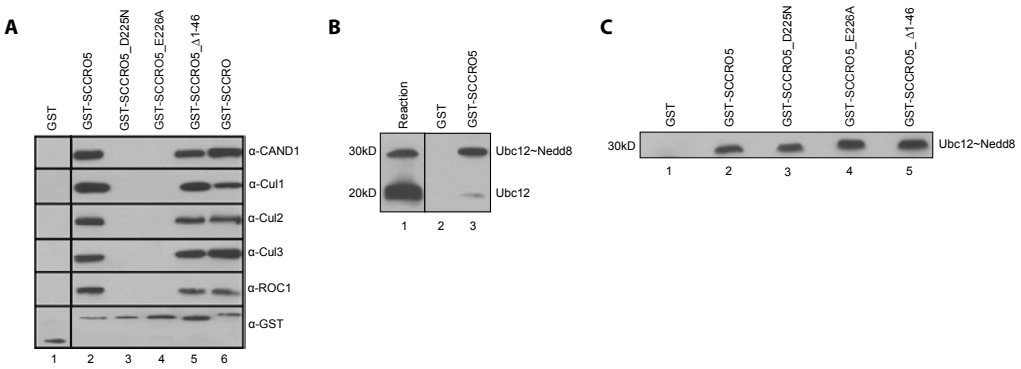

(**A**), Western blot analysis of the products of GST-SCCRO, GST-SCCRO5, and selected GST-SCCRO5 mutants after pull-down assays from HeLa lysates probed with the indicated antibodies, which shows that, like SCCRO, SCCRO5 binds to CAND1, Cul1, Cul2, Cul3, and ROC1. Mutations in the PONY domain (SCCRO5_D225N and SCCRO5_E226A), but not the N-terminal NLS (SCCRO5_ Δ1–46), result in loss of binding. The dividing line between lane 1 and lane 2 indicates the position of omitted lanes from the same gel. (**B**), Western blot analysis of Ubc12 after GST and GST-SCCRO5 pulldown assays on products from a thioester reaction (lane 1), which shows preferential binding to Ubc12~Nedd8, even in the presence of excess free Ubc12. C, Western blot analysis of Ubc12 after pull-down assays on products of thioester reaction, which shows that GST-SCCRO5 and PONY and NLS mutants bind equally to Ubc12~Nedd8.

SCCRO5 promotes cullin neddylation

Structural and biochemical studies have shown that SCCRO promotes cullin neddylation by promoting complex assembly, nuclear translocation of neddylation E3 components, enhanced E2 recruitment, and structural orientation to optimize the efficiency of the transfer of Nedd8 from Ubc12 to cullin (42, 43). To determine whether SCCRO5 also promotes cullin neddylation, we performed in vitro neddylation reactions containing Nedd8, recombinant APPBP1/Uba3 (E1), Ubc12 (E2), ATP, and whole-cell lysate from HeLa cells (as a source of Cullin-ROC substrates), with and without SCCRO5. Western blotting of reaction products for cullins showed a dose-dependent increase in neddylation of Cul1, Cul2, and Cul3 with the addition of SCCRO5 (Fig. 2A). A time-course in vitro neddylation reaction showed that SCCRO5 enhanced the rate of cullin neddylation (Fig. 2B). To determine the domains required for the observed effects on neddylation, we supplemented in vitro reactions with SCCRO5 or selected SCCRO5 mutants. PONY domain mutants (SCCRO5_D225N and SCCRO5_E226A) failed to augment Cul3 neddylation beyond basal levels, whereas N-terminus deletion mutants (SCCRO5_ Δ1–46) enhanced Cul3 neddylation to levels similar to those observed in reactions supplemented with wild-type SCCRO5 (Fig. 2C). Combined, these findings suggest that, as with SCCRO (17), the effect of SCCRO5 on cullin neddylation *in vitro* requires its interaction with neddylation E3 components through its PONY domain but not its NLS domain.

Figure 2. SCCRO5 augments cullin neddylation.

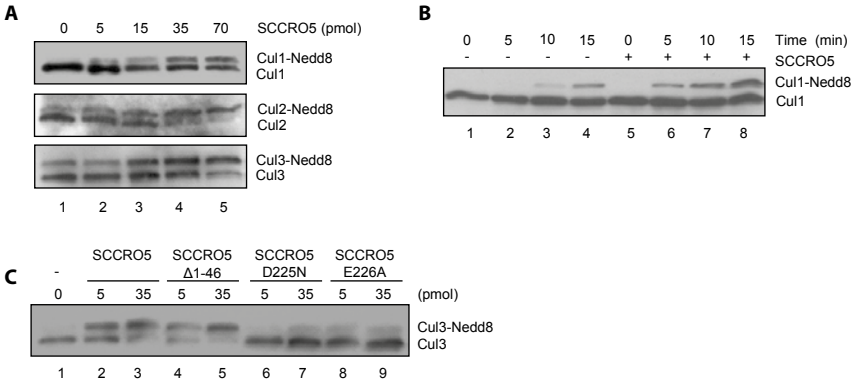

(**A**), Western blot analysis of the indicated cullins on products of an in vitro neddylation reaction using HeLa lysates as a source for Cullin-ROC1 complexes supplemented with a gradient of SCCRO5, which shows a dose-dependent increase in neddylation of Cul1, Cul2, and Cul3 with the addition of recombinant SCCRO5. (**B**), Western blot analysis of Cul1 on products of an in vitro neddylation reaction with (lanes 5–8) or without (lanes 1–4) the addition of SCCRO5, which shows enhanced efficiency of Cul1 neddylation by SCCRO5. (**C**), Western blot analysis of Cul3 on products of an in vitro neddylation reaction with concentration gradients of SCCRO5, SCCRO5_Δ1–46, SCCRO5_D225N, or SCCRO5_E226A (quantities in pmol), which shows a dose-dependent increase in neddylation of Cul3 with SCCRO5 and SCCRO5_Δ1–46 but not with SCCRO5_D225N or SCCRO5_E226A.

SCCRO5 promotes cell proliferation and anchorage-independent cell growth

With SCCRO5's function in cullin neddylation established, we next asked whether this activity is required for transformation. To determine this, we transfected NIH-3T3 cells with pBABE-SCCRO5, selected pBABE-SCCRO5 mutants or empty vector, and developed two stably expressing clones for each construct by use of puromycin selection. Equal expression of SCCRO5 and SCCRO5 mutants in selected clones was confirmed by qRT-PCR and Western blot analysis (Supplemental Fig. S2A and S2B). The results of MTS assays showed that the proliferation rate was significantly higher in SCCRO5-expressing clones than in SCCRO5_D195N/A219R/D225N, SCCRO5_ Δ1–10, or empty vector transfected NIH-3T3 cells (Fig. 3A). NIH-3T3 clones were then subjected to soft agar colony formation assay to assess transforming ability, which showed that SCCRO5-transfected clones had significantly higher anchorage-independent growth, compared with SCCRO5_D195N/A219R/D225N, SCCRO5_ Δ1–10, or empty vector transfected cells (Fig. 3B). Combined, these findings suggest that SCCRO5's oncogenic activity requires its neddylation-promoting activity as well as its compartmentalization to the nucleus.

SCCRO5 overexpression is associated with an oncogene addiction phenotype

Consistent with the concept of oncogene addiction, we previously reported that cancer cell lines with amplification and high levels of SCCRO expression are more susceptible to apoptosis with RNAi knockdown of SCCRO, compared with cell lines with normal copy numbers and low levels of SCCRO expression (16, 44). To validate the role that SCCRO5 plays in cancer pathogenesis, we sought to determine whether an oncogene addiction to SCCRO5 was present in cancer cell lines. Results of qRT-PCR and Western blot analysis showed a wide range of SCCRO5 expression in a panel of head and neck cancer cell lines, with the highest levels of expression in SCC15 and MDA1483 and the lowest level in MDA1386 (Fig. 3C). Representative cell lines with low (MDA1386) and high (MDA1483) endogenous SCCRO5 expression were transfected with two independent anti-SCCRO5 shRNA constructs and with anti-lacZ shRNA as a control. Western blot analysis, after transfection with anti-SCCRO5 shRNA constructs, showed efficient knockdown of SCCRO5 levels, compared with those in the anti lacZ shRNA-transfected cells (Fig. 3D). SCCRO levels were not affected by transfection with any of the shRNA constructs, which confirmed specificity. Results of MTS assays showed a more significant decrease in the viability of MDA1483 cells, compared with MDA1386 cells, after SCCRO5 knockdown (Fig. 3E and F). These results indicate the presence of an oncogene addiction phenotype and validate the role of SCCRO5 in cancer pathogenesis.

Figure 3. Transgenic expression of SCCRO5 promotes proliferation and anchorage-independent growth.

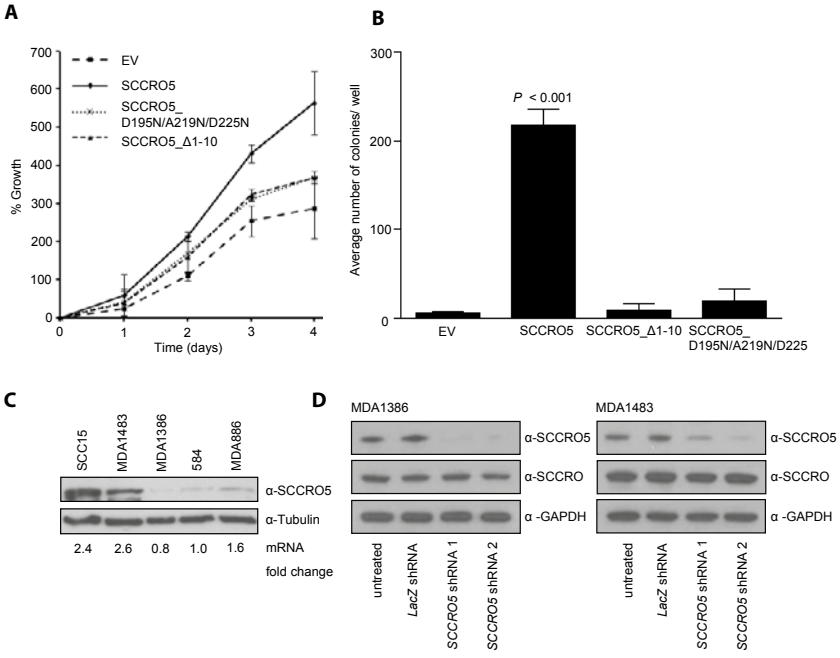

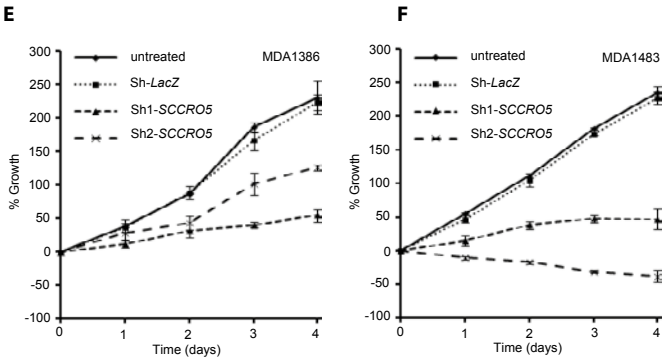

(**A**), graph showing results from an MTS assay on NIH-3T3 cells stably expressing SCCRO5 and indicated mutants, which shows increased proliferation in cells expressing SCCRO5 but not NLS (SCCRO5_Δ1–10) or PONY (SCCRO5_D195N/A219R/D225N) domain mutants. (**B**), results from a soft agar assay, which shows increased colony formation in NIH-3T3 cells stably transfected with SCCRO5, compared with that in cells transfected with empty vector and SCCRO5 NLS and PONY domain mutants (bars represent the mean _ SD number of colonies per well of 6-well plates; $P < 0.001$). (**C**), Western blot analysis, which shows SCCRO5 protein levels and corresponding mRNA levels, on the basis of real-time PCR, in head and neck cancer cell lines. (**D**), Western blot analysis of SCCRO5, with GAPDH as a loading control, on lysates fromMDA1386 (low endogenous SCCRO5) and MDA1483 (high endogenous SCCRO5), before and after transfection of two independent shRNA constructs against SCCRO5 or lacZ control, which shows efficient and specific knockdown of SCCRO5. (**E**) and (**F**), graphs from MTS assays showing a more pronounced decrease in the viability of MDA1483 cells, compared with MDA1386 cells, with knockdown of SCCRO5.

SCCRO5 overexpression is associated with an aggressive clinical course

To establish the clinical significance of SCCRO5 overexpression, we sought to identify mutations and to determine the prevalence of SCCRO5 overexpression, as well as the association of mutations and overexpression with outcome in a panel of randomly selected human tumors. Sequenome-based mutational screening of all cases did not identify any mutations in SCCRO5 (data not shown). To investigate the presence and frequency of overexpression, SCCRO5 mRNA levels were determined by qRT-PCR in cancer tissue and matched histologically normal tissue for each case. The highest prevalence of SCCRO5 mRNA overexpression was observed in cancer types known to harbor 11q22 amplification, including gliomas (4/10; 40%), lung SCCs (14/30; 47%), and oral cavity SCCs (16/40; 40%). SCCRO5 mRNA overexpression was less common in cancer types with a lower prevalence of 11q22 amplification, including lung adenocarcinomas (2/27; 7%), lung neuroendocrine carcinomas (6/54; 11%), ovarian carcinomas (1/40; 3%), and thyroid carcinomas (5/56; 9%; Fig. 4A; refs. 26, 27, 30). Moreover, in the cohort of lung SCCs and oral cavity SCCs, SCCRO5 mRNA levels correlated with SCCRO5 protein levels (Fig. 4B).

To validate the prevalence of SCCRO5 dysregulation, we analyzed interim results from TCGA projects, which showed that the highest prevalence of SCCRO5 dysregulation (amplification and/or overexpression) was in head and neck SCCs (11.6%), followed by ovarian serous cystadenocarcinomas

(3%; copy number change only; expression data not available), cervical carcinomas (8.7%; copy number change only; expression data not available), and bladder urothelial carcinomas (7%), with a significant correlation between copy number and mRNA expression in head and neck SCCs (Supplemental Fig. S3). The difference in the prevalence of dysregulation between our tumor cohort and that in the TCGA likely represents differences in the sensitivity of the analytic techniques used to assess SCCRO5 mRNA levels (cDNA array vs. qRT-PCR) and in the type of control tissue used for analysis (matched normal tissue vs. blood).

To determine clinical relevance, we performed a post hoc analysis to determine the association between SCCRO5 overexpression and disease-free survival. We limited survival comparisons to patients undergoing treatment for head and neck or lung SCC as these datasets had: (i) reasonable power (more than 10 cases with SCCRO5 over expression), (ii) had sufficient events (only 2 recurrences were observed in the thyroid cancer cohorts; Supplemental Table 3), and (iii) had uniform histology (thyroid cohort included papillary, follicular and Hurthle cell carcinomas and lung neuroendocrine carcinomas included large cell carcinomas, small cell carcinomas, and carcinoid tumors; Supplemental Table S4). All patients in the study cohort underwent uniform treatment that included primary surgery with or without adjuvant treatment (on the basis of the extent of disease), in accordance with established institutional protocols. Clinicopathologic parameters, including age, sex, tumor node metastasis stage, and tobacco use, were not significantly different according to SCCRO5 expression status for either cancer cohort (Supplemental Tables S1 and S2). We found that SCCRO5 overexpression (SCCRO5+), which is defined in the Materials and Methods section, compared with normal expression of SCCRO5 (SCCRO5-), negatively correlated with disease-free survival for both head and neck SCCs and lung SCCs ($P = 0.05$; Fig. 4C and D). Interestingly, time to survival analysis for lung neuroendocrine carcinomas also shows worse outcome in tumors with SCCRO5 over expression (Supplemental Fig. S4; $P = 0.05$). However, the differences in outcome in the lung neuroendocrine carcinoma need to be considered with caution given the limited sample size and variable behavior of histologic subtypes of neuroendocrine carcinomas. Moreover, limitation of sample size and number of events in the study cohorts do not support multivariate analyses. Nonetheless, the correlation of overexpression with an aggressive clinical course supports SCCRO5's clinical relevance.

Figure 4. SCCRO5 overexpression is common in human tumors and correlates with outcomes.

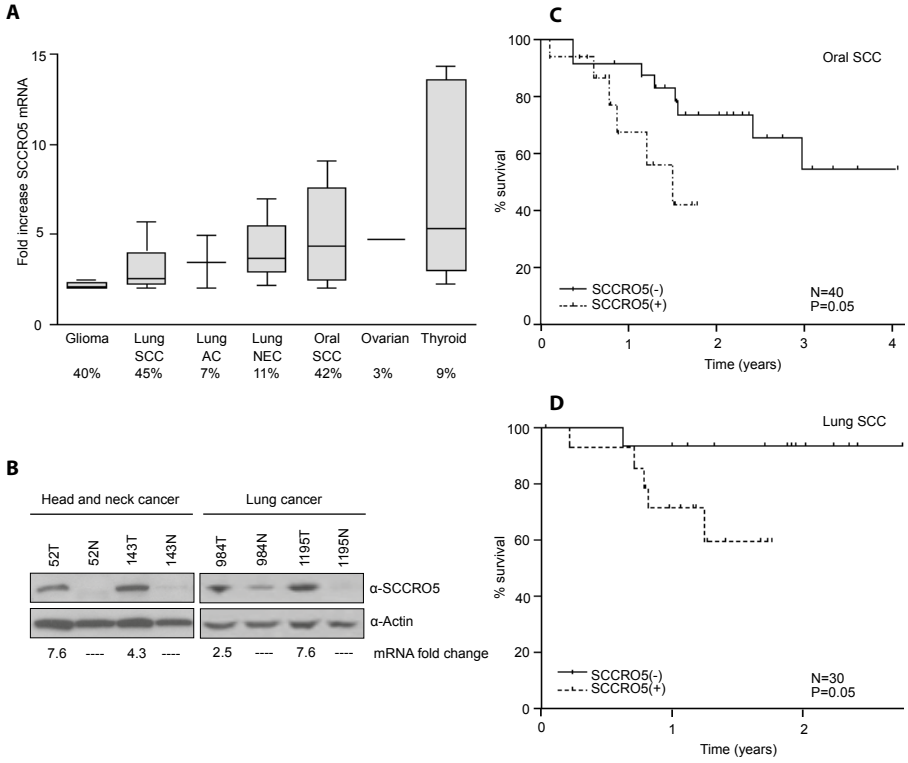

(**A**), box plot showing fold increase in SCCRO5 mRNA expression, analyzed by qRT-PCR, in 10 gliomas, 30 lung SCCs, 27 lung adenocarcinomas (AC), 54 lung neuroendocrine (NEC) tumors, 40 oral SCCs, 40 ovarian carcinomas, and 56 thyroid carcinomas, compared with matched normal tissues (boxes represent the lower through the upper quartile; the median is shown as a horizontal line; whiskers represent minimum and maximum levels). The percentage of cases with overexpression is given below each plot. (**B**), Western blot analysis showing SCCRO5 protein expression in representative head and neck and lung SCCs (T) and matched normal (N) samples. The corresponding fold change in mRNA levels, determined by real-time PCR, is noted below. (**C**), Kaplan–Meier survival curves from post-hoc analysis showing recurrence-free survival based on SCCRO5 mRNA expression status in primary oral SCCs. (**D**), Kaplan–Meier survival curves showing recurrence-free survival from post hoc analysis based on SCCRO5 mRNA expression status in primary lung SCCs.

Discussion

SCCRO and its paralogs are commonly dysregulated in human cancers, with aberrations of one or more paralogs present in 50% of head and neck cancers, in 70% of lung SCCs, in 55% of ovarian serous cystadenocarcinomas, in 34% of cervical and endometrial carcinomas, in 26% of lung adenocarcinomas, and in 15% of glioblastomas, on the basis of analysis of interim data from respective TCGA projects. Of the SCCRO paralogs, SCCRO and SCCRO5 are the most commonly dysregulated and have a tendency toward mutual exclusivity, which suggests that they act independently in oncogenesis. It is well established that overexpression of SCCRO promotes its function as an oncogene (16, 18). By showing that overexpression of SCCRO5 has transforming activity and by associating it with an aggressive clinical course in human cancers, our data support the position that SCCRO5 may function as an oncogene as well (20). Its role in cancer pathogenesis is further validated by our findings, which indicate the presence of an oncogene addiction phenotype in cancer cell lines that have high endogenous levels of SCCRO5 expression. Structure-function analyses show that, as with SCCRO, SCCRO5's conserved PONY domain is required for binding to neddylation components, as well as for its neddylation and transforming activities (16, 17, 41, 42). Of interest, SCCRO5's N-terminal NLS was not required for neddylation- promoting activity in vitro, which is similar to the case for the UBA domain in SCCRO (41).

Given that SCCRO's subcellular localization is important to its neddylation activity, the direct or indirect association of the N-terminal motifs with subcellular localization of the SCCRO paralogs suggests that they may regulate neddylation activity in vivo (43–45). Consistent with this finding, SCCRO's UBA is involved in monoubiquitination by Nedd4-1, which promotes nuclear export, thereby inhibiting its neddylation activity (unpublished data; refs. 43, 45). Similarly, the myristoylation sequence localizes SCCRO3 to the membrane, which affects its neddylation promoting activity (unpublished data; ref. 46). Our finding showing that the NLS is required for SCCRO5's transforming activity suggests that, as with the UBA, the NLS may modulate neddylation activity in vivo. However, these findings raise a question about SCCRO5's role in neddylation. Our previous work showed that SCCRO promotes nuclear translocation of Cullin-ROC1, which is required for neddylation in vivo. Given that SCCRO5 is present almost exclusively in the nucleus, it is unclear how cytoplasmic Cullin-ROC1 complexes are delivered to the nucleus to allow for interaction with SCCRO5. Several possibilities exist, including cooperative activity between other SCCRO paralogs and NLS-containing variants, presence of alternative mechanisms for nuclear translocation of Cullin-ROC1 complexes, and selective activity on cullins situated in the nucleus. The functional effects of neddylation are mediated by downstream targets that CRLs activate.

The recent publication by Monda and colleagues showing that SCCRO and its paralogs have overlapping affinity to E2s (Ube2M and Ube2F) and cullins (42) suggests that they may have redundant effects on CRL activity in vivo. This idea is supported by the differential requirements of SCCRO for viability in yeast, whose genome does not contain other SCCRO paralogs, and in higher

organisms, where paralogs can compensate for SCCRO loss (unpublished data; refs. 40, 43). As SCCRO5 promotes neddylation of all cullins (with the possible exception of Cul4A), it putatively can regulate the ubiquitination of a myriad of proteins, resulting in diverse cellular effects (42). Guo and colleagues suggest that SCCRO5 may be involved in regulating ubiquitination of the proteins involved in DNA damage repair (20). Consistent with this suggestion, SCCRO5 was found to be part of a panel of seven genes whose expression score predicts radiation response in patients with cervical cancer (47). Further work is required to define the CRLs and protein targets that are dependent on SCCRO5 in the DNA damage response, cellular activities, and oncogenesis.

Supplemental figure 1.

A

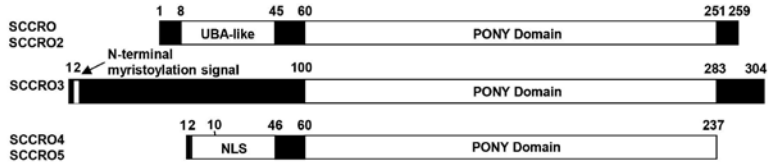

B

```
SCCRO   206   RSIPKDTWNLLLDFSTMIADDMSNYDEEGAWPVLIDDFVEFA-RPQI   251
SCCRO2  206   RSIPRDTWNLLLDFGNMIADDMSNYDEEGAWPVLIDDFVEYA-RPVV   251
SCCRO3  237   KGISRDTWNMFLNFTQVIGPDLSNYSEDEAWPSLFDTFVEWEMERRKR   283
SCCRO4  190   KVINKDQWCNVLEFSRTINLDLSNYDEDGAWPVLLDEFVEWYKDKQMS   237
SCCRO5  190   RVMNKDQWYNVLEFSRTVHADLSNYDEDGAWPVLIDEFVEWQKVRQTS   237
```

(**A**), Schematic representation of domain structures of SCCRO and its paralogs. (**B**), Alignment of PONY domain of SCCRO and its paralogs. SCCRO5 residues critical for binding to neddylation components are shown.

Supplemental figure 2.

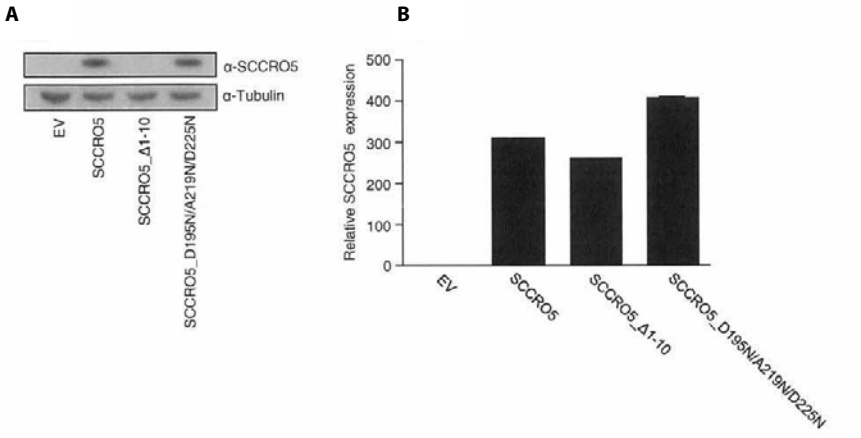

(**A**), Western blot analysis of lysates of NIH-3T3 cells stably transfected with vector alone, *SCCRO5*, *SCCRO5*_Δ1-10 or *SCCRO5*_D195N/A219R/D225N and probed with antibody against SCCRO5 or tubulin as a loading control. SCCRO5_Δ1-10 is not detected as the antibody recognizes an epitope that included this region. (**B**), Bar graph depicting results of qRT-PCR on the same cells as in A showing expression of transgenes.

Supplemental figure 3.

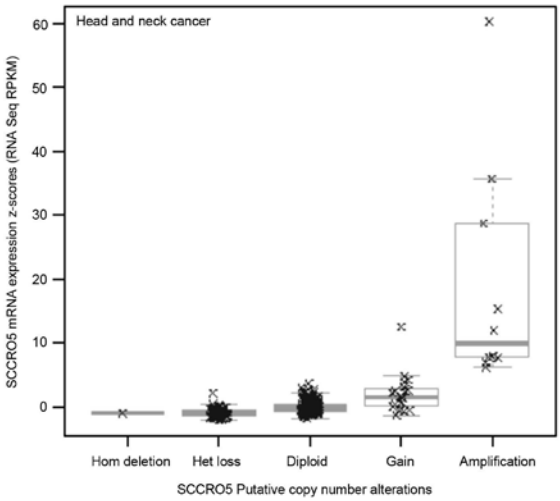

Correlation between *SCCRO5* copy number alterations and mRNA expression measured by RNA seq (deep sequencing for RNA), in head and neck squamous cell carcinomas from The Cancer Genome Atlas, normalized by z-score transformation. Het, heterozygous; Hom, homologous; RPKM, reads per kilobase for million mapped reads.

Supplemental figure 4.

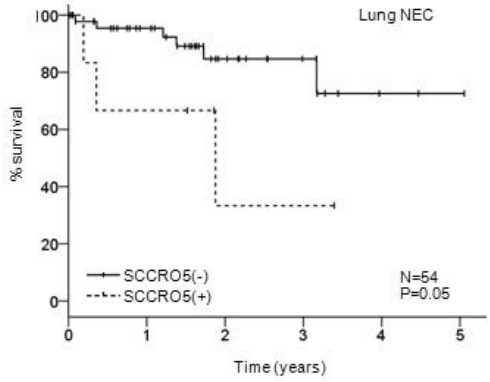

Kaplan-Meier survival curves from post-hoc analysis showing recurrence-free survival based on SCCRO5 mRNA expression status in primary lung neuroendocrine carcinomas.

Supplemental Table S1. Oral squamous cell carcinoma- patient and tumor characteristics.

Characteristic	Total (N=40)	SCCRO5 overexpression		*P*
		Present (N=16)	Absent (N=24)	
Median age (range), years	57 (26-89)	57 (36-89)	58 (26-80)	NS*
Gender				NS#
Male	24	9	15	
Female	16	7	9	
TNM Stage				NS#
Early (I-II)	29	12	17	
Advanced (III-IV)	11	4	7	
Tumor site in oral cavity				NS#
Tongue	24	11	13	
Other	16	5	11	
Tobacco use				NS#
Yes	25	10	15	
No	15	6	9	

*Mann-Whitney U test.
#Fisher's exact test.

Supplemental Table S2. Lung squamous cell carcinoma –patient and tumor characteristics.

Characteristic	Total (N=30)	SCCRO5 overexpression		*P*
		Present (N=15)	Absent (N=15)	
Median age (range), years	67 (43-84)	67 (43-84)	65 (48-76)	NS*
Gender				NS#
Male	21	9	12	
Female	9	6	3	
TNM Stage				NS#
Early (I-II)	25	12	13	
Advanced (III-IV)	5	3	2	
Tobacco use				NS#
Yes	29	15	14	
No	1	0	1	

*Mann-Whitney U test.
#Fisher's exact test.

Supplemental Table S3. Thyroid carcinoma –patient and tumor characteristics.

Characteristic	SCCRO5 overexpression		*P Value*
	Present (N=5)	Absent (N=51)	
Age			NS#
<45 years	3	23	
>45 years	2	28	
Gender			NS#
Female	4	41	
Male	1	10	
Type of operation			NS#
Total	4	31	
Lobectomy	1	20	
Tumor size			NS#
0-2 cm	2	29	
>2.1 cm	3	22	
Lymph node metastasis			NS#
Present	3	41	
Absent	2	10	
Capsular invasion			NS#
Present	1	29	
Absent	4	22	
Tumor encapsulation			NS#
Present	4	31	
Absent	1	20	
Extrathyroidal extension			NS#
Present	2	33	
Absent	3	18	
Recurrence			NS#
Present	1	1	
Absent	4	50	

#Fisher's exact test.

Supplemental Table S4. Lung neuroendocrine carcinoma –patient and tumor characteristics.

Characteristic	SCCRO5 overexpression		*P Value*
	Present (N=6)	Absent (N=48)	
Median age (range), years	58.5 (48-79)	63.5 (31-83)	NS*
Gender			NS#
Female	3	20	
Male	3	28	
Tobacco use			NS#
Yes	39	6	
No	9	0	
Tumor type			NS+
Carcinoid	2	16	
Large cell carcinoma	3	25	
Small cell carcinoma	1	7	
TNM Stage			NS#
Early (I-II)	5	45	
Advanced (III-IV)	1	3	
Recurrence			0.05#
Present	3	6	
Absent	3	42	

*Mann-Whitney U test.
#Fisher's exact test.
+Chi Square Test

Supplemental Table S5. Sequences of the real-time PCR primers for *SCCRO5* and housekeeping gene *GAPDH* (in 5'-3' direction).

Gene	Forward primer	Reverse primer
SCCRO5	'TGCGCTCACAGTTGAATGATATTTCGTC'	'CAGTGGCCATGTCCTCCCAAGCAG'
GAPDH	'GCACCACCAACTGCTTAG'	'CATGGACTGTGGTCATGAG'

Supplemental Table S6. Sequences of the DNA mutation analysis primers for *SCCRO5*.

DNA mutation analysis primer	Sequence
SCCRO5_450608_L_13706892_chr11_102467638_20	GTAAAACGACGGCCAGTGGGGAAGCGCAATTTACATA
SCCRO5_450608_R_13706893_chr11_102468531_20	CAGGAAACAGCTATGACCAGTTTCACTTTTTGGCGGTG
SCCRO5_450609_L_13160312_chr11_102465192_20	GTAAAACGACGGCCAGTTCAGCCTAAATTGGCAACAA
SCCRO5_450609_R_13160313_chr11_102465562_20	CAGGAAACAGCTATGACCACAATGCCAACCGAAGAAAA
SCCRO5_450610_L_chr11_102459030	GTAAAACGACGGCCAGTCATTTGCCCAACTTAAACTGA
SCCRO5_450610_R_chr11_102459353	CAGGAAACAGCTATGACCTGGTGTGTTCATGGGTACCTT
SCCRO5_450611_L_13158842_chr11_102458527_20	GTAAAACGACGGCCAGTCTGCCCAACGAACATACTCC
SCCRO5_450611_R_13158843_chr11_102458999_20	CAGGAAACAGCTATGACCTGCTGACTTTTCCCCTATCC
SCCRO5_450612_L_12038772_chr11_102442443_20	GTAAAACGACGGCCAGTATGTCCTCCCAAGCAGAAGA
SCCRO5_450612_R_12038773_chr11_102442863_20	CAGGAAACAGCTATGACCATTGGTAGATGCAGGGCAAG
SCCRO5_450613_L_15099538_chr11_102442179_20	GTAAAACGACGGCCAGTCTTTTATTTGGGGGACTGGG
SCCRO5_450613_R_15099539_chr11_102442597_20	CAGGAAACAGCTATGACCATGCCTTTGATTTTGCAAGG
SCCRO5_450614_L_14044750_chr11_102440195_20	GTAAAACGACGGCCAGTGTTGCCGAGGAACTGAAAAC
SCCRO5_450614_R_14044751_chr11_102440890_20	CAGGAAACAGCTATGACCGCCAAACTCAAAATGTGGCT
SCCRO5_450615_L_12063632_chr11_102438024_20	GTAAAACGACGGCCAGTAAGGCCAACAGTCTTCCAAA
SCCRO5_450615_R_12063633_chr11_102438925_20	CAGGAAACAGCTATGACCGCTGATCCCTCTCAACAAGC

Supplemental Table S7. Sequences of the primers used for SCCRO5 PCR for deletion and mutagenesis.

Mutation primer	Sequence
Δ1-10	CGCGGATCCATGGGGGTG
Δ1-46	CGCGGATCCATGTCAAGCAAGAAGT
Δ189-237	CTTTGATTGCTCCAGGTACTGGTAAAATAC
A219R	ACAGGCCAACGACCATCTTCAT
D195N	CATTGTACCATTGATTTTTGTTCATAACACGATAC
D225N	GCCACTCAACAAATTCATTAAGAAGAACAGG
E226A	CACTCAACAAATGCATCAAGAAGAACAGG

References

1. Liu Z, Zanata SM, Kim J, Peterson MA, Di Vizio D, Chirieac LR, et al. The ubiquitin-specific protease USP2a prevents endocytosis-mediated EGFR degradation. Oncogene 2013;32:1660–9.
2. Grim JE, Knoblaugh SE, Guthrie KA, Hagar A, Swanger J, Hespelt J, et al. Fbw7 and p53 cooperatively suppress advanced and chromosomally unstable intestinal cancer. Mol Cell Biol 2012;32:2160–7.
3. Soucy TA, Dick LR, Smith PG, Milhollen MA, Brownell JE. The Nedd8 conjugation pathway and its relevance in cancer biology and therapy. Genes Cancer 2010;1:708–16.
4. Hsu JM, Lee YC, Yu CT, Huang CY. Fbx7 functions in the SCF complex regulating Cdk1-cyclin B-phosphorylated hepatoma up-regulated protein (HURP) proteolysis by a proline-rich region. J Biol Chem 2004;279:32592–602.
5. Lehman NL, van de Rijn M, Jackson PK. Screening of tissue microarrays for ubiquitin proteasome system components in tumors. Methods Enzymol 2005;399:334–55.
6. Chen LC, Manjeshwar S, Lu Y, Moore D, Ljung BM, Kuo WL, et al. The human homologue for the Caenorhabditis elegans cul-4 gene is amplified and overexpressed in primary breast cancers. Cancer Res 1998;58:3677–83.
7. Melchor L, Saucedo-Cuevas LP, Munoz-Repeto I, Rodriguez-Pinilla SM, Honrado E,Campoverde A, et al. Comprehensive characterization of the DNA amplification at 13q34 in human breast cancer reveals TFDP1 and CUL4A as likely candidate target genes. Breast Cancer Res 2009;11:R86.
8. Chen A, Wu K, Fuchs SY, Tan P, Gomez C, Pan ZQ. The conserved RING-H2 finger of ROC1 is required for ubiquitin ligation. J Biol Chem 2000;275:15432–9.
9. Kawakami T, Chiba T, Suzuki T, Iwai K, Yamanaka K, Minato N, et al. Nedd8 recruits E2-ubiquitin to SCF E3 ligase. EMBO J 2001;20:4003–12.
10. Zheng J, Yang X, Harrell JM, Ryzhikov S, Shim EH, Lykke-Andersen K, et al. CAND1 binds to unneddylated CUL1 and regulates the formation of SCF ubiquitin E3 ligase complex. Mol Cell 2002;10:1519–26.
11. Goldenberg SJ, Cascio TC, Shumway SD, Garbutt KC, Liu J, Xiong Y, et al. Structure of the Cand1-Cul1-Roc1 complex reveals regulatory mechanisms for the assembly of the multisubunit cullin-dependent ubiquitin ligases. Cell 2004;119:517–28.
12. Sakata E, Yamaguchi Y, Miyauchi Y, Iwai K, Chiba T, Saeki Y, et al. Direct interactions between Nedd8 and ubiquitin E2 conjugating enzymes upregulate cullin-based E3 ligase activity. Nat Struct Mol Biol 2007;14:167–8.
13. Wimuttisuk W, Singer JD. The Cullin3 ubiquitin ligase functions as a Nedd8-bound heterodimer. Mol Biol Cell 2007;18:899–909.
14. Gong L, Yeh ET. Identification of the activating and conjugating enzymes of the Nedd8 conjugation pathway. J Biol Chem 1999; 274:12036–42.
15. Zhao Y, Sun Y. Cullin-RING ligases (CRLs) as attractive anti-cancer targets. Curr Pharm Des 2013;19:3215–25.
16. Sarkaria I, O-charoenrat P, Talbot SG, Reddy PG, Ngai I, Maghami E, et al. Squamous cell carcinoma related oncogene/DCUN1D1 is highly conserved and activated by amplification in squamous cell carcinomas. Cancer Res 2006;66:9437–44.
17. Kim AY, Bommeljé CC, Lee BE, Yonekawa Y, Choi L, Morris LG, et al. SCCRO (DCUN1D1) is an essential component of the E3 complex for neddylation. J Biol Chem 2008;283:33211–20.
18. Broderick SR, Golas BJ, Pham D, Towe CW, Talbot SG, Kaufman A, et al. SCCRO promotes glioma formation and malignant progression in mice. Neoplasia 2010;12:476–84.
19. Ma T, Shi T, Huang J, Wu L, Hu F, He P, et al. DCUN1D3, a novel UV-responsive gene that is involved in cell cycle progression and cell growth. Cancer Sci 2008;99:2128–35.
20. Guo W, Li GJ, Xu HB, Xie JS, Shi TP, Zhang SZ, et al. In vitro biological characterization of DCUN1D5 in DNA damage response. Asian Pac J Cancer Prev 2012;13:4157–62.
21. Abba MC, Fabris VT, Hu Y, Kittrell FS, Cai WW, Donehower LA, et al. Identification of novel amplification gene targets in mouse and human breast cancer at a syntenic cluster mapping to mouse ch8A1 and human ch13q34. Cancer Res 2007;67:4104–12.
22. Salgado R, Toll A, Alameda F, Baro T, Martin-Ezquerra G, Sanmartin O, et al. CKS1B amplification is a frequent event in cutaneous squamous cell carcinoma with aggressive clinical behaviour. Genes Chromosomes Cancer 2010;49:1054–61.

23. Barrow J, Adamowicz-Brice M, Cartmill M, MacArthur D, Lowe J, Robson K, et al. Homozygous loss of ADAM3A revealed by genome-wide analysis of pediatric high-grade glioma and diffuse intrinsic pontine gliomas. Neuro Oncol 2011;13:212–22.
24. Lockwood WW, Chari R, Chi B, Lam WL. Recent advances in array comparative genomic hybridization technologies and their applications in human genetics. Eur J Hum Genet 2006;14:139–48.
25. Brown J, Bothma H, Veale R, Willem P. Genomic imbalances in esophageal carcinoma cell lines involve Wnt pathway genes. World J Gastroenterol 2011;17:2909–23.
26. Ambatipudi S, Gerstung M, Gowda R, Pai P, Borges AM, Schaffer AA, et al. Genomic profiling of advanced-stage oral cancers reveals chromosome 11q alterations as markers of poor clinical outcome. PLoS ONE 2011;6:e17250.
27. Dai Z, Zhu WG, Morrison CD, Brena RM, Smiraglia DJ, Raval A, et al. A comprehensive search for DNA amplification in lung cancer identifies inhibitors of apoptosis cIAP1 and cIAP2 as candidate oncogenes. Hum Mol Genet 2003;12:791–801.
28. Muramatsu T, Imoto I, Matsui T, Kozaki K, Haruki S, Sudol M, et al. YAP is a candidate oncogene for esophageal squamous cell carcinoma. Carcinogenesis 2011;32:389–98.
29. Wu C, Xu B, Yuan P, Miao X, Liu Y, Guan Y, et al. Genome-wide interrogation identifies YAP1 variants associated with survival of smallcell lung cancer patients. Cancer Res 2010;70:9721–9.
30. Baldwin C, Garnis C, Zhang L, Rosin MP, Lam WL. Multiple microalterations detected at high frequency in oral cancer. Cancer Res 2005;65:7561–7.
31. Zender L, Spector MS, Xue W, Flemming P, Cordon-Cardo C, Silke J, et al. Identification and validation of oncogenes in liver cancer using an integrative oncogenomic approach. Cell 2006;125:1253–67.
32. Lockwood WW, Coe BP, Williams AC, MacAulay C, Lam WL. Whole genome tiling path array CGH analysis of segmental copy number alterations in cervical cancer cell lines. Int J Cancer 2007;120:436–43.
33. Singh B, Gogineni S, Goberdhan A, Sacks P, Shaha A, Shah J, et al. Spectral karyotyping analysis of head and neck squamous cell carcinoma. Laryngoscope 2001;111:1545–50.
34. Essentials of real time PCR [Internet]. Applied Biosystems; 2012. Available from: http://www3.appliedbiosystems.com/cms/groups/mcb_marketing/documents/generaldocuments/cms_039996.pdf.
35. Gene Quantification [Internet]. Reference genes/housekeeping genes. Available from: http://www.gene-quantification.de/hkg.html.
36. Vandesompele J, De Preter K, Pattyn F, Poppe B, Van Roy N, De Paepe A, et al. Accurate normalization of real-time quantitative RT-PCR data by geometric averaging of multiple internal control genes. GenomeBiol 2002;3:RESEARCH0034.
37. Rozen S, Skaletsky H. Primer3 on the WWW for general users and for biologist programmers. Methods Mol Biol 2000;132:365–86.
38. Little SE, Vuononvirta R, Reis-Filho JS, Natrajan R, Iravani M, Fenwick K, et al. Array CGH using whole genome amplification of fresh-frozen and formalin-fixed, paraffin-embedded tumor DNA. Genomics 2006;87:298–306.
39. Marks JL, McLellan MD, Zakowski MF, Lash AE, Kasai Y, Broderick S, et al. Mutational analysis of EGFR and related signaling pathway genes in lung adenocarcinomas identifies a novel somatic kinase domain mutation in FGFR4. PLoS ONE 2007;2:e426.
40. Kurz T, Chou YC, Willems AR, Meyer-Schaller N, Hecht ML, Tyers M, et al. Dcn1 functions as a scaffold-type E3 ligase for cullin neddylation. Mol Cell 2008;29:23–35.
41. Kurz T, Ozlu N, Rudolf F, O'Rourke SM, Luke B, Hofmann K, et al. The conserved protein DCN-1/Dcn1p is required for cullin neddylation in C. elegans and S. cerevisiae. Nature 2005;435:1257–61.
42. Monda JK, Scott DC, Miller DJ, Lydeard J, King D, Harper JW, et al. Structural conservation of distinctive N-terminal acetylation-dependent interactions across a family of mammalian Nedd8 ligation enzymes. Structure 2013;21:42–53.
43. Huang G, Kaufman AJ, Ramanathan Y, Singh B. SCCRO (DCUN1D1) promotes nuclear translocation and assembly of the neddylation E3 complex.J Biol Chem 2011;286:10297–304.
44. Weinstein IB, Joe A. Oncogene addiction. Cancer Res 2008;68:3077–80.
45. Wu K, Yan H, Fang L, Wang X, Pfleger C, Jiang X, et al. Monoubiquitination drives nuclear export of the human DCN1-like protein hDCNL1. J Biol Chem 2011;286:34060–70.

46. Meyer-Schaller N, Chou YC, Sumara I, Martin DD, Kurz T, Katheder N, et al. The human Dcn1-like protein DCNL3 promotes Cul3 neddylation at membranes. Proc Natl Acad Sci U S A 2009;106:12365–70.

47. Rajkumar T, Vijayalakshmi N, Sabitha K, Shirley S, Selvaluxmy G, Bose MV, et al. A 7 gene expression score predicts for radiation response in cancer cervix. BMC Cancer 2009;9:365.

Chapter 9

SCCRO and its paralogs are frequently dysregulated in human cancers and are associated with an aggressive clinical course and activation of neddylation

C.C. Bommeljé, H. Sun, S. Bains, R. Ghossein, Y. Ramanathan, B. Singh

Submitted to Annals of Surgical Oncology

Abstract

Background: SCCRO is now established as an oncogenic driver in many types of cancer. Recently, SCCRO's paralogs were shown to play a role in cancer pathogenesis. The focus of this work was to determine the prevalence of dysregulation of SCCRO and its family members and to assess their clinical and biological significance in human cancers.

Methods: Expression of SCCRO and its family members was assessed in a cohort of 257 human cancer samples and in interim results from The Cancer Genome Atlas (TCGA) for head and neck cancers. Expression of SCCRO and its family members was then correlated with clinical outcomes and biochemical activity in neddylation and ubiquitination, using selected cohorts.

Results: SCCRO and its family members were commonly dysregulated in many types of cancer, with the highest prevalence in squamous cell carcinomas (SCCs) of the lung and oral cavity and neuroendocrine carcinomas of the lung. The prevalence of dysregulation was similar in the interim TCGA data. Expression of SCCRO and its paralogs was associated with poorer survival outcomes for oral SCC in our study cohort and for head and neck cancer in the TCGA data. Moreover, levels of endogenous SCCRO correlated with neddylation and ubiquitination activity in representative tumor samples of oral cavity and thyroid cancers.

Conclusions: SCCRO and its paralogs are commonly dysregulated in human cancers. Given the biochemical functions of SCCRO and its family members in neddylation, targeting their function may have therapeutic benefit.

Introduction

Our group previously identified squamous cell carcinoma related oncogene (*SCCRO*, aka *DCUN1D1*) within an amplification peak at 3q that is present with a high prevalence in head and neck cancers, lung squamous cell carcinomas (SCCs), and many other cancer types.[1-6] Its role as a cancer driver was validated by (1) independent correlation of SCCRO overexpression with worse clinical outcomes, (2) the presence of oncogenic activity *in vitro* and *in vivo*, and (3) the presence of an oncogene addiction phenotype.[7, 8] A subsequent analysis of The Cancer Genome Atlas (TCGA) data for lung SCC validated our findings by showing that SCCRO is a driver within the 3q amplicon in lung SCC.[9, 10] In addition, SCCRO was identified as one of the top 42 druggable cancer driver genes amplified across multiple TCGA datasets.[11] Combined, these data established the role of SCCRO as an oncogenic driver in a wide range of cancer types.

We and others found that SCCRO functions in neddylation, a process analogous to ubiquitination, in which a tripartite enzymatic cascade results in covalent modification of primarily cullin family members with the ubiquitin-like protein Nedd8.[12] Neddylation of cullins promotes assembly and activity of cullin-RING-ligase (CRL) type ubiquitination E3s. As such, neddylation regulates the activity of the largest class of E3s involved in ubiquitination.[13-15] Dysfunction of the ubiquitin-proteasome pathway contributes to deregulated cell-cycle control and aberrant cell proliferation and has been implicated in the pathogenesis of numerous human diseases, including cancer.[16-18] Although SCCRO was not required for neddylation *in vitro*, our findings suggest that its subcellular localization of neddylation components is essential for *in vivo* neddylation activity.

Starting as a single gene in one-cell organisms, SCCRO has evolved to include four additional paralogs in mammals: SCCRO2, SCCRO3, SCCRO4, and SCCRO5. Each of these paralogs has a highly conserved potentiation of neddylation (PONY) domain in common, which is required for binding to neddylation components and for promoting neddylation activity. We have shown that SCCRO, SCCRO2, SCCRO4, and SCCRO5 all promote neddylation and function as oncogenes.[8, 10, 12, 19] In contrast, the expression of SCCRO3 is decreased, compared with its expression in matched adjacent normal tissues, and it functions as a tumor suppressor gene.[20] The frequency of dysregulation of each of all these genes in head and neck and other cancers remains to be determined.

Materials and methods

Bioinformatic analyses

The ClustalW program (Conway Institute UCD, Dublin, Ireland) was used for multiple sequence alignments (Supplemental Figure S1, Supplemental Table S1). Data from TCGA projects were accessed and analyzed using the cBio Cancer Genomics Portal (http://www.cbioportal.org).

Human tissues, cell lines, and antibodies

A total of 257 randomly selected primary cancer tissue and adjacent matched histologically normal tissue samples were obtained from patients undergoing surgical treatment at Memorial Sloan Kettering Cancer Center between January 1, 2004, and October 1, 2007, as previously described.[19] The study group included 30 lung SCCs, 27 lung adenocarcinomas, 54 lung neuroendocrine carcinomas, 40 oral SCCs, 10 oligodendromas, 40 ovarian carcinomas, 9 benign nodular hyperplasias, 9 follicular adenomas, 10 Hürthle cell carcinomas, 18 well-differentiated papillary thyroid carcinomas, and 10 tall cell variant papillary thyroid carcinomas. Demographic and tumor data for all patients are described in Supplemental Tables S2 and S3.

The origins, maintenance, and growth of the cell lines used in this study have been described previously.[1,8] The following antibodies were used in this study: anti-SCCRO (developed and validated as previously described)[8], anti-Cul1 (Invitrogen, Grand Island, NY), anti-Ponceau S (Millipore, Billerica, MA), and anti-ubiquitin (Santa Cruz Biotechnology, Santa Cruz, CA).

RNA isolation, cDNA synthesis, and quantitative real-time PCR (qRT-PCR)

RNA isolation and, cDNA synthesis in this study were performed, as previously described.[19] Primers were designed for all *SCCRO* paralogs and glyceraldehyde-3-phosphate-dehydrogenase *(GAPDH)* (Supplemental Table S4). To confirm their specificity, the primer sets were tested on plasmids for all *SCCRO* paralogs. qRT-PCR for all *SCCRO* paralogs was performed on the 257 tumor and paired normal samples and the comparative threshold cycle method was used to calculate the expression ratio in each sample relative to the value observed in the control standard curve, as previously described.[8,19, 21, 22, 23]

Mutation profiling

Primers were designed, using Primer3, to cover putative exon regions of all SCCRO paralogs (National Center for Biotechnology Information Human Genome Build 36.1); products were ≤500 bp in length.[24] Tumor DNA extraction and mutation analysis were performed in this study, as described previously.[19, 25,26]

Protein extraction and Western blot analysis

For protein extraction, primary tumor tissues were mechanically homogenized in 1× cell lysis buffer (Cell Signaling Technology, Danvers, MA). Protein concentrations were determined using the standard Bradford assay. Twenty-five micrograms of primary tissue extracts (25 µg) in 6× Laemmli buffer were loaded onto 4% to 12% Bis-Tris polyacrylamide gel, and Western blotting was performed in accordance with the standard protocol.

Activated neddylation assay and global ubiquitination

A biochemical assay was developed to assess neddylation activity in tissue lysates. The assay has been validated to accurately represent neddylation activity, using lysates from murine embryonic fibroblasts (MEFs) harvested from wild-type and $SCCRO^{-/-}$ mice in which levels of endogenous SCCRO, basal neddylation, and ubiquitination are known. Tumor tissue extracts served as a source of Cullin-ROC1 substrate for activated neddylation reactions. In total, 50 µg of wild-type MEF lysates or 200 µg of tumor tissue extracts were added to reactions containing 10 nM APPBP1/Uba3, 200 nM Ubc12, 2 µM Nedd8, and 100 mM ATP. All reactions were performed in 1× neddylation buffer (50 mM Tris-HCl [pH 7.6], 1 Mm NaF, 55 mM NaCl, and 5mM MgCl2) and incubated at 30°C for the indicated times. Reactions were stopped by the addition of 6× Laemmli buffer, loaded onto 7.5% Tris-HCl polyacrylamide gel, and Western blotting was performed in accordance with the standard protocol. The antibodies used were rabbit anti-Cul1 (1:1000; Invitrogen) and mouse anti-ubiquitin (1:1000; Santa Cruz Biotechnology). The blots were visualized using a chemiluminescent detection kit (Millipore). To quantify protein levels on Western blots, densitometric analysis was performed using ImageJ software. Ponceau-S was used as loading control, Ponceau-S levels were quantified using ImageJ, and protein levels were normalized against Ponceau-S levels. To assess global levels of ubiquitinated proteins, Western blots from the neddylation assays were stripped and reprobed with anti-ubiquitin antibody.

Statistical analysis

All statistical analyses were performed using the SPSS statistical software package (version 19; IBM, Armonk, NY). qRT-PCR results were expressed as means ± SD, and only tumor samples with values at least 2-fold different from the matched normal samples and at least 2-fold different from the SD of the mean of all normal samples of the same histologic profile were considered to overexpress or underexpress a particular gene. The nonparametric Wilcoxon test was used to compare the levels of mRNA expression between tumor and normal samples and to compute the relationship between SCCRO expression and neddylation activity. Survival curves were generated using the Kaplan-Meier method, by use of GraphPad Prism software for Windows (San Diego, California), and were compared using the log-rank test. A p level ≤ 0.05 was considered to indicate statistical significance, and all tests were two-sided.

Results

SCCRO paralogs are commonly dysregulated in human cancers

To determine the prevalence of dysregulation of SCCRO and its family members in various human cancers, we first assessed mRNA expression levels using qRT-PCR analysis in a variety of human cancer and matched normal tissues. The most commonly dysregulated paralogs in human cancers were SCCRO (27%), SCCRO3 (41%), and SCCRO5 (14%). SCCRO was most commonly overexpressed in lung SCCs, oral SCCs, and oligodendromas. SCCRO2 was most commonly overexpressed in lung SCCs and oligodendromas. A decrease in SCCRO3 expression was common in multiple cancer types, with the highest prevalence of dysregulation observed in SCCs, adenocarcinomas, neuroendocrine carcinomas of the lung, and Hürthle cell carcinomas. Although overexpression of SCCRO4 was not common, it occurred with the highest frequency in all SCCs and Hürthle cell carcinomas. SCCRO5 overexpression was most common in oral SCCs and oligodendromas (Table 1).

Table 1. Expression of SCCRO1-5 in primary human cancers, analyzed by RT-PCR.

Tumor type	SCCRO	SCCRO2	SCCRO3	SCCRO4	SCCRO5
Lung squamous cell carcinoma (n=30)	57	23	57	7	11
Lung adenocarcinoma (n=27)	4	11	48	0	7
Lung neuroendocrine carcinoma (n=54)	35	13	85	7	11
Oral squamous cell carcinoma (n=40)	44	3	17	17	42
Oligodendroma (n=10)	60	70	0	10	40
Ovarian carcinoma (n=40)	18	6	20	5	3
Thyroid benign nodular hyperplasia (n=9)	11	11	22	0	0
Thyroid follicular adenoma (n=9)	0	0	22	0	0
Thyroid Hürthle cell carcinomas (n=10)	10	10	60	20	10
Thyroid papillary carcinoma (n=18)	5	5	11	5	11
Thyroid tall cell variant (n=10)	0	20	10	10	20

Shown are the percentages of cases with mRNA overexpression; for SCCRO3, the percentage of cases in which expression was decreased is shown.

To validate the prevalence of dysregulation of SCCRO and its family members, we analyzed interim results from TCGA projects using the BioPortal for all available tumors. In the TCGA data set, copy number changes in SCCRO and its paralogs were common; the highest prevalence for SCCRO was in lung SCC (79 of 178; 44.3%), ovarian carcinoma (187 of 570; 32.8%), and head and neck SCC (75 of 279; 26.8%) (Figure 1A). Copy number changes were less common for other SCCRO paralogs (data not shown). A strong correlation was found between SCCRO copy number and mRNA expression in head and neck cancers (Figure 1B), as well as other cancers (data not shown).

Combined, these findings suggest that SCCRO and its paralogs are commonly dysregulated in human cancers. Moreover, the common codysregulation of SCCRO paralogs suggests that they may play cooperative roles in oncogenesis; these roles remain to be determined.

Mutations in SCCRO paralogs are rare in human cancers

Mutations are a mechanism for activation of oncogenes. To begin to determine whether mutations contribute to the oncogenic activation of SCCRO and its paralogs, we subjected our tumor cohort to exon sequencing. We identified only 1 case with a mutation in the UBA domain of SCCRO (data not shown). Exon sequencing revealed several single nucleotide polymorphisms (SNPs), shown in Supplemental Table S5. The significance of these SNPs, if any, has yet to be determined. In the TCGA data set, mutations of SCCRO and its paralogs were present in many cancer types, with the highest prevalence in melanomas (12 of 228; 5.2%), uterine carcinomas (10 of 248; 4%), lung adenocarcinomas (8 of 229; 3.5%), and head and neck SCCs (4 of 306; 1.3%) (Figure 1C). We have previously shown that mutations found in the UBA domain of SCCRO (and identified in the TCGA data set) enhance its oncogenic activity.[27] The effects that mutations in SCCRO's paralogs have on their function remain to be determined.

Figure 1. TCGA data analysis.

A

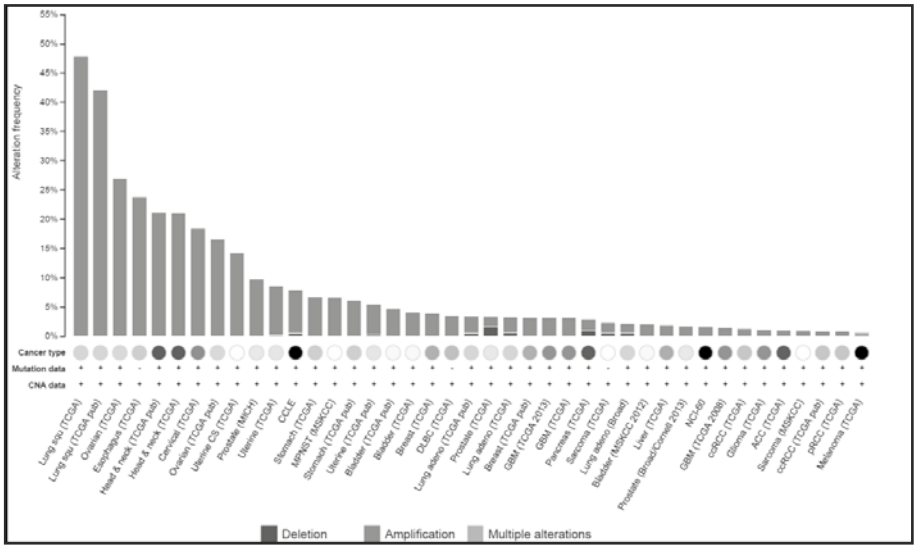

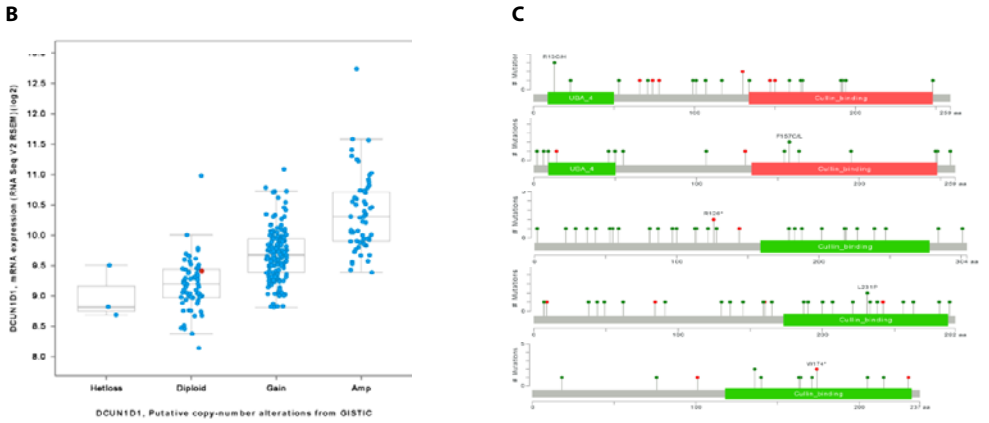

(**A**), Results from analysis of the TCGA data set for all tumors for SCCRO, showing copy number alterations. (**B**), Correlation between SCCRO expression and copy number for head and neck cancers in the TCGA data set. (**C**), Mutations in SCCRO1-5 identified in the TCGA data set.

Correlation between expression of SCCRO and its family members and outcomes

To assess the effects of dysregulation of SCCRO and its family members on clinical factors, we focused our analyses on oral SCCs, owing to the availability of outcomes data, a sufficient sample size, and the high frequency of 3q amplification in these tumors. Dysregulation of any SCCRO paralog was significantly correlated with worse outcomes in the oral SCC cohort (p=0.05) (Figure 2A). In the TCGA data set, a correlation between SCCRO overexpression and worse outcomes was present in the data set for head and neck cancers (Figure 2B). However, the presence or the number of SCCRO paralogs dysregulated did not correlate with outcomes (data not shown). These findings suggest that a complex interaction may exist between the dysregulation of SCCRO and its paralogs in their contributions to tumor behavior.

Figure 2. SCCRO dysregulation correlates with an aggressive clinical course.

A

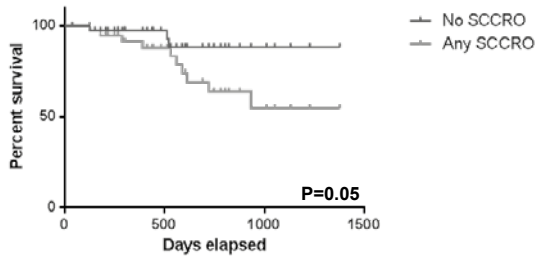

B

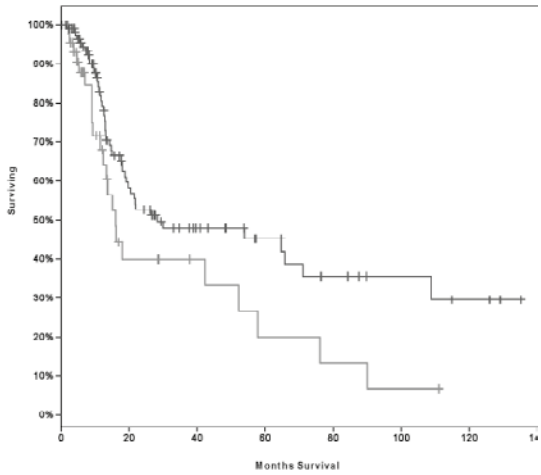

(**A**), Kaplan-Meier survival curve from post hoc analysis, showing recurrence-free survival based on SCCRO1-5 expression status in oral SCCs. (**B**), Correlation between SCCRO expression and outcomes for head and neck cancers in the TCGA data set, red: cases with SCCRO overexpression, blue: cases without SCCRO overexpression.

SCCRO levels correlate with biochemical activity

We next aimed to determine whether dysregulation of SCCRO has functional consequences in human cancers. To determine this, we assessed Hürthle cell carcinomas, as these tumors had the cleanest profile of misexpression of SCCRO and its paralogs. We screened for levels of endogenous SCCRO protein in Hürthle cell carcinomas and matched normal samples by Western blotting. We quantified SCCRO protein levels using densitometric analysis and found samples with low, intermediate, and high SCCRO levels (Figure 3A and Supplemental Table S6A). To assess the biochemical effects of SCCRO expression, we measured neddylation activity in these samples using a novel neddylation assay developed and validated in our laboratory.[12] Western blotting with Cul1 antibody, quantified using densitometric analysis, was used to determine the ratio of neddylated Cul1 (representing the active form of the protein) to unneddylated Cul1 (representing the inactive form of the protein). This showed that SCCRO protein expression levels correlated with Cul1 neddylation (Figure 3B). Specifically, the ratios of neddylated to unneddylated Cul1 in the low, intermediate, and high SCCRO groups were 0.25, 0.47, and 0.74, respectively (Figure 3C and Supplemental Table S6B).

Neddylation of cullins promotes their activity in CRL complexes, which is expected to lead to increases in protein ubiquitination. We next asked whether SCCRO protein expression levels were also associated with ubiquitination in this set of tumors. We assessed the levels of global ubiquitination in these primary tissue lysates, after subjecting them to activated neddylation assays, and found that increasing SCCRO protein expression corresponded with an increase in

global levels of ubiquitinated proteins in primary Hürthle cell carcinoma tissue lysates (Figure 3D). These findings show that increased SCCRO expression in tumors is associated with an increase in the level of neddylated cullins and CRL activity, suggesting that SCCRO overexpression has functional consequences.

Figure 3. SCCRO overexpression correlates with activation of neddylation.

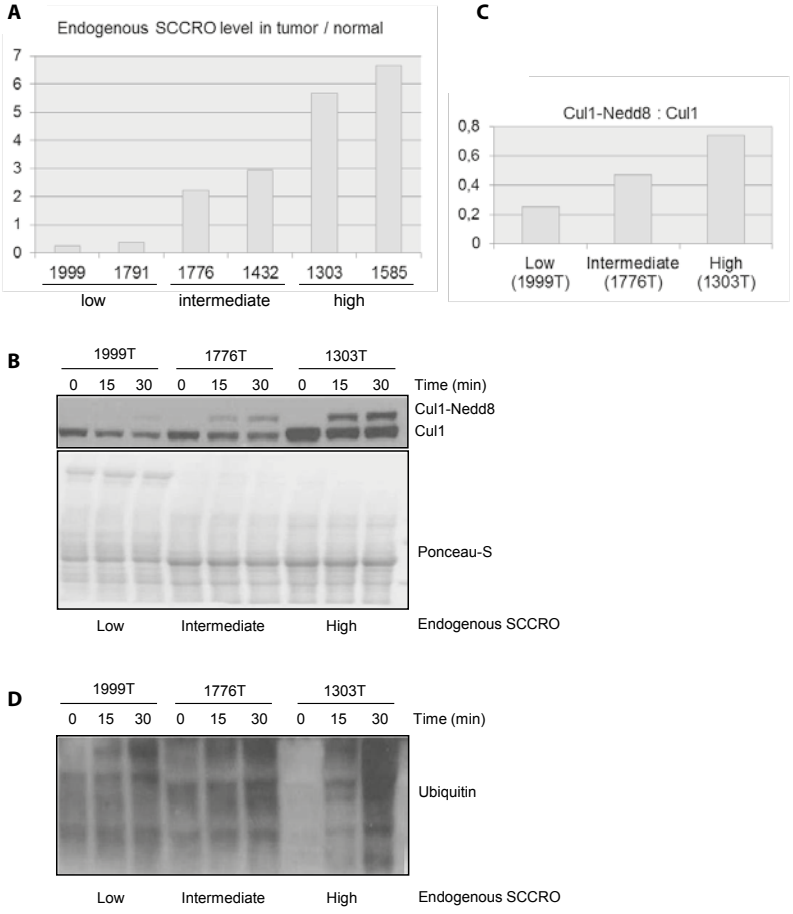

(**A**), Bar graph showing the ratio of tumor to normal levels of endogenous SCCRO protein in 6 tumor and matched normal tissue specimens from patients with Hürthle cell carcinoma. (**B**), Western blot analysis of Cul1 on products of an in vivo neddylation reaction using tumor tissue lysates with low (1999T), intermediate (1776T), and high (1303T) levels of endogenous SCCRO, with Ponceau-S as a loading control, which shows a time-dependent increase in neddylation of Cul1 that correlates with higher levels of endogenous SCCRO; the upper band is neddylated Cul1, the lower band is unneddylated Cul1. (**C**), Bar graph showing an increase in the ratio of Cul1-Nedd8 to Cul1 in Hürthle cell carcinomas containing low, intermediate, and high levels of endogenous SCCRO. (**D**), Ubiquitination signaling was assessed by probing the same blot from activated neddylation in panel B with ubiquitin antibody; there is a pattern of increased global ubiquitination with increasing levels of endogenous SCCRO.

Discussion

SCCRO amplification supports oncogenesis by promoting neddylation of cullins. The conservation of functional domains, and their locations on chromosomal loci that are aberrant in human cancers, suggests that all SCCRO paralogs may contribute to human cancer pathogenesis. We have shown that all SCCRO paralogs are dysregulated in human cancers. The most commonly dysregulated paralogs were SCCRO (27%) and SCCRO3 (41%), followed by SCCRO5 (14%), SCCRO2 (13%), and SCCRO4 (7%). One or more SCCRO paralog was dysregulated in 75% of oral and 80% of lung SCCs. The prevalence of dysregulation of SCCRO paralogs in the TCGA data sets was similar to that in our findings. These findings suggest that SCCRO and its paralogs play a role in the pathogenesis of a wide range of cancers.

We and others have previously shown that SCCRO's primary role is to promote neddylation as part of the E3 complex. Similar to ubiquitination, the activity of the E3 complex serves as the rate-limiting step in neddylation. Consistent with the importance of SCCRO's role in neddylation, we found that overexpression of SCCRO was associated with an increase in neddylation activity in primary tumors. Interestingly, the PONY domain is required for neddylation, and its mutation abrogates SCCRO's oncogenic activity. While PONY domains are present in all SCCRO paralogs, it is quite evident that their various N-terminal domains have a significant impact on functional activity. We have shown that subcellular localization is a major mechanism by which SCCRO affects neddylation activity. The restriction of SCCRO3 to the membrane, caused by its myristoyl sequence in the N-terminus, is a key mechanism by which it inhibits neddylation and promotes oncogenesis. Consistent with the role of SCCRO3 as a tumor suppressor,. SCCRO3's effect on neddylation results from its inhibition of SCCRO-promoted neddylation.[20] Interestingly, the SCCRO paralogs were commonly codysregulated, suggesting that they may have cooperative activity in human cancers. However, the oncologic and clinical significance of codysregulation of SCCRO paralogs remains to be determined.

We and others have shown that SCCRO can promote the neddylation of multiple cullins. As such, it can affect the activity of a myriad of CRL complexes. CRL complexes are the most common class of E3s in ubiquitination. Consistent with its role in regulating CRL activity, overexpression of SCCRO correlated with an increase in the global pool of ubiquitinated proteins in primary tumors. Although many CRL E3 complex targets are known, specific targets regulated by SCCRO-promoted neddylation remain to be determined. Combined, our data suggest that SCCRO and its paralogs are commonly dysregulated and may be targetable for therapeutic benefit in many types of human cancers.

Supplemental Table 1. Chromosomal loci of the SCCRO family.

Gene	Entrez gene name	Gene bank sequence accession no.	Locus	ORF	AA
hDCNL1/SCCRO	DCUN1D1	NM_020640	3q26.3	780bp	259
hDCNL2/SCCRO2	DCUN1D2	NM_001014283	13q34	780bp	259
hDCNL3/SCCRO3	DCUN1D3	NM_173475	16p12.3	915bp	304
hDCNL4/SCCRO4	DCUN1D4	NM_001040402	4q12	879bp	292
hDCNL5/SCCRO5	DCUN1D5	NM_032299	11q22.3	714bp	237

Supplemental Table 2. Demographic characteristics of patients with thyroid cancer.

Characteristics	No. of patients (N=56)
Age, years	
≤45	27
>45	29
Median	47.4
Range	22-87
Sex	
Male	12
Female	44
Histologic diagnosis	
Nodular hyperplasia	9
Follicular adenoma	9
Hürthle cell carcinoma	10
Well-differentiated papillary thyroid carcinoma	18
Tall cell variant papillary thyroid carcinoma	10
Tumor size	
0-2.0	31
>2.0	25
Capsular invasion	
Negative	30
Positive	26
Lymph node metastasis	
Negative	44
Positive	12
Distant metastasis	
Negative	55
Positive	1
Extent of surgical resection	
Lobectomy	21
Total thyroidectomy	35

Supplemental Table 3. Demographic characteristics of patients with oral squamous cell carcinoma.

Characteristics	No. of patients (N=40)
Age, years	
Median	57
Range	26-89
Sex	
Male	24
Female	16
TNM stage	
Early (I-II)	29
Advanced (III-IV)	11
Tumor site in oral cavity	
Tongue	24
Other	16
Tobacco use	
Yes	25
No	15

Supplemental Table 4. Sequences of the real-time PCR primers for SCCRO1-5 and housekeeping gene GAPDH (in the 5'-3' direction).

Gene of interest	Forward primer	Reverse primer
SCCRO	'CTGGAGGACACCAACATG'	'TTCACTAGATTGTGTGAAGATC'
SCCRO2	'GTTCACCTCCATTTCTCAATGTG'	'CTTAGAAATGGCTGTTGCGT'
SCCRO3	'CACAGAATTTCGAGTGCTG'	'TGCACTTATTGCTTTGCAG'
SCCRO4	'CTGGCAAATATTCATAAGATCTACC'	'AAGACCGCAGACTTCCTG'
SCCRO5	'TGCGCTCACAGTTGAATGATATTTCGTC'	'CAGTGGCCATGTCCTCCCAAGCAG'
GAPDH	'GCACCACCAACTGCTTAG'	'CATGGACTGTGGTCATGAG'

Supplemental Table 5. SNPs in thyroid and oral squamous cell carcinoma samples from the present study.

Sample	SCCRO		SCCRO3				SCCRO4	
	rs4859146	rs4859147	rs7187522	rs1858901	rs34248677	rs35094690	rs13531	rs2271046
Thyroid								
FA 880	X	X	X					X
WDPTC 493		X	X				X	X
WDPTC 550		X	X	X				
WDPTC 228							X	X
WDPTC 256	X	X	X				X	X
TCVPTC 662	X	X	X				X	X
TCVPTC 696	X	X	X	X				
TCVPTC 726	X	X	X				X	X
TCVPTC 960		X	X	X			X	X
HCC 416	X	X	X	X			X	X
HCC 526	X	X	X				X	X
HCC 637	X	X	X				X	X
HCC 892	X	X	X				X	X
HCC 895	X	X	X				X	X
HCC 1039	X	X	X				X	X
Oral SCC	X	X	X	X	X	X	X	X

Supplemental Table 6. Raw data used for Figure 3A and 3C.

A

Endogenous SCCRO protein level	Low		Intermediate		High	
Sample name	1999T	1791T	1776T	1432T	1303T	1585T
Normalized SCCRO densitometry	279.164	738.087	1054.688	1265.886	2135.076	2431.475
Sample name	1999N	1791N	1776N	1432N	1303N	1585N
Normalized SCCRO densitometry	1123.773	2009.617	482.342	129.435	377.672	365.451

B

Cul1		Cul1-Nedd8		Cul1-Nedd8 : Cul1
Low (1999T)	2265.84	Low (1999T)	569.75	0.25
Intermediate (1776T)	3004.89	Intermediate (1776T)	1411.16	0.47
High (1303T)	5374.94	High (1303T)	3977.41	0.74

(**A**) shows data on the normalized SCCRO densitometry protein levels in tumor and matched normal tissue samples. (**B**) shows data on Cul1 and Cul1-Nedd8 densitometry in tumor samples with low, intermediate, and high levels of endogenous SCCRO protein; in the last column, the ratio of Cul1-Nedd8 to Cul1 in these samples is shown.

Supplemental Figure 1. Alignment of the PONY domain of SCCRO1-5.

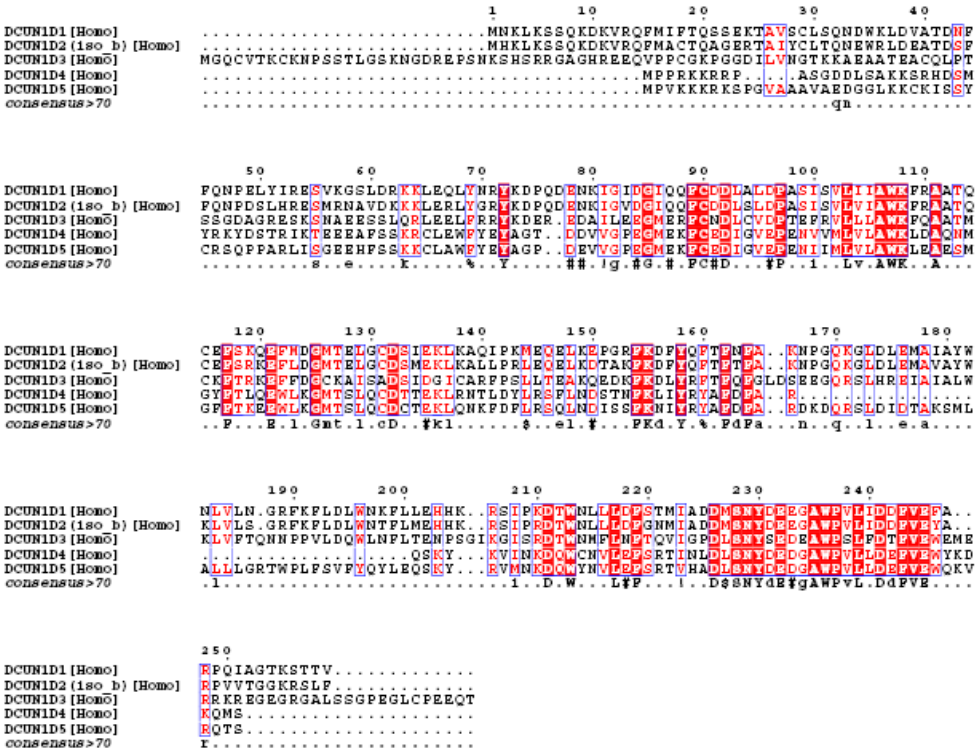

References

1. Singh B, Gogineni S, Goberdhan A, et al. Spectral karyotyping analysis of head and neck squamous cell carcinoma. Laryngoscope 2001;111(9):1545-50.
2. Singh B, Gogineni SK, Sacks PG, et al. Molecular cytogenetic characterization of head and neck squamous cell carcinoma and refinement of 3q amplification. Cancer Research 2001;61(11):4506-4513.
3. Singh B, Stoffel A, Gogineni S, et al. Amplification of the 3q26.3 locus is associated with progression to invasive cancer and is a negative prognostic factor in head and neck squamous cell carcinomas. American Journal of Pathology 2002;161(2):365-371.
4. Singh B, Wreesmann VB, Pfister D, et al. Chromosomal aberrations in patients with head and neck squamous cell carcinoma do not vary based on severity of tobacco/alcohol exposure. Bmc Genetics 2002;3.
5. Estilo CL, O-charoenrat P, Nagi I, et al. The role of novel oncogenes squamous cell carcinoma-related oncogene and phosphatidylinositol 3-kinase p110 alpha in squamous cell carcinoma of the oral tongue. Clinical Cancer Research 2003;9(6):2300-2306.
6. Sarkaria IS, Pham D, Ghossein RA, et al. SCCRO expression correlates with invasive progression in Bronchioloalveolar carcinoma. Annals of Thoracic Surgery 2004;78(5):1734-1741.
7. Weinstein IB, Joe A. Oncogene addiction. Cancer Res 2008;68(9):3077-80; discussion 3080.
8. Sarkaria I, O-charoenrat P, Talbot SG, et al. Squamous cell carcinoma related oncogene/DCUN1D1 is highly conserved and activated by amplification in squamous cell carcinomas. Cancer Res 2006;66(19):9437-44.
9. Wang J, Qian J, Hoeksema MD, et al. Integrative Genomics Analysis Identifies Candidate Drivers at 3q26-29 Amplicon in Squamous Cell Carcinoma of the Lung. Clinical Cancer Research 2013;19(20):5580-5590.
10. Huang GC, Singh B. Coamplification and Cooperation: Toward Identifying Biologically Relevant Oncogenes. Clinical Cancer Research 2013;19(20):5549-5551.
11. Chen Y, Mcgee J, Chen XM, et al. Identification of Druggable Cancer Driver Genes Amplified across TCGA Datasets. Plos One 2014;9(5).
12. Kim AY, Bommeljé CC, Lee BE, et al. SCCRO (DCUN1D1) is an essential component of the E3 complex for neddylation. J Biol Chem 2008;283(48):33211-20.
13. Kurz T, Chou YC, Willems AR, et al. Dcn1 functions as a scaffold-type E3 ligase for cullin neddylation. Mol Cell 2008;29(1):23-35.
14. Huang G, Kaufman AJ, Ramanathan Y, Singh B. SCCRO (DCUN1D1) promotes nuclear translocation and assembly of the neddylation E3 complex. J Biol Chem 2011;286(12):10297-304.
15. Wu K, Yan H, Fang L, et al. Mono-ubiquitination drives nuclear export of the human DCN1-like protein hDCNL1. J Biol Chem 2011;286(39):34060-70.
16. Hershko A, Ciechanover A. The ubiquitin system. Annual Review of Biochemistry 1998;67:425-479.
17. Petroski MD, Deshaies RJ. Function and regulation of Cullin-RING ubiquitin ligases. Nature Reviews Molecular Cell Biology 2005;6(1):9-20.
18. Dye BT, Schulman BA. Structural mechanisms underlying posttranslational modification by ubiquitin-like proteins. Annual Review of Biophysics and Biomolecular Structure 2007;36:131-150.
19. Bommeljé CC, Weeda VB, Huang GC, et al. Oncogenic Function of SCCRO5/DCUN1D5 Requires Its Neddylation E3 Activity and Nuclear Localization. Clinical Cancer Research 2014;20(2):372-381.
20. Huang GC, Stock C, Bommeljé CC, et al. SCCRO3 (DCUN1D3) Antagonizes the Neddylation and Oncogenic Activity of SCCRO (DCUN1D1). Journal of Biological Chemistry 2014;289(50):34728-34742.
21. Essentials of real time PCR. http://www3.appliedbiosystems.com/cms/groups/mcb_marketing/documents/generaldocuments/cms_039996.pdf. In; 2012.
22. Reference genes/housekeeping genes. Gene Quantification website. http:// www.gene-quantification.de/hkg.html. . In.
23. Vandesompele J, De Preter K, Pattyn F, et al. Accurate normalization of real-time quantitative RT-PCR data by geometric averaging of multiple internal control genes. Genome Biol 2002;3(7):RESEARCH0034.
24. Rozen S, Skaletsky H. Primer3 on the WWW for general users and for biologist programmers. Methods Mol Biol 2000;132:365-86.
25. Little SE, Vuononvirta R, Reis-Filho JS, et al. Array CGH using whole genome amplification of fresh-frozen and formalin-fixed, paraffin-embedded tumor DNA. Genomics 2006;87(2):298-306.

26. Marks JL, McLellan MD, Zakowski MF, et al. Mutational analysis of EGFR and related signaling pathway genes in lung adenocarcinomas identifies a novel somatic kinase domain mutation in FGFR4. PLoS One 2007;2(5):e426.
27. Huang G, Towe CW, Choi L, et al. The ubiquitin-associated (UBA) domain of SCCRO/DCUN1D1 protein serves as a feedback regulator of biochemical and oncogenic activity. J Biol Chem 2015;290(1):296-309.

Chapter 7

General discussion

Genomic abnormalities

The genome of cancer cells is characterized by various forms of aberrations such as copy-number alterations, loss of heterozygosity, and epigenetic changes (1). Earlier studies aimed on development of genome-wide screening tools, such as comparative genomic hybridization (CGH) and spectral karyotyping (SKY). This allowed to determine common genomic copy number alterations and their frequency in a wide range of tumors. In head and neck squamous cell carcinomas (HNSCC), this low resolution mapping refined a region of frequent amplification to 3q25-27 (2,3). Further analysis, in a systemic, positional cloning approach, identified *Squamous Cell Carcinoma Related Oncogene* (SCCRO, aka DCUN1D1) as a candidate oncogene within this region of frequent amplification, located on 3q26.3 (4-6).

New technologies

Technology advancement resulted in the development of world-wide appraised assays that are able to detect abnormalities at the gene and nucleotide level, like whole genome sequence analysis. In 2003 the Human Genome Project was declared complete (7). Also for head and neck cancers more and more information is coming into the world about mutation status (8). For example tumors from patients with a history of tobacco use have more mutations than tumors from patients who did not use tobacco, and tumors that are negative for HPV have twice as many mutations compared to HPV-positive tumors (9). One of the latest successes in new technologies was The Cancer Genome Atlas (TCGA), a platform for researchers to search, download, and analyze data sets with the goal of comprehensively mapping cancer genomes (10).

Gateway to targeted therapies

These novel technologies make us able to now move to an era in which integrating several types of data from high-throughput biological assays will be essential to understand complex diseases such as cancer. The last years tremendous steps have been made in tumor DNA and RNA sequencing and the subsequent development of novel drugs targeting the mutated pathways. In an attempt to improve outcomes for head and neck cancers, new targeted therapeutic strategies have been developed, including new anti-EGFR monoclonal antibodies (mAb), tyrosine kinase inhibitors (TKI) targeting other members of the erbB/HER family besides EGFR, other nodes along the EGFR- mitogen-activated protein kinase, MAPK pathway, or oncogenic pathways, such as the phosphoinositide 3-kinase (PI3K), insulin-like growth factor 1 receptor and MET pathways (11). This novel drug development has led to improved outcome survival, for example in head and neck cancer by Cetuximab targeting EGFR, Vumerafenib, targeting the V600E activating mutation in the BRAF gene (12,13). Recently the BRAF V600E mutation has been appraised in aggressive papillary thyroid cancer and Pembrolizumab, an antibody against the anti-programmed-death-receptor-1 (PD-1) has been shown to have activity in PD-1 positive HNSCC (14,15).

Understanding the function of SCCRO- implications for cancer

The genomic complexity of human cancers and perpetual genetic evolution in cancer cells has made characterization of the cancer genome difficult. But, as described above, developments in basic science research has led to a broad range of new therapeutic strategies and the function of many cellular pathways involved in carcinogenesis are revealed. Every piece of the puzzle solved, is needed to, in the future, be able to better treat cancer patients and improve clinical outcomes.

In further elucidating the molecular biology behind cancer, we focused in this thesis on the function of SCCRO, an established oncogene in HNSCC (6). As known, dysregulation of DCN-1, the *C. elegans* ortholog of SCCRO, results in severe developmental defects, and dysregulation of SCCRO leads to tumor formation in mice (6,16). Taken together, this made the elucidation of the exact molecular function of SCCRO very interesting, both for unravelling the normal cellular function of SCCRO and for the implications in carcinogenesis. In chapter 2, we describe that SCCRO is part of a complex that functions as the E3 for neddylation. We showed that SCCRO binds to the components of the neddylation pathway (Cullin-ROC1, Ubc12, and CAND1), that SCCRO helps to recruit the Ubc12~Nedd8 thioester to the neddylation E3 complex, SCCRO promotes cullin neddylation and is necessary to dissociate CAND1.

The completion of the human genome sequencing project and analysis of sequence databases revealed a variety of vertebrate genes with sequence homology to SCCRO; four highly conserved members of the defective in cullin neddylation domain containing (DCUN1D) proteins. As SCCRO was found to be a novel oncogene that functions as an oncogene by its function in the cullin neddylation pathway, we sought to elucidate whether these four other paralogs function in the neddylation pathway and whether they play a role in carcinogenesis as well.

CRL systems

Due to the complexity of the Cullin Ring ubiquitin Ligase (CRL) system, and the neddylation pathway, it is difficult to make *a priori* hypotheses about the mechanism by which SCCRO overexpression and increased neddylation activity contributes to tumor development. There are a wide variety of potentially oncogenic and tumor-suppressing pathways which are known to be affected by specific CRL E3 complexes, and an even greater number likely remain uncharacterized. Further work is required to define the CRL's and protein targets that are dependent on the SCCRO family in cellular activities, specifically what is downstream for each individual paralog as CRL's regulate the ubiquitination of a myriad of proteins, resulting in diverse cellular effects (18). The identification of CRL targets downstream of SCCRO is more complex given the presence of 7 Cullins in eukaryotic species, each forming a part of a multi-subunit ubiquitin complex modified by Nedd8, regulating many different processes. Moreover, the identification of CRL targets downstream of SCCRO is even more complex given the multiple SCCRO's that have neddylation activity and probably different

affinity for each Cullin.

One strategy for approaching the mechanism of SCCRO-mediated oncogenicity would be to individually assay each of the many "candidate" CRL complexes and ubiquitination targets for altered activity in SCCRO-overexpressing tumors or SCCRO-transformed cell lines. Another approach would be to further identify specific cellular processes or tissues in vertebrates which are dependent on the SCCRO family for their normal function. By learning more about the endogenous role of the SCCRO family, it may help to further determine the focus of studies of SCCRO family's role in carcinogenesis.

Elucidating factors that control SCCRO

Since SCCRO promotes cullin neddylation, which serves as a signal for assembly of ubiquitination E3 complexes, factors controlling SCCRO likely regulate ubiquitination. As noted by Kurz and colleagues, the UBA domain is lost in one of two isoforms of *C. elegans* DCN-1, and we showed that the UBA domain is not necessary for the neddylation-enhancing function of SCCRO proteins, since the UBA-lacking proteins SCCRO4 and SCCRO5 enhance *in-vitro* neddylation reactions with roughly the same efficiently as the UBA-containing SCCRO (24). In chapter 3 we describe the finding that binding of polyubiquitinated proteins to the N-terminal UBA domain of SCCRO inhibits neddylation activity, suggesting the presence of a classical negative feedback loop that regulates CRL-promoted ubiquitination activity (25). The effects of the UBA domain do not appear to be allosteric, often resulting in a conformational change, as the addition of polyubiquitin chains or mutation of the UBA domain has no effect on SCCRO's neddylation function *in vitro*, whereas accumulation of polyubiquitinated proteins shows classical negative-feedback dynamics *in vivo*. We suggest that binding of polyubiquitinated proteins to the UBA domain affect the subcellular localization and function of SCCRO by serving as a signal for the monoubiquitination of SCCRO (26,27). How SCCRO is translocated from the nucleus to the cytoplasm and vice versa is very interesting. A possibility is that monoubiquitination of SCCRO inhibits interactions with NLS-containing protein partners involved in nuclear import. Another possibility is that monoubiquitination of SCCRO leads to an interaction with an unknown protein that inhibits nuclear translocation. The role of the UBA domain in cancer pathogenesis is well-established and the activity of an oncogene may be mitigated by agents that bind to or mimic the oncoprotein's UBA domain (28-32). Future research should therefore be focused on further elucidating the effects of polyubiquitination and monoubiquitination of SCCRO.

Because SCCRO3, SCCRO4 and SCCRO5 do not contain a UBA domain and do not possess any other novel functional domains than the myristoyl sequence and the NLS in comparison to SCCRO and SCCRO2, it is tempting to infer that these genes perform a restricted subset of the functions performed by the UBA subfamily, that they do not require UBA-mediated interactions and they are not likely to replicate all functions of the UBA containing SCCRO proteins *in vivo*. As we suggest that binding of polyubiquitinated proteins to the UBA domain affect the subcellular localization and function of SCCRO, it remains a question how the two other subfamilies of the SCCRO family are

controlled. The myristoyl sequence of SCCRO3 that localizes to the membrane does not serve as a negative feedback loop domain. Neither does the NLS in SCCRO4 and SCCRO5. What controls these subfamilies might be useful to identify as it may add information on factors that control the UBA domain containing SCCRO proteins. Further experiments with chimeric *SCCRO* genes containing both the UBA and NLS domains, or containing a nuclear export sequence, could help clarify these possibilities. But keeping in mind the following restrictions; *in vitro* studies of the neddylation pathway are useful for determining the basic molecular mechanisms of proteins in this system, but do not fully capture the complexity of the system *in vivo*.

Interaction of the five SCCRO family members

One of the puzzling features of the SCCRO family is why there is such a great conservation of five separate genes in three subfamilies, given their nearly identical structure and similar functional properties. The various expression of the SCCRO family in various human tissues as in human cancers suggests that certain tissues have a higher need for neddylation activity than others, and that the diversification of *SCCRO* genes in higher organisms may be related to the need for more complex regulation of this system.

The question is if the five SCCRO family members also have functional interaction, overlapping or indirect, in the nuclear translocation of Cullin-ROC1 and such in the regulation of cullin neddylation. We showed that SCCRO promotes nuclear translocation of Cullin-ROC1, which is required for neddylation *in vivo* (26). In chapter 4 we show that co-expression of SCCRO3 blocked SCCRO-promoted transformation of a benign transformed cell line, suggesting that competition between SCCRO and SCCRO3 for cullin substrate had functional implications *in vivo* (33). These findings led us to propose that SCCRO3 functions as a tumor suppressor by sequestering Cul1 to the membrane and antagonizing SCCRO-mediated nuclear translocation and neddylation of cullins. Another reason to hypothesize that the SCCRO's functionally interact in the nuclear translocation of Cullin-ROC1 is shown in chapter 5; our finding showing that the NLS is required for SCCRO5's transforming activity suggests that, as with the UBA, the NLS may modulate neddylation activity *in vivo* (24). However, these findings raise a question about SCCRO5's role in neddylation. Given that SCCRO5 is present almost exclusively in the nucleus, it is unclear how cytoplasmic Cullin-ROC1 complexes are delivered to the nucleus to allow for interaction with SCCRO5. Several possibilities exist, including cooperative activity between the other SCCRO paralogs and the NLS-containing variants, presence of alternative mechanisms for nuclear translocation of Cullin-ROC1 complexes, and selective activity on cullins situated in the nucleus.

Targeting the neddylation pathway

Nedd8-activating enzyme (NAE) is the E1 of the neddylation pathway. MLN4924 is a selective inhibitor of NAE. MLN4924 disrupts cullin-RING ligase-mediated protein turnover leading

to apoptotic death in human tumour and has proven successful in the treatment of human malignancies (34-38). The success of MLN4924 highlights the benefits of targeting neddylation pathway components in anticancer treatment (39). As SCCRO is frequently dysregulated in various human cancers and SCCRO is the E3 ligase of cullin neddylation, targeting the activity of SCCRO and its paralogs may prove beneficial in the treatment of a significant proportion of patients with HNSCC, as well as many other cancers. Several findings suggest that inhibiting SCCRO activity may be an effective way to target the neddylation pathway activity in human cancers: (i) in contrast with NAE, which is rarely dysregulated in human cancers, SCCRO dysregulation is common and is associated with an oncogene addiction phenotype, which was confirmed by results from Wang and colleagues (40), (ii) although knocking out other core components of neddylation is associated with lethality in mice, *SCCRO* knockout mice are viable and have no appreciable defects in essential functions (26). This suggests that inhibiting *SCCRO* may have limited detrimental effect on normal cells. (iii) SCCRO's molecular interactions and crystal structure are suitable for inhibition by small molecules (17, 26, 41, 42).

Towards multiple approach therapies

The treatment of cancer is continuing to evolve, and physicians who are treating patients with locally advanced disease have multiple treatment options. The treatment team should consider the patient's overall condition and his or her ability to tolerate aggressive therapy. The risk of local and distant recurrence needs to be considered as a treatment is implemented, and a multi-disciplinary approach is crucial. However, the next goal, in the near future, is to be able to clinically test each patients' tumor genome and the search for new molecularly targeted agents for head and neck cancers will lead to the ability to treat each individual specifically, based on its tumor genetics and epigenetics. The incorporation of such therapies into current treatment regimens is priority, in conjunction with a good understanding of the underlying mechanisms of action of such targeted agents.

Conclusion

Little was known about the significance and function of the SCCRO family in vertebrates. To our knowledge, the Laboratory of Epithelial Cell Biology under supervision of dr. Singh is the first to provide functional and clinical data about the protein products of these genes. Our original interest in SCCRO arose from evidence that SCCRO is a gene-amplified, overexpressed oncogene in human squamous cell cancers of mucosal origin. The discovery of four additional human genes with many similar molecular properties raised the question whether they might also be involved in the neddylation pathway and carcinogenesis which we have shown in chapter 4 and 5. We hope, with elucidating the function of the SCCRO family, to provide important knowledge in the cure of cancer. The shown molecular function, oncogenic activity and aggressive clinical course of the

SCCRO family support their clinical relevance in cancer pathogenesis. Innovative molecular targets, like the human SCCRO gene family, may add improved outcomes in the treatment of (head and neck) cancer in the future and provide much hope (43).

References

1. Cowell JK, Hawthorn L. The application of microarray technology to the analysis of the cancer genome. Curr Mol Med. 2007;7(1):103-20.
2. Singh B, Gogineni S, Goberdhan A, et al. Spectral karyotyping analysis of head and neck squamous cell carcinoma. Laryngoscope. 2001;111:1545–50.
3. Singh B, Gogineni SK, Sacks PG, et al. Molecular cytogenetic characterization of head and neck squamous cell carcinoma and refinement of 3q amplification. Cancer Res. 2001;61:4506-13.
4. Singh B, Stoffel A, Gogineni S. Amplification of the 3q26.3 locus is associated with progression to invasive cancer and is a negative prognostic factor in head and neck squamous cell carcinomas. Am J Pathol. 2002;161:365–71.
5. Estilo CL, O-charoenrat P, Ngai I, et al. The role of novel oncogenes squamous cell carcinoma-related oncogene and phosphatidylinositol 3-kinase p110alpha in squamous cell carcinoma of the oral tongue. Clin Cancer Res. 2003;9(6):2300-6
6. Sarkaria I, O-charoenrat P, Talbot SG, Reddy PG, Ngai I, Maghami E, et al. Squamous cell carcinoma related oncogene/DCUN1D1 is highly conserved and activated by amplification in squamous cell carcinomas. Cancer Res. 2006;66:9437–44.
7. Hudson TJ, Anderson W, Artez A, et al. International network of cancer genome projects. Nature. 2010;15:464:993-8.
8. Chin L, Hahn WC, Getz G, et al. Making sense of cancer genomic data. Genes Dev. 2011;25:534-55.
9. Agrawal N, Frederick MJ, Pickering CR, et al. Exome sequencing of the head and neck squamous cell carcinoma reveals inactivating mutations in NOTCH1. Science. 2011;333:1154-7.
10. www.tcga-data.nci.nih.gov/tcga/dataAccessMatrix.htm.
11. Boeckx C, Baay M, Wouters A, et al. Anti-epidermal growth factor therapy in head and neck squamous cell carcinoma: focus on potential molecular mechanisms of drug resistance. Oncologist. 2013;18(7): 850-64.
12. Lidsky M, Antoun G, Speicher P, et al. Mitogen-activated protein kinase (MAPK) hyperactivation and enhanced NRAS expression drive acquired vemurafenib resistance in V600E BRAF melanoma cells. J Biol Chem. 2014;289:27714-26.
13. Xing M, Alzahrani AS, Carson KA, et al. Association between BRAF V600E mutation and recurrence of papillary thyroid cancer. J Clin Oncol. 2014.56.8253.
14. Weintraub K. Drug development: releasing the brakes. Nature. 2013;504:S6-8.
15. Zandberg DP, Strome SE. The role of the PD-L1:PD-1 pathway in squamous cell carcinoma of the head and neck. Oral Oncol. 2014;50:627-32.
16. Kurz T, Ozlu N, Rudolf F, et al. The conserved protein DCN-1/Dcn1p is required for cullin neddylation in C. elegans and S. cerevisiae. Nature 2005;435:1257–61.
17. Kim AY, Bommeljé CC, Lee BE, et al. SCCRO (DCUN1D1) is an essential component of the E3 complex for neddylation. J Biol Chem. 2008;283:33211-33220.
18. Monda JK, Scott DC, Miller DJ, et al. Structural conservation of distinctive N-terminal acetylation-dependent interactions across a family of mammalian Nedd8 ligation enzymes. Structure. 2013;21:42–53.
19. Kipreos ET, Lander LE, Wing JP, et al. Cul-1 is required for cell cycle exit in C. elegans and identifies a novel gene family. Cell. 1996;85:829–39.
20. Petroski MD, Deshaies RJ. Function and regulation of cullin-RING ubiquuitin ligases. Nat Rev Mol Cell Biol. 2005;6:9-20.
21. Zheng N, Schulman BA, Song L, et al. Structure of the Cul1-Rbx1-Skp1-F boxSkp2 SCF ubiquitin ligase complex. Nature. 2002;416:703–9.
22. Goldenberg SJ, Cascio TC, Shumway SD, et al. Structure of the Cand1-Cul1-Roc1 complex reveals regulatory mechanisms for the assembly of the multisubunit cullin-dependent ubiquitin ligases. Cell. 2004;119:517-28.
23. Pan ZQ, Kentsis A, Dias DC, et al. Nedd8 on cullin: building an expressway to protein destruction. Oncogene. 2004;23:1985-97.
24. Bommeljé CC, Weeda VB, Huang G, et al. Oncogenic function of SCCRO5/DCUN1D5 requires its Neddylation E3 activity and nuclear localization. Clin Cancer Res. 2014;20:372-381.
25. Huang G, Towe CW, Choi L, et al. The UBA domain of SCCRO/DCUN1D1 serves as a feedback regulator of biochemical and oncogenic activity. J Biol Chem. 2014. Ahead of print.

26. Huang G, Kaufman AJ, Ramanathan Y, et al. SCCRO (DCUN1D1) promotes nuclear translocation and assembly of the neddylation E3 complex. J Biol Chem. 2011;286:10297-10304.
27. Wu K, Yan H, Fang L, et al. Monoubiquitination drives nuclear export of the human DCN1-like protein hDCNL1. J Biol Chem. 2011;286:34060–70.
28. Seibenhener ML, Geetha T, Wooten MW. Sequestosome 1/p62--more than just a scaffold. FEBS Lett 2007;581:175-179.
29. Layfield R, Searle MS. Disruption of ubiquitin-mediated processes in diseases of the brain and bone. Biochem Soc Trans. 2008;36:469-471.
30. Lucas GJ, Daroszewska A, Ralston SH. Contribution of genetic factors to the pathogenesis of Paget's disease of bone and related disorders. J Bone Miner Res. 2006; 21:31-37.
31. Daroszewska A, Ralston SH. Genetics of Paget's disease of bone. Clin Sci. 2005;109: 257-263.
32. Lee JJ, Kim YM, Jeong J, et al. Ubiquitin-associated (UBA) domain in human Fas associated factor 1 inhibits tumor formation by promoting Hsp70 degradation. PLoS One. 2012;7:e40361.
33. Huang G, Stock C, Bommeljé CC, et al. SCCRO3 (DCUN1D3) antagonizes the neddylation and oncogenic activity of SCCRO (DCUN1D1). J Biol Chem. 2014;289:34728-42.
34. Gao Q, Yu GY, Shi JY, et al. Neddylation pathway is up-regulated in human intrahepatic cholangiocarcinoma and serves as a potential therapeutic target. Oncotarget. 2014;5:7820-32.
35. Wang X, Li L, Liang Y, et al. Targeting the neddylation pathway to suppress the growth of prostate cancer cells: therapeutic implication for the men's cancer. Biomed Res Int. 2014;974309.
36. Li L, Wang M, Yu G, et al. Overactivated neddylation pathway as a therapeutic target in lung cancer. J Natl Cancer Inst. 2014;106(6).
37. Gu Y, Kaufman JL, Bernal L, et al. MLN4924, an NAE inhibitor, suppresses AKT and mTOR signaling via upregulation of REDD1 in human myeloma cells. Blood. 2014;123:3269-76.
38. Xu GW, Toth JI, da Silva SR, et al. Mutations in UBA3 confer resistance to the Nedd8-activating enzyme inhibitor MLN4924 in human leukemic cells. PLos One. 2014;9:e93530.
39. Soucy TA, Smith PG, Milhollen MA, et al. An inhibitor of Nedd8-activating enzyme as a new approach to treat cancer. Nature. 2009;458:732–6.
40. Wang J, Qian J, Hoeksema MD, et al. Integrative genomics analysis identifies candidate drivers at 3q26-29 amplicon in squamous cell carcinoma of the lung. Clin Cancer Res. 2013;19:5580-90.
41. Scott DC, Monda JK, Bennett EJ, et al. N-terminal acetylation acts as an avidity enhancer within an interconnected multiprotein complex. Science. 2011;334:674–8.
42. Huang G, Singh B. Coamplification and cooperation: toward identifying biologically relevant oncogenes. Clin Cancer Res. 2013;19:5549-5551.
43. Denaro N, Russi EG, Adamo V, et al. State-of-the-art and emerging treatment options in the management of head and neck cancer: news from 2013. Oncology. 2014;86:212-29.

Chapter 8

Summary

Samenvatting

Summary

SCCRO (a.k.a. DCUN1D1) is an oncogene that is commonly activated by amplification in human cancers, especially in head and neck squamous cell carcinomas. The identification of highly conserved paralogs that like SCCRO are located in chromosomal loci that are recurrently amplified in human cancers (SCCRO2 at 13q34, SCCRO4 at 4q12, and SCCRO5 at 11q22) raised the possibility that these paralogs also play a role in cancer pathogenesis. In this thesis the molecular function of the SCCRO gene family is described, focusing on their role in the neddylation pathway and in carcinogenesis.

First, we wanted to investigate SCCRO's function in the neddylation pathway, a pathway highly relevant to cancer pathogenesis. The neddylation pathway is an enzymatic cascade involving the sequential activity of a dedicated E1 (APPBP1/Uba3), E2 (Ubc12), and E3 enzyme. Nedd8, a ubiquitin like protein (UBL), is transferred from the E1, E2 to the E3 enzyme. Covalent modification of cullins by the ubiquitin-like protein Nedd8 regulates protein ubiquitination by promoting the assembly of cullin-RING ligase (CRL) E3 complexes. We show that SCCRO functions as a component of the E3 in neddylation; SCCRO binds to the components of the neddylation pathway (Cullin-ROC1, Ubc12, and CAND1) in its C-terminal PONY domain and augments, but is not required for, cullin neddylation in reactions using purified recombinant proteins.

In its N-terminal, SCCRO contains a ubiquitin associated (UBA) domain. We found that the UBA domain of SCCRO preferentially binds to polyubiquitin chains in a linkage-independent manner. Binding of polyubiquitin chains to the UBA domain inhibits SCCRO's neddylation activity *in vivo* by inhibiting SCCRO-promoted nuclear translocation of neddylation components and results in a corresponding decrease in cullin-RING-ligase promoted ubiquitination. Mutations in the UBA domain lead to loss of inhibitory control, which results in increased biochemical and oncogenic activity, which may be a mechanism of oncogene activity in human cancers.

The specific characteristics of the four paralogs of SCCRO had not yet been studied and the next purpose of the research described in this thesis was to screen the role of the SCCRO paralogs in human cancers. SCCRO3 and SCCRO5 were shown to be frequently dysregulated in human cancers. Therefore, we further elucidated the role of SCCRO3 and SCCRO5 in cancer pathogenesis. SCCRO3 contains a myristoyl sequence which localizes it to the membrane. We found that SCCRO3 binds to components of the neddylation pathway, but contrary to the other SCCRO paralogs, it does not efficiently bind to Ubc12 nor does it promote cullin neddylation and so, does not seem to have E3 activity. We found that SCCRO3 inhibits SCCRO's transforming activity by sequestering cullins to the membrane and we suggest that, in that way, SCCRO3 may function as a tumor suppressor by antagonizing SCCRO's neddylation activity by sequestering cullins.

In chapter 5 the role of SCCRO5 in human cancers and the neddylation pathway is described. SCCRO5 contains a nuclear localization sequence (NLS). Correlation between copy number, mRNA, and protein expression and association with clinical outcome was performed showing that increased expression of SCCRO5 correlates with a worse clinical outcome. Further on, transforming activity *in vitro* and *in vivo*, its function in the neddylation pathway and the role of its NLS are elucidated. We found that SCCRO5's NLS is essential for *in vivo* neddylation activity.

In chapter 6 we further analyzed the translational importance for this basic science research as we examined the role of the SCCRO family of genes in various cancers and describe a novel biochemical assay to look for ubiquitination activities in human tissue and use this in a subset of thyroid cancer.

In conclusion, in this thesis we have set the first steps in understanding the molecular function and mechanisms of the human SCCRO gene family in neddylation and cancer pathogenesis by correlation between copy number, mRNA, and protein expression, association with clinical outcome, presence of oncogene addiction in cancer cell lines, transforming activity *in vitro* and *in vivo*, and by analyzing its function in the neddylation pathway, a pathway highly relevant to cancer pathogenesis. The high frequency of dysregulation, association with a worse clinical outcome, combined with an oncogene addiction phenotype, function in a targetable pathway and crystal structure suggesting that their activity is amenable to inhibition by small molecules, SCCRO family members represent ideal targets for drug development efforts.

The main goal of this research is to develop therapeutic targets, targeting the neddylation pathway, in the treatment of human cancers.

Samenvatting

In dit proefschrift wordt de functie beschreven van de SCCRO gen familie. De SCCRO gen familie bestaat uit *Squamous Cell Carcinoma Related Oncogene* (SCCRO) èn vier genen die in de evolutie verwand zijn aan elkaar en functionele gelijkenissen hebben, genaamd SCCRO2, SCCRO3, SCCRO4 en SCCRO5. SCCRO is een gen dat betrokken is bij de ontwikkeling van tumoren, o.a. in hoofd-hals plaveiselcelcarcinomen. In het onderzoek beschreven in dit proefschrift wordt gekeken naar de functie van de SCCRO gen familie, naar hun klinische relevantie en naar hun rol in de ontwikkeling van kanker.

Ten eerste werd de moleculaire functie van SCCRO bestudeerd. Er waren aanwijzingen dat SCCRO functioneert in de 'neddylation' cascade. De neddylation cascade is een enzym-cascade waarbij Nedd8, een op ubiquitine lijkend eiwit, wordt opeenvolgend verplaatst van een bepaalde E1 (APPBP1/Uba3), naar een E2 (Ubc12), naar een E3 enzym. Cullin Ring ligases (CRL) zijn het doel van deze Nedd8. Modificatie van cullins door Nedd8 reguleert ubiquitinatie van eiwitten; ubiquitinatie is een proces in de cel wat leidt tot eiwitafbraak of het veranderen van de functie van eiwitten. Wij tonen in hoofdstuk 2 aan dat SCCRO functioneert als een component van de E3 in cullin neddylation.

SCCRO bevat een ubiquitin geassocieerd (UBA) domein in zijn N-terminus welke wij omschrijven en ontrafelen in hoofdstuk 3. Wij tonen aan dat het UBA domein van SCCRO bij voorkeur bindt aan polyubiquitine ketens. Binding van polyubiquitine ketens aan het UBA domein van SCCRO verhindert SCCRO's neddylation activiteit *in vivo* doordat door SCCRO gepromote translocatie van componenten van de neddylation cascade wordt verhinderd wat resulteert in een afname van cullin-RING ligase gepromote ubiquitinatie. Mutaties in het UBA domein leiden tot verlies van een remmende werking op SCCRO's neddylation activiteit, wat mogelijk een van de onderliggende mechanismen is in de ontwikkeling van tumoren door SCCRO.

De volgende stap in ons onderzoek was het verder specificeren van het moleculair mechanisme van de aan SCCRO verwante genen en hun rol in de ontwikkeling van tumoren, waarbij we ons richten op SCCRO3 en SCCRO5, omdat deze twee paralogen het meest frequent gedereguleerd zijn in tumoren. SCCRO3 bevat een 'myristoylation' signaal waardoor SCCRO3 aan de celmembraan gebonden is. SCCRO3 bindt ook aan de componenten van de neddylation cascade, maar in tegenstelling tot de andere SCCRO paralogen, bindt SCCRO3 niet aan Ubc12 en versnelt het niet de neddylation van cullins. Tevens wordt bij het screenen van genexpressie levels in verscheidene humane tumoren gezien dat SCCRO3 expressie is verlaagd in tumoren. Wij tonen aan dat SCCRO3 cullins naar de celmembraan sekwestert en zo de neddylation activiteit van SCCRO verhindert. Wij suggereren dat hierdoor SCCRO3 als een tumor suppressor functioneert.

In hoofdstuk 5 wordt de rol van SCCRO5 beschreven. SCCRO5 bevat een nuclear localization sequence (NLS). Gekeken wordt naar de correlatie tussen copy number, mRNA en eiwit expressie en klinische parameters. Dit laat zien dat overexpressie van SCCRO5 correleert met een slechtere overleving. De *in vivo* en *in vitro* eigenschappen van SCCRO5, de functie in de neddylation cascade en de rol van de NLS worden bestudeerd waaruit blijkt dat SCCRO5 als een E3 in de neddylation cascade functioneert en hiervoor *in vivo* de NLS nodig heeft.

In hoofdstuk 6 analyseren we het translationele belang van dit basaal wetenschappelijk onderzoek door de rol van de SCCRO familie in verscheidene humane tumoren in kaart te brengen. We introduceren een nieuwe biochemische test waarmee de ubiquitinatie activiteit in weefsel kan worden gemeten en passen deze toe in Hürthle cell carcinomen.

Tot slot, in dit proefschrift hebben we de eerste stappen gezet in het ontrafelen van de moleculaire functie en de klinische relevantie van de SCCRO familie in de neddylation cascade en in de ontwikkeling van tumoren, o.a. hoofd-hals plaveiselcelcarcinomen. 1) De hoge frequentie van deregulatie, 2) de associatie met een slechtere overleving, 3) het 'oncogene' addiction phenotype, 4) de functie in een te behandelen cascade en 5) een bekende kristalstructuur suggereren dat de SCCRO familie in aanmerking komt voor behandeling met ‘small molecules’.

Het doel van het onderzoek is om uiteindelijk therapieën te ontwikkelen die aangrijpen op de SCCRO gen familie in de neddylation cascade teneinde de behandeling van (hoofd-hals) kanker en daarmee de prognose voor (hoofd-hals) kanker patiënten te verbeteren.

Addendum

List of abbreviations

a.k.a.	also known as
CA	carcinoma
CAND1	cullin associated Nedd8 dissociated-1
CGH	comparative genomic hybridization
CRL	cullin-RING ubiquitin ligase
DCUN1D1/DCN-1	defective in cullin neddylation 1
DTT	dithiothreitol
E1	ubiquitin (or Nedd8)-activating enzyme
E2	ubiquitin (or Nedd8) carrier protein
E3	ubiquitin (or Nedd8)-protein isopeptide ligase
EGFR	epidermal growth factor receptor
EV	empty vector
FCS	fetal calf serum
FISH	fluorescent in situ hybridization
GST	glutathione-Sepharose transferase
HA	hemagglutinin
HECT	homologous to E6-AP carboxy terminus
HNSCC	head and neck squamous cell carcinoma
IB	immunoblotting
IP	immunoprecipitation
mAB	monoclonal antibodies
MALDI-reTOF	matrix-assisted laser desorption/ionization reflectron time-of-flight
MEF	murine embryonic fibroblasts
MEM	minimal essential media
NAE	Nedd8 activating enzyme
NE(C)	neuroendocrine carcinoma
NLS	nuclear localization sequence
NSCLC	non-small-cell lung cancer
PCAF	p300/CBP-associated factor
PD	pulldown
PCR	polymerase chain reaction
PONY	potentiating of neddylation
RING	really interesting new gene; part of the E3 ligase CRL complex
RNAi	RNA-mediated interference
RT	radiotherapy
SCC	squamous cell carcinoma
SCCRO	squamous cell carcinoma related oncogene

SCF complex	SKP1 cullin1 F-box
SKP1	S-phase kinase-associated protein 1
SKP2	S-phase kinase-associated protein 2
SKY	spectral karyotyping
TCGA	the cancer genome atlas
TKI	tyrosine kinase inhibitor
Ub	ubiquitin
UBA	ubiquitin associated
UBD	ubiquitin binding domain
UBL or Ublp	ubiquitin like protein
UPS	ubiquitin proteasome system

PhD portfolio

Summary of PhD training and teaching activities

Name PhD student: C.C. Bommeljé Erasmus MC Department: KNO-heelkunde	PhD period: 2006-2014 Promotor(s): prof.dr. B. Singh and prof.dr. R.J. Baatenburg de Jong	
1. PhD training		
	Year	**Workload (Hours/ECTS)**
General academic skills		
Desiderius Education: discipline overstijgend onderwijs	2008-2014	4 ECTS
Research skills		
Research fellowship with weekly basic science training	2006-2008	8 ECTS
In-depth courses (e.g. Research school, Medical Training)		
Head and neck anatomy (dissection)	2008-2014	4 ECTS
Skillslab Course Hands-on in Otology	2014	4 ECTS
Presentations		
Poster AAES, Monterey	2008	3 ECTS
Poster AHNS, San Francisco (best poster)	2008	3 ECTS
KNO vergadering (april)	2009	1 ECTS
KNO vergadering (november)	2009	1 ECTS
Poster AHNS, Arlington	2010	3 ECTS
KNO vergadering (april)	2012	1 ECTS
Poster AHNS-IFHNOS, New York City	2014	4 ECTS
KNO vergadering (november)	2014	1 ECTS
International conferences		
AAES, Monterey	2008	
AHNS, San Francisco	2008	
European Skull Base Society, Rotterdam	2009	0,5 ECTS
AHNS, Arlington	2010	
AHNS-IFHNOS, New York City	2014	
KNO vergadering (2 / year)	>2008	1 ECTS
Lecturing		
Onderwijs verpleegkundigen KNO “chirurgische ingrepen”.	2008	0,5 ECTS
Seminars and workshops		
Module: “Knopen en hechten”.	2008	0.5 ECTS
Workshop: “Geavanceerde beeldvormende technieken voor dokters”	2009	0.5 ECTS
Workshop: “Otology course”	2014	1 ECTS
Other		
Refereeravond KNO (4 / year)	>2008	1 ECTS

Acknowledgments

This thesis is the work of many people who I am grateful to.

First of all, I gratefully acknowledge dr. Shah for welcoming me at the Head and Neck Service of Memorial Sloan Kettering Cancer Center, for the hospitality and for the opportunity to work several years in the laboratory.

I am profoundly indebted to my mentor, Dr. Singh, for this unique opportunity, for introducing the scientific world to me and for the great support during my development as a research fellow. Your enthousiasm, knowledge and ongoing motivation have inspired me tremendously. It has been a great privilege and honor to work for you. You continuously raised the bar and pursued the very best. Many thanks for your intensive help and guidance. I learned a lot from your way of thinking.

During the years at MSKCC I have been very fortunate to be able to attend many educational lectures, including the Thursday morning conferences held in presence of dr. Ghossein, Dr. Lee, Dr. Stambuck, Dr. Tuttle and the attending head and neck surgeons Dr. Shah, Dr. Shaha, Dr. Boyle, Dr. Patel, Dr. Wong, Dr. Kraus and Dr. Singh who generously shared their immense knowledge of genetics, pathology, radiology, radiotherapy, medicine and surgery. They are exemplary role models, both professionally and personally.

Geachte professor Baatenburg de Jong, beste Rob, dank dat u mijn promotor wilde zijn. Ik waardeer het vertrouwen dat u in dit proefschrift had. Bedankt voor de geweldige opleiding tot KNO arts.

Geachte leden van de promotiecommissie; professor Looijenga, professor van Kemenade, professor Speel, professor Sleijfer, professor Verhoef en professor Berns, hartelijk dank voor uw tijd en expertise voor het beoordelen van mijn manuscript en uw komst naar de verdediging van dit proefschrift. I gratefully acknowledge our American Ph.D. committee opponents, including Dr. Singh and Guochang Huang for taking time out of their busy schedules and their commitment to join the PhD committee and travel to The Netherlands for the defense of this thesis.

I am grateful to all the colleagues in the laboratory; they taught me a complete laboratory-novice, the basics of proper work and thinking in a very inspiring environment. Thanks Alex, Anne, Ben, Cameron, Chris, Luc, Manish, Pete, Sarina and Stephen for excellent team work and for the great time we had. Dr. Y. Ramanathan, dear Rama, we had daily contact about the progress of my research. Thank you for the trust in my abilities.
Special thanks to Viola Weeda and Guochang Huang. We got to know each other at a later stage of this research project. Your quick replies and helpful criticism have helped this thesis to a good ending.

Alle stafleden en medewerkers van de afdeling KNO-heelkunde van het Erasmus MC, Reinier de Graaf Gasthuis en het Haga Ziekenhuis, hartelijk dank voor jullie bijdrage aan mijn opleiding tot KNO-arts. Ik heb veel geleerd, het waren ontzettend leuke jaren en het vloog voorbij!

Dr. Poublon, beste Pou, nog een apart woord voor u. Bedankt voor de leerzame tijd en de begeleiding als A-opleider tijdens de opleiding tot KNO arts. U was vanaf het eerste moment van mijn passen op de afdeling KNO in Rotterdam getuige; van mijn wetenschapsstage in het laatste studiejaar, het oudste co-schap, de daaropvolgende onderzoekstijd en mijn positie als AIOS.

KNO sportdag – commissie – genoten; Emilie, Laura en Laura, ik kijk altijd uit naar onze reuze gezellige etentjes waarbij we er 10 inplannen om in 1 avond de sportdag te regelen. Het bezoek naar het AMC om 'duifje' terug te halen, zal ik lang herinneren!

Charlotte, buddy, semi-huisgenoot, de logeerkamer blijft beschikbaar voor al je diensten. Gezellig!

Alle arts assistenten van de afdeling KNO; dank voor de gezelligheid gedurende mijn opleidingstijd, zowel binnen als buiten het werk!

Verder dank ik alle vriendinnen en vrienden die op hun eigen manier een bijdrage hebben geleverd aan de totstandkoming van dit proefschrift.

Lieve paranimfen, Dorine en Susanne, wat fijn dat jullie naast mij zullen staan op deze bijzondere dag. Naast afstuderen, trouwen, kinderen krijgen en promoveren, hoop ik nog vele life events met jullie mee te maken!

Lieve familie. Schoonouders, Willem en Annemarie, dank voor jullie getoonde interesse in mij en mijn proefschrift! Mijn ouders, Simon en Corien, ik wil jullie bedanken voor de steun en liefde die jullie mij altijd hebben gegeven. Datgene afmaken waar je aan begonnen bent, hebben jullie meegegeven als belangrijke waarde. Ik heb het met dit proefschrift geweten! Dit boekje is dan ook met trots aan jullie opgedragen. Mijn broers, Paul en Willem, bedankt voor alles.

Mijn lieve Paul, dank voor al je voortdurende steun, liefde en eindeloze begrip. Met jou en onze twee mooie zoons, Berend en Otto, wil ik voor altijd samenzijn! Op naar het volgende avontuur.

About the author

Claire Cornelia Bommeljé was born in Breda on July 25th, 1980. In 1998, she graduated cum laude from the Mencia de Mendoza Lyceum in Breda. The subsequent year she went a year abroad to New Braunfels (USA) where she followed anatomy and physiology courses. In 1999 she started medical school at the Erasmus University of Rotterdam. During her studies she followed an extracurricular surgical internship at the Academic Hospital in Paramaribo, Suriname and she participated in a research project on nasal NO measurements which led to her first scientific publication. She completed medical school cum laude in 2006.

In the same year, she started as a research fellow in the Laboratory of Epithelial Cancer Biology of the Head and Neck Service at Memorial Sloan Kettering Cancer Center, New York, under supervision of dr. Bhuvanesh Singh. The research collected in this thesis was mainly done in this time. In August 2008 she moved back to Rotterdam and started working at the department of Otorhinolaryngology and Head and Neck Surgery of the Erasmus Medical Center (EMC). In July 2009 she started her residency in the same department under supervision of Prof.dr. R.J. Baatenburg de Jong, dr. R.M.L. Poublon and dr. R.M. Metselaar. Rotations were done at the Haga Ziekenhuis in The Hague (mentor: dr. H.M. Blom and dr. J.P. Koopman) and Reinier de Graaf Gasthuis in Delft (mentor: dr. F.A.W. Peek and dr. H.C. Hafkamp). The expected end-date of her residency is June 20th, 2015. The author is married to Paul Verkleij and together they have two sons, Berend (2011) and Otto (2013).

List of publications

V.M.D. Struben, M.H. Wieringa, C.J. Mantingh, **C.C. Bommeljé**, M. Don, L. Feenstra, J.C. de Jongste. Nasal NO: normal values in children age 6 through to 17 years. *Eur Respir J*. 26:453-7, 2005.

L.G. Morris, O. Burschtin, J. Setlur, **C.C. Bommeljé**, K.C. Lee, J.B. Jacobs, R.A. Lebowitz. Acoustic rhinometric evaluation of nasal airway patency in REM and non-REM sleep. *Otolaryngology - Head and Neck Surgery*. Nov;139: 619-23, 2008.

C.C. Bommeljé*, A.Y. Kim*, B.E. Lee, Y. Yonekawa, L. Choi, L.G. Morris, R. Ryan, A. Kaufman, B.Hao, Y. Ramanathan, B. Singh. SCCRO (DCUN1D1) is an essential component of the E3 complex for neddylation. *J. Biol. Chem*. Nov 28; 283:33211-20, 2008.* these authors contributed equally.

C.C. Bommeljé, R. Poublon. Hyperostosis frontalis interna, een toevalsbevinding. *Ned Tijdsch KNO-heelkunde.* 3:144-147, 2010.

C.C. Bommeljé, B. Pullens. Respiratoire insufficiëntie door plastic bronchitis. *Ned Tijdsch KNO-heelkunde.* 1:16-18, 2012.

C.C. Bommeljé, D. Monserez, J.A.U. Hardillo. Heterotoop maagslijmvlies in het cavum oris. *Ned Tijdsch KNO-heelkunde.* 2:51-54, 2012.

C.C. Bommeljé, V. Weeda, G. Huang, K. Shah, S. Bains, E. Buss, M. Shaha, M. Gonen, R. Ghossein, Y. Ramanathan, B. Singh. Oncogenic function of SCCRO5/DCUN1D5 requires its neddylation E3 activity and nuclear localization. *Clin Cancer Res*. Jan 15;20(2):372-81, 2014.

C.C. Bommeljé, S.F. Meinesz, H.M. Blom. Achondroplasie: cave aberrante vaatstructuren in het os temporale. *Ned Tijdsch KNO-heelkunde.* 2:50-54, 2014.

G.C. Huang, C. Stock, **C.C. Bommeljé**, V.B. Weeda, K. Shah, S. Bains, E. Buss, M. Shaha, W. Rechler, Y. Ramanathan, B. Singh. SCCRO3 (DCUN1D3) antagonizes the neddylation and oncogenic activity of SCCRO (DCUN1D1). *J. Biol. Chem.* Dec 12;289(50):34728-42, 2014.

G.C. Huang, C.W. Towe, L. Choi, Y. Yonekawa, **C.C. Bommeljé**, S. Bains, W. Rechler, B. Hao, Y. Ramanathan, B. Singh. The UBA domain of SCCRO/DCUN1D1 serves as a feedback regulator of biochemical and oncogenic activity. *J. Biol. Chem.* Jan 2;290(1):296-309, 2015.

C.A. Hellingman, H.C. Hafkamp, J.M. Kruyt, **C.C. Bommeljé**. Plaatsbepaling van subcutane immunotherapie bij inhalatieallergie: eerste of tweede lijn? *Ned Tijdsch KNO-heelkunde* 1:13-18, 2015.

B.J. Noordman, F.W. Schalekamp, **C.C. Bommeljé**, T. Smith, R.H. Heijmen, J.A.D. Jol. Linker nervus recurrens parese ten gevolge van een staande ruptuur van een aneurysma van de arcus aortae. *Ned Tijdsch KNO-heelkunde* 2:79-82, 2015.

C.C. Bommeljé, J. Sun, S. Bains, R.A. Ghossein, Y. Ramanathan, B. Singh. SCCRO and its paralogs are frequently dysregulated in human cancers and associated with an aggressive clinical course and activation of neddylation. *Submitted to Annals of Surgical Oncology.*